An OFDM and MC-CDMA Primer

by

L. Hanzo and T. Keller

We dedicate this monograph to the numerous contributors of this field, many of whom are listed in the Author Index

Contents

[1]This section is based on M. Münster, T. Keller and L. Hanzo, "Co-Channel Interference Suppression Assisted Adaptive OFDM in Interference Limited Environments", ©IEEE, VTC'99, Amsterdam, NL, 17-19 Sept. 1999.

About the Authors

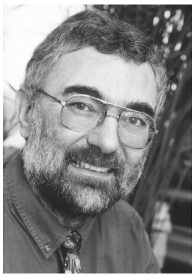

Lajos Hanzo, Fellow of the Royal Academy of Engineering, received his first-class degree in electronics in 1976 and his doctorate in 1983. In 2004 he was awarded the Doctor of Sciences (DSc) degree by the University of Southampton, UK. During his career in telecommunications he has held various research and academic posts in Hungary, Germany and the UK. Since 1986 he has been with the Department of Electronics and Computer Science, University of Southampton, UK, where he holds the chair in telecommunications. He has co-authored 12 books, totalling 9000 pages on mobile radio communications, published in excess of 600 research papers, has acted as TPC Chair of numerous major IEE and IEEE conferences, presented various keynote lectures and has been awarded a number of distinctions. Currently he heads an academic research team, working on a range of research projects in the field of wireless multimedia communications sponsored by industry, the Engineering and Physical Sciences Research Council (EPSRC) UK, the European IST Programme and the Mobile Virtual Centre of Excellence (VCE), UK. He is an enthusiastic supporter of industrial and academic liaison and he offers a range of industrial courses. Lajos is also an IEEE Distinguished Lecturer of both the Communications as well as the Vehicular Technology Society, a Fellow of both the IEEE and the IEE. He is an editorial board member of the Proceedings of the IEEE and a Governer of the IEEE VT Society. For further information on research in progress and associated publications, please refer to http://www-mobile.ecs.soton.ac.uk

Thomas Keller studied Electrical Engineering at the University of Karlsruhe, Ecole Superieure d'Ingenieurs en Electronique et Electrotechnique, Paris, and the University of Southampton. He graduated with a Dipl.-Ing. degree in 1995. Between 1995 and 1999 he was with the Wireless Multimedia Communications Group at the University of Southampton, where he completed his PhD in mobile communications. His areas of interest include adaptive OFDM transmission, wideband channel estimation, CDMA and error correction coding. Following the completion of hos PhD he joined Ubinetics, Cambridge, UK, where he was involved in the research and development of third-generation wireless systems. Following a reorganization, he was part of a team that was transferred to Analog Devices, Cambridge, UK. Dr. Keller has co-authored three monographs and about 30 various research papers.

Other Wiley and IEEE Press Books on Related Topics [2]

- R. Steele, L. Hanzo (Ed): *Mobile Radio Communications: Second and Third Generation Cellular and WATM Systems*, John Wiley and IEEE Press, 2nd edition, 1999, ISBN 07 273-1406-8, 1064 pages
- L. Hanzo, F.C.A. Somerville, J.P. Woodard: *Voice Compression and Communications: Principles and Applications for Fixed and Wireless Channels*; IEEE Press and John Wiley, 2001, 642 pages
- L. Hanzo, P. Cherriman, J. Streit: *Wireless Video Communications: Second to Third Generation and Beyond*, IEEE Press and John Wiley, 2001, 1093 pages
- L. Hanzo, T.H. Liew, B.L. Yeap: *Turbo Coding, Turbo Equalisation and Space-Time Coding*, John Wiley and IEEE Press, 2002, 751 pages
- J.S. Blogh, L. Hanzo: *Third-Generation Systems and Intelligent Wireless Networking: Smart Antennas and Adaptive Modulation*, John Wiley and IEEE Press, 2002, 408 pages
- L. Hanzo, C.H. Wong, M.S. Yee: *Adaptive Wireless Transceivers: Turbo-Coded, Turbo-Equalised and Space-Time Coded TDMA, CDMA and OFDM Systems*, John Wiley and IEEE Press, 2002, 737 pages
- L. Hanzo, L-L. Yang, E-L. Kuan, K. Yen: *Single- and Multi-Carrier CDMA: Multi-User Detection, Space-Time Spreading, Synchronisation, Networking and Standards*, John Wiley and IEEE Press, June 2003, 1060 pages
- L. Hanzo, M. Münster, T. Keller, B-J. Choi, *OFDM and MC-CDMA for Broadband Multi-User Communications, WLANs and Broadcasting*, John-Wiley and IEEE Press, 2003, 978 pages
- L. Hanzo, S-X. Ng, T. Keller and W.T. Webb, *Quadrature Amplitude Modulation: From Basics to Adaptive Trellis-Coded, Turbo-Equalised and Space-Time Coded OFDM, CDMA and MC-CDMA Systems*, John Wiley and IEEE Press, 2004, 1105 pages

[2] For detailed contents and sample chapters please refer to http://www-mobile.ecs.soton.ac.uk

Acknowledgements

We are indebted to our many colleagues who have enhanced our understanding of the subject, in particular to Prof. Emeritus Raymond Steele. These colleagues and valued friends, too numerous to be mentioned, have influenced our views concerning various aspects of wireless multimedia communications. We thank them for the enlightenment gained from our collaborations on various projects, papers and books. We are grateful to Steve Braithwaite, Jan Brecht, Jon Blogh, Marco Breiling, Marco del Buono, Sheng Chen, Peter Cherriman, Stanley Chia, Joseph Cheung, Sheyam Lal Dhomeja, Dirk Didascalou, Lim Dongmin, Stephan Ernst, Peter Fortune, Eddie Green, David Greenwood, Hee Thong How, Ee Lin Kuan, W. H. Lam, C. C. Lee, Xiao Lin, Chee Siong Lee, Tong-Hooi Liew, Vincent Roger-Marchart, Jason Ng, Michael Ng, M. A. Nofal, Jeff Reeve, Redwan Salami, Clare Somerville, Rob Stedman, David Stewart, Jürgen Streit, Jeff Torrance, Spyros Vlahoyiannatos, William Webb, Stephan Weiss, John Williams, Jason Woodard, Choong Hin Wong, Henry Wong, James Wong, Lie-Liang Yang, Bee-Leong Yeap, Mong-Suan Yee, Kai Yen, Andy Yuen, and many others with whom we enjoyed an association.

We also acknowledge our valuable associations with the Virtual Centre of Excellence (VCE) in Mobile Communications, in particular with its chief executive, Dr Walter Tuttlebee, and other leading members of the VCE, namely Dr Keith Baughan, Prof. Hamid Aghvami, Prof. Ed Candy, Prof. John Dunlop, Prof. Barry Evans, Prof. Peter Grant, Prof. Mike Walker, Prof. Joseph McGeehan, Prof. Steve McLaughlin and many other valued colleagues. Our sincere thanks are also due to the EPSRC, UK for supporting our research. We would also like to thank Dr Joao Da Silva, Dr Jorge Pereira, Dr Bartholome Arroyo, Dr Bernard Barani, Dr Demosthenes Ikonomou, Dr Fabrizio Sestini and other valued colleagues from the Commission of the European Communities, Brussels, Belgium.

Without the kind support of Mark Hammond, Sarah Hinton, Jinnifer Beal and their colleagues at the Wiley editorial office in Chichester, UK this monograph would never have reached the readers. *Finally, our sincere gratitude is due to the numerous authors listed in the Author Index — as well as to those whose work was not cited owing to space limitations — for their contributions to the state of the art, without whom this book would not have materialised.*

Lajos Hanzo and Thomas Keller
School of Electronics and Computer Science
University of Southampton, UK

Chapter 10

Maximum-Likelihood Enhanced Sphere Decoding of MIMO-OFDM [1] [2]

J. Akhtman and L. Hanzo

10.1 Classification of Smart Antennas

In recent years various smart antenna designs have emerged, which have found application in diverse scenarios, as seen in Table 10.1. The main objective of employing smart antennas is that of combating the effects of multipath fading on the desired signal and suppressing interfering signals, thereby increasing both the performance and capacity of wireless systems [351]. Specifically, in smart antenna-assisted systems, multiple antennas may be invoked at the transmitter and/or the receiver, where the antennas may be arranged for achieving spatial diversity, directional beamforming or for attaining both diversity and beamforming. In smart antenna systems the achievable performance improvements are usually a function of the antenna spacing and that of the algorithms invoked for processing the signals received by the antenna elements.

In beamforming arrangements [217] typically $\lambda/2$-spaced antenna elements are used for the sake of creating a spatially selective transmitter/receiver beam. Smart antennas using beamforming have been widely employed for mitigating the effects of various interfering signals and for providing beamforming gain. Furthermore, the beamforming arrangement is capable of suppressing co-channel interference, which allows the system to support multiple

[1] Acknowledgements: The work reported in this paper has formed part of the Wireless Enabling Techniques work area of the Core 3 Research Programme of the Virtual Centre of Excellence in Mobile and Personal Communications, Mobile VCE, www.mobilevce.com, whose funding support, including that of EPSRC, is gratefully acknowledged. Fully detailed technical reports on this research are available to Industrial Members of Mobile VCE.
OFDM and MC-CDMA: A Primer. L.Hanzo, T. Keller, ©2006 John Wiley & Sons, Ltd. ISBN 0-470-03007-0

Beamforming [217]	Typically $\lambda/2$-spaced antenna elements are used for the sake of creating a spatially selective transmitter/receiver beam. Smart antennas using beamforming have been employed for mitigating the effects of co-channel interfering signals and for providing beamforming gain.
Spatial Diversity [216] and Space-Time Spreading	In contrast to the $\lambda/2$-spaced phased array elements, in spatial diversity schemes, such as space-time block or trellis codes [216] the multiple antennas are positioned as far apart as possible, so that the transmitted signals of the different antennas experience independent fading, resulting in the maximum achievable diversity gain.
Space Division Multiple Access	SDMA exploits the unique, user-specific "spatial signature" of the individual users for differentiating amongst them. This allows the system to support multiple users within the same frequency band and/or time slot.
Multiple Input Multiple Output Systems [123]	MIMO systems also employ multiple antennas, but in contrast to SDMA arrangements, not for the sake of supporting multiple users. Instead, they aim for increasing the throughput of a wireless system in terms of the number of bits per symbol that can be transmitted by a given user in a given bandwidth at a given integrity.

Table 10.1: Applications of multiple antennas in wireless communications

users within the same bandwidth and/or same time-slot by separating them spatially. This spatial separation however becomes only feasible, if the corresponding users are separable in terms of the angle of arrival of their beams. These beamforming schemes, which employ appropriately phased antenna array elements that are spaced at distances of $\lambda/2$ typically result in an improved SINR distribution and enhanced network capacity [217].

In contrast to the $\lambda/2$-spaced phased array elements, *in spatial diversity schemes*, such as space-time coding aided transmit diversity arrangements [216], the multiple antennas are positioned as far apart as possible. A typical antenna element spacing of 10λ [351] may be used, so that the transmitted signals of the different antennas experience independent fading, when they reach the receiver. This is because the maximum diversity gain can be achieved, when the received signal replicas experience independent fading. Although spatial diversity can be achieved by employing multiple antennas at either the base station, mobile station, or both, it is more cost-effective and practical to employ multiple transmit antennas at the base station. A system having multiple receiver antennas has the potential of achieving receiver diversity, while that employing multiple transmit antennas exhibits transmit diversity. Recently, the family of transmit diversity schemes based on space-time coding, either space-time block codes or space-time trellis codes, has received wide attention and has been invoked in the 3rd-generation systems [217,352]. The aim of using spatial diversity is to provide both transmit as well as receive diversity and hence enhance the system's integrity/robustness. This typically results in a better physical-layer performance and hence a better network-layer performance, hence space-time codes indirectly increase not only the transmission integrity, but also the achievable spectral efficiency.

A third application of smart antennas is often referred to as *Space Division Multiple Access* (SDMA), which exploits the unique, user-specific ”spatial signature” of the individual users for differentiating amongst them. In simple conceptual terms one could argue that both a conventional CDMA spreading code and the Channel Impulse Response (CIR) affect the transmitted signal similarly - they are namely convolved with it. Hence, provided that the CIR is accurately estimated, it becomes known and is certainly unique, although - as opposed to orthogonal Walsh-Hadamad spreading codes, for example - not orthogonal to the other CIRs. Nonetheless, it may be used for uniquely identifying users after channel estimation and hence for supporting several users within the same bandwidth. Provided that a powerful multi-user detector is available, one can support even more users than the number of antennas. Hence this method enhances the achievable spectral efficiency directly.

Finally, Multiple Input Multiple Output (MIMO) systems [123, 353–356] also employ multiple antennas, but in contrast to SDMA arrangements, not for the sake of supporting multiple users. Instead, they aim for increasing the throughput of a wireless system in terms of the number of bits per symbol that can be transmitted by a single user in a given bandwidth at a given integrity.

10.2 Introduction to Space-Time Processing

The ever-increasing demand for both high data-rates, as well as for improved transmission integrity requires efficient utilisation of the limited system resources, while supporting a high grade of mobility in diverse propagation environments. Consequently, the employment of an appropriate modulation format, as well as efficient exploitation of the available bandwidth constitute crucial factors in achieving high performance.

The Orthogonal Frequency Division Multiplexing (OFDM) modulation scheme employed in conjunction with a Multiple-Input Multiple-Output (MIMO) architecture [90], where multiple antennas are employed at both the transmitter and the receiver of the communication system, constitutes an attractive solution in terms of satisfying these requirements. Firstly, the OFDM modulation technique is capable of coping with the highly frequency-selective, time-variant channel characteristics associated with mobile wireless communication channels, while possessing a high grade of structural flexibility for exploiting the beneficial properties of MIMO architectures.

It is highly beneficial that OFDM and MIMOs may be conveniently combined, since the information-theoretical analysis predicts [357] that substantial capacity gains are achievable in communication systems employing MIMO architectures. Specifically, if the fading processes corresponding to different transmit-receive antenna pairs may be assumed to be independently Rayleigh distributed,[3] the attainable capacity has been shown to increase linearly with the smaller of the numbers of the transmit and receive antennas [357]. Additionally, the employment of MIMO architectures allows the efficient exploitation of the spatial diversity available in wireless MIMO environments, thus improving the system's BER, as well as further increasing the system's capacity, as a benefit of the reduced channel quality fluctuations.

[3] This assumption is typically regarded as valid, if the appropriate antenna spacing is larger than $\lambda/2$, where λ is the corresponding wavelength.

The family of space-time signal processing methods, which allow the efficient implementation of communication systems employing MIMO architectures, are commonly referred to as smart antennas. In recent years, the concept of smart antennas has attracted intense research interest in both the academic and the industrial communities. As a result, a multiplicity of smart antenna-related methods has been proposed. These include methods implemented at the transmitter, the receiver or both.

The classification of smart-antenna aided wireless transmission techniques was already briefly addressed in the context of Table 10.1. A slightly more detailed classification is illustrated in Figure 10.1. It should be noted, however, that the classification presented here is somewhat informal and its sole purpose is to appropriately position the content of this chapter in the context of the extensive material available on the subject.

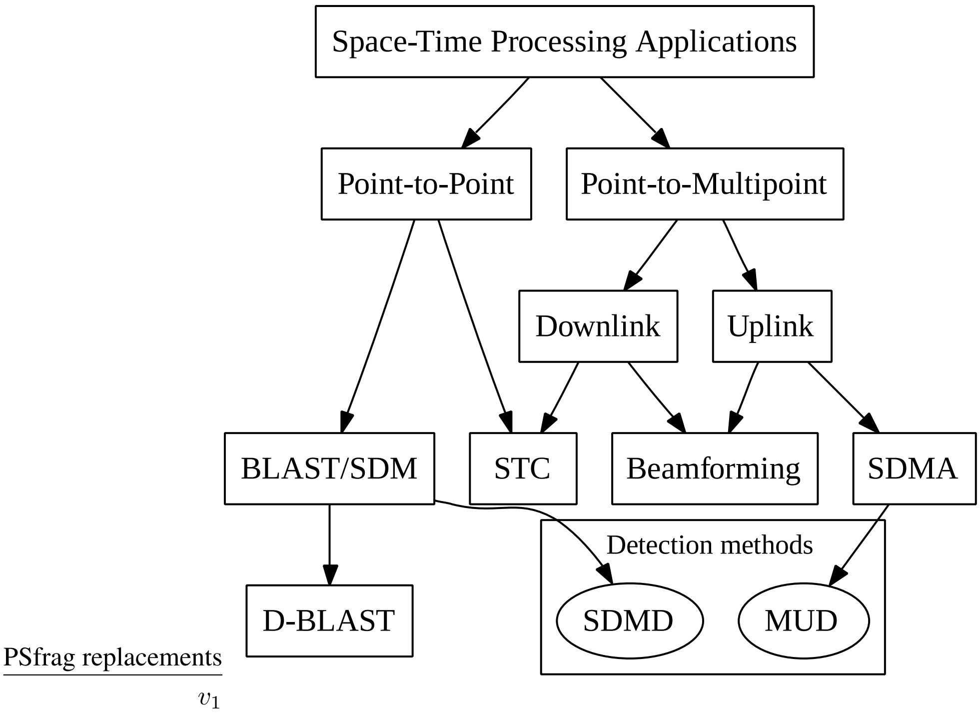

Figure 10.1: Classification of space-time processing techniques

Two distinctive system scenarios employing smart antennas can be identified. The first is the point-to-point SDM-type scenario, where two peer terminals each employing multiple antennas, communicate with each other over a MIMO channel and the multiple antennas are primarily used for achieving a multiplexing gain, i.e. a higher throughput [123]. The second scenario corresponds to the point-to-multipoint configuration, where a single base-station, employing multiple antennas communicates simultaneously using a single carrier frequency with multiple user terminals, each employing one or several antennas.

The various point-to-multipoint smart antenna applications can be further subdivided into uplink- and downlink-related applications. The uplink-related methods constitute a set of techniques, which can be employed in the base station in order to detect the signals simultaneously transmitted by multiple user terminals. More specifically, provided that the Channel Impulse Response (CIR) of all users is accurately estimated, it may be used as their unique, user-specific spatial signature for differentiating them, despite communicating within the same frequency band [90]. Hence, the corresponding space-time signal processing problem is commonly referred to as Multi-User Detection (MUD) [90], while the multi-antenna multi-user systems employing uplink space-time MUD are commonly referred to as Space Division Multiple Access (SDMA) systems [90]. In contrast to the SDM-type systems designed for achieving the highest possible multiplexing gain, the design objective of the SDMA techniques is the maximisation of the number of users supported. By contrast, the class of beamformers [217] creates angularly selective beams for both the uplink and downlink in the direction of the desired user, while forming nulls towards the interfering users. Finally, the family of Space-Time Codes (STC) [216] was optimised for achieving the highest possible transmit diversity gain, rather than for attaining the highest possible spatial multiplexing gain in the context of a single user or for increasing the number of users supported. At the time of writing new research is aiming for increasing both the attainable diversity and multiplexing gain with the aid of eigen-value decomposition [358].

On the other hand, the host of downlink-related smart antenna applications comprises techniques which can be employed in both the base station terminal and/or each of the user terminals in order to efficiently resolve the high-datarate signal concurrently communicated from multiple antennas of the base station terminal. The downlink smart antenna implementations, which rely on transmitter-end space-time processing only are usually jointly referred to as beamforming [217]. Other downlink methods, which involve space-time processing at both the transmitter and the receiver ends are largely associated with Space-Time Codes (STC) [216].

As stated above, two benefits of employing smart antennas are the system's improved integrity, as well as the increased aggregate throughput. Hence an adequate performance criterion of the particular smart antenna implementation is a combination of the system's attainable aggregate data-throughput, as well as the corresponding data integrity, which can be quantified in terms of the average BER. Consequently, in the context of point-to-multipoint-related smart antenna applications, the achievable capacity associated with the particular space-time processing method considered may be assessed as a product of the simultaneously supported number of individual users and the attainable data-rate associated with each supported user. The measure of data-integrity may be the average BER of all the users supported. Thus, the typical objective of the multi-user-related smart antenna implementations, such as that of an SDMA scheme is that of increasing the number of the simultaneously supported users, while sustaining the highest possible integrity of all the data communicated.

For the sake of distinction, in this work we employ the alternative terminology of Space Division Multiplexing (SDM) in order to refer to a generic MIMO architecture. The corresponding detection methods are referred to as SDM Detection (SDMD) techniques, as opposed to the MUD techniques employed in the context of SDMA systems [90]. Naturally, however, the SDMD and MUD schemes share the same signal detection methods, regardless of whether the signal has arrived from multiple antennas of the same or different users. The classification of the most popular SDMD/MUD schemes is depicted in Figure 10.2. The methods considered include the linear LS and MMSE techniques, as well as non-linear techniques, such as Maximum Likelihood (ML), Successive Interference Cancellation (SIC), Genetic Algorithm-aided MMSE (GA-MMSE) [359,360] as well as the novel OHRSA methods proposed in this chapter.

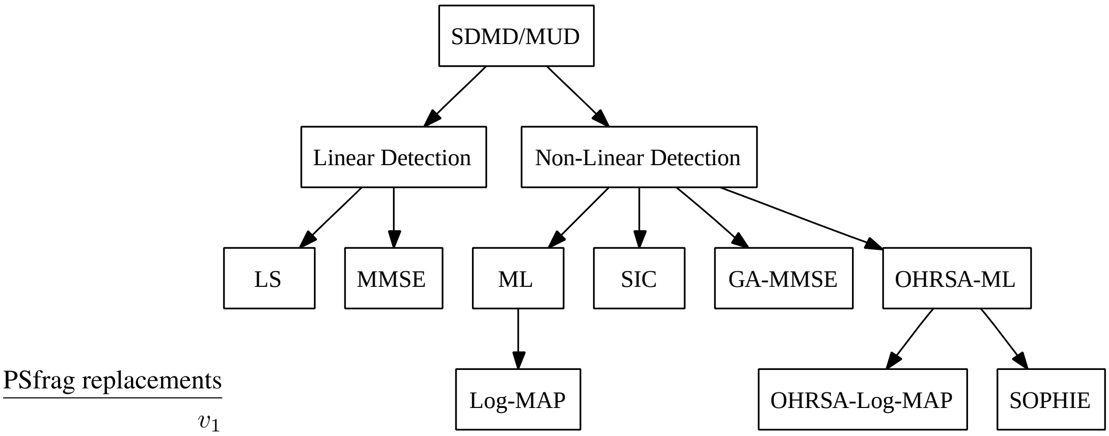

Figure 10.2: SDM detection methods classification.

The rest of this chapter is structured as follows. Both the MIMO channel model considered as well as the SDM-OFDM system model are described in Section 10.3. The OHRSA-aided SDM detection methods considered are outlined in Section 10.4. Specifically, in Section 10.4.1 we derive the OHRSA-aided ML SDM detector, which benefits from the optimal performance of the ML detector briefly introduced in Chapter 9, while exhibiting a relatively low computational complexity, which is only slightly higher than that required by the low-complexity MMSE detector of Chapter 12 in [90]. To elaborate a little further, in Section 10.4.3 we will derive a bit-wise OHRSA-aided ML SDM detector, which allows us to apply the OHRSA method of Section 10.4 in high-throughput systems, which employ multi-level modulation schemes, such as M-ary QAM [90].

In Section 10.4.4 our discourse evolves further by deducing the OHRSA-aided Log-MAP SDM detector, which allows an efficient evaluation of the soft-bit information and therefore results in highly efficient turbo decoding. Unfortunately however, in comparison to the OHRSA-aided ML SDM detector of Section 10.4.3 the OHRSA-aided Log-MAP SDM detector of Section 10.4.4 exhibits a substantially higher complexity. Consequently, in Section 10.4.5 we derive an approximate Log-MAP method, which we refer to as Soft-output OPtimised HIErarchy (SOPHIE) SDM detector. The SOPHIE SDM detector combines the advantages of both the OHRSA-aided ML and the OHRSA-aided Log-MAP SDM detectors of Sections 10.4.3 and 10.4.4, respectively. Specifically, it exhibits a similar performance to that of the optimal Log-MAP detector, while imposing a modest complexity, which is only slightly higher than that required by the low-complexity MMSE SDM detector [90]. The computational complexity as well as the achievable performance of the SOPHIE SDM detector of Section 10.4.5 are analysed and quantified in Sections 10.4.5.1 and 10.4.5.2, respectively. Finally, our conclusions are summarised in Section 10.5.

10.3 SDM-OFDM System Model

10.3.1 MIMO Channel Model

We consider a MIMO wireless communication system employing m_{t} transmit and n_{r} receive antennas, hence, the corresponding MIMO wireless communication channel is constituted by $(n_{\mathrm{r}} \times m_{\mathrm{t}})$ propagation links, as illustrated in Figure 10.3. Furthermore, each of the corresponding $(n_{\mathrm{r}} \times m_{\mathrm{t}})$ Single Input Single Output (SISO) propagation links comprises a multiplicity of statistically independent components, termed as paths. Thus, each of these SISO propagation links can be characterised as a multipath SISO channel discussed in detail in [90]. Similarly to the SISO case, the multi-carrier structure of our SDM-OFDM transceiver allows us to characterise the broadband frequency-selective channel considered as an OFDM subcarrier-related vector of flat-fading Channel Transfer Function (CTF) coefficients. However, as opposed to the SISO case, for each OFDM symbol n and subcarrier k the MIMO channel is characterised by a $(n_{\mathrm{r}} \times m_{\mathrm{t}})$-dimensional matrix $\mathbf{H}[n,k]$ of the CTF coefficients associated with the different propagation links, such that the element $H_{ij}[n,k]$ of the CTF matrix $\mathbf{H}[n,k]$ corresponds to the propagation link connecting the jth transmit and ith receive antennas.

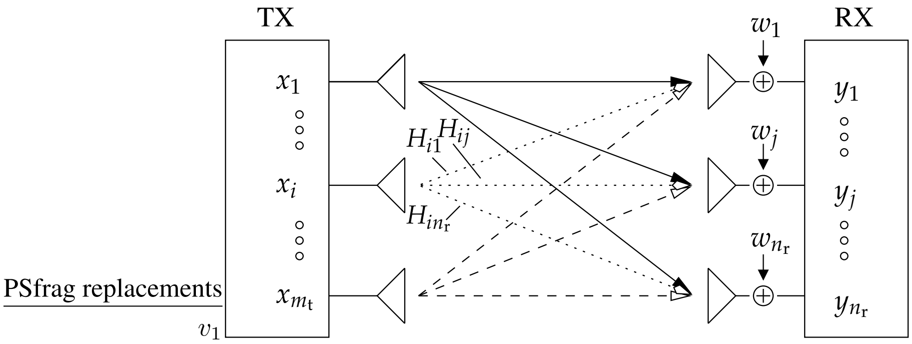

Figure 10.3: Illustration of a MIMO channel constituted by m_{t} transmit and n_{r} receive antennas. The corresponding MIMO channel is characterized by the $(n_{\mathrm{r}} \times m_{\mathrm{t}})$-dimensional matrix $\mathbf{H}$ of CTF coefficients.

Furthermore, the correlation properties of the MIMO-OFDM channel can readily be derived as a generalisation of the SISO-OFDM channel scenario discussed in detail in [90]. As was shown in [361], the cross-correlation function $r_H[m,l]$, which characterises both the time- and frequency-domain correlation properties of the discrete CTF coefficients $H_{ij}[n,k]$ associated with the particular (i,j)th propagation link of the MIMO channel, as well as with the different OFDM symbol and subcarrier indices n and k can be described as

$$\begin{aligned} r_{H;ij}[m,l] &= \mathtt{E}\left\{H_{ij}^*[n+m,k+l], H_{ij}[n,k]\right\} \\ &= \sigma_H^2 r_t[m] r_f[l], \end{aligned} \tag{10.1}$$

where $r_t[m]$ is the time-domain correlation function, which may be characterised by a time-domain correlation model proposed by Jakes in [362], where we have

$$r_t[m] \triangleq r_J[m] = J_0(nw_d), \tag{10.2}$$

and $J_0(x)$ is a zero-order Bessel function of the first kind, while $w_d = 2\pi T f_D$ is the normalised Doppler frequency. On the other hand, the frequency-domain correlation function $r_f[l]$ can be expressed as [93]

$$r_f[l] = |C(l\Delta f)|^2 \sum_{i=1}^{L} \frac{\sigma_i^2}{\sigma_H^2} e^{-\jmath 2\pi l \Delta f \tau_i}, \tag{10.3}$$

where $C(f)$ is the frequency response of the pulse-shaping filter employed by the particular system, σ_i^2 and $\tau_i,\ i = 1, \cdots, L$ are the average power and the corresponding delay of the L-tap Power Delay Profile (PDP) encountered, while σ_H^2 is the average power per MIMO channel link, such that we have $\sigma_H^2 = \sum_{i=1}^{L} \sigma_i^2$.

In this chapter we assume the different MIMO channel links to be mutually uncorrelated. This common assumption is usually valid, if the spacing between the adjacent antenna elements exceeds $\lambda/2$, where λ is the wavelength corresponding to the RF signal employed. Thus, the overall cross-correlation function can be described as

$$\begin{aligned} r_{H;ij}[m,l] &= \mathtt{E}\left\{H^*_{i'j'}[n+m, k+l], H_{ij}[n,k]\right\} \\ &= \sigma_H^2 r_t[m] r_f[l] \delta[i-i'] \delta[j-j'], \end{aligned} \tag{10.4}$$

where $\delta[i]$ is the discrete Kronecker Delta function.

10.3.2 SDM-OFDM Transceiver Structure

The schematic of a typical SDM-OFDM system's physical layer is depicted in Figure 10.4.

The transmitter of the SDM-OFDM system considered is typically constituted by the Encoder and Modulator seen in Figure 10.4, generating a set of m_t complex-valued base-band time-domain signals [90]. The modulated base-band signals are then processed in parallel. Specifically, they are oversampled and shaped using a Nyquist filter, such as, for example, a root-raised-cosine filter. The resultant oversampled signals are then converted into an analog pass-band signal using a bank of D/A converters and upconverted to the Radio Frequency (RF) band. At the receiver side of the SDM-OFDM transceiver the inverse process takes place, where the set of received RF signals associated with the n_r receive antenna elements are amplified by the RF amplifier and down-converted to an intermediate frequency passband. The resultant pass-band signals are then sampled by a bank of A/D converters, downconverted to the base-band, filtered by a matched Nyquist filter and finally decimated, in order to produce a set of discrete complex-valued base-band signals. The resultant set of discrete signals is processed by the corresponding Demodulator and Decoder module seen in Figure 10.4, where the transmitted information-carrying symbols are detected.

In this chapter we consider the link between the output of the SDM-OFDM Modulator and the input of the corresponding SDM-OFDM Demodulator of Figure 10.4 as an effective baseband MIMO channel. The proof of feasibility for this assumption is beyond the scope this chapter, however it can be found for example in [249,363]. The structure of the resultant base-

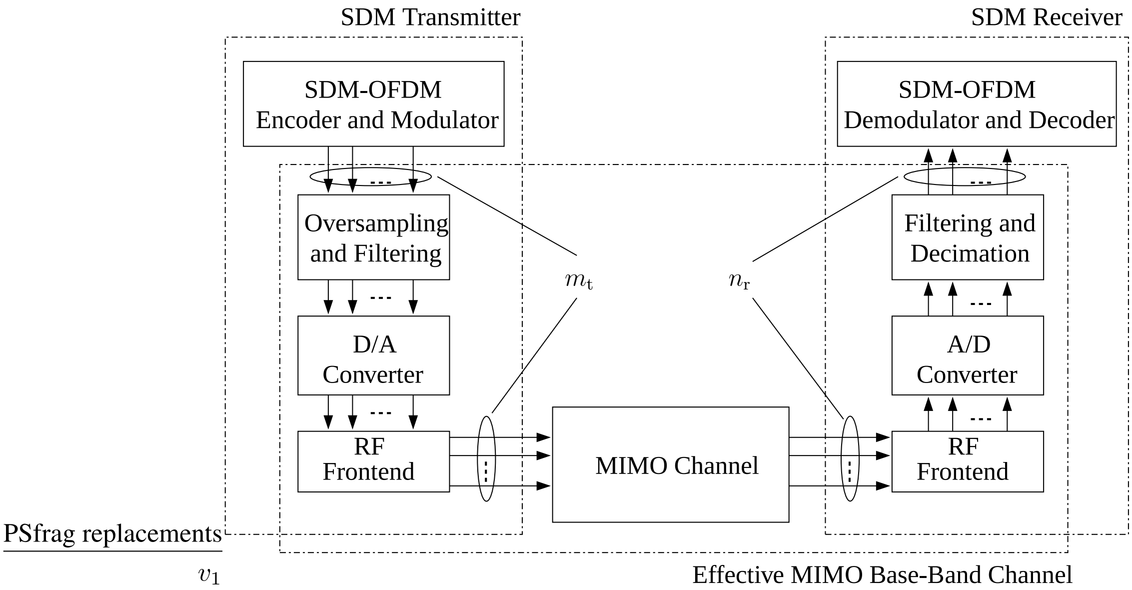

Figure 10.4: Schematic of a typical SDM-OFDM system's physical layer.

band SDM-OFDM system is depicted in Figure 10.5, where the bold grey arrows illustrate subcarrier-related signals represented by the vectors $\mathbf{x}_i$ and $\mathbf{y}_i$, while the black thin arrows accommodate scalar time-domain signals.

The discrete frequency-domain model of the SDM-OFDM system, illustrated in Figure 10.5, may be characterised as a generalisation of the SISO case described in [90]. Namely, we have

$$y_i[n,k] = \sum_{j=1}^{m_t} H_{ij}[n,k]x_j[n,k] + w_i[n,k], \tag{10.5}$$

where $n = 0, 1, \cdots$ and $k = 0, \ldots, K-1$ are the OFDM symbol and subcarrier indices, respectively, while $y_i[n,k], x_j[n,k]$ and $w_i[n,k]$ denote the symbol received at the ith receive antenna, the symbol transmitted from the jth transmit antenna and the Gaussian noise sample encountered at the ith receive antenna, respectively. Furthermore, $H_{ij}[n,k]$ represents the complex-valued CTF coefficient associated with the propagation link connecting the jth transmit and ith receive antennas at the kth OFDM subcarrier and time instance n. Note that in the case of an M-QAM modulated OFDM system, $x_j[n,k]$ corresponds to the M-QAM symbol accommodated by the kth subcarrier of the nth OFDM symbol transmitted from the jth transmit antenna element.

The SDM-OFDM system model described by Equation (10.5) can be interpreted as the per OFDM-subcarrier vector expression of

$$\mathbf{y}[n,k] = \mathbf{H}[n,k]\mathbf{x}[n,k] + \mathbf{w}[n,k], \tag{10.6}$$

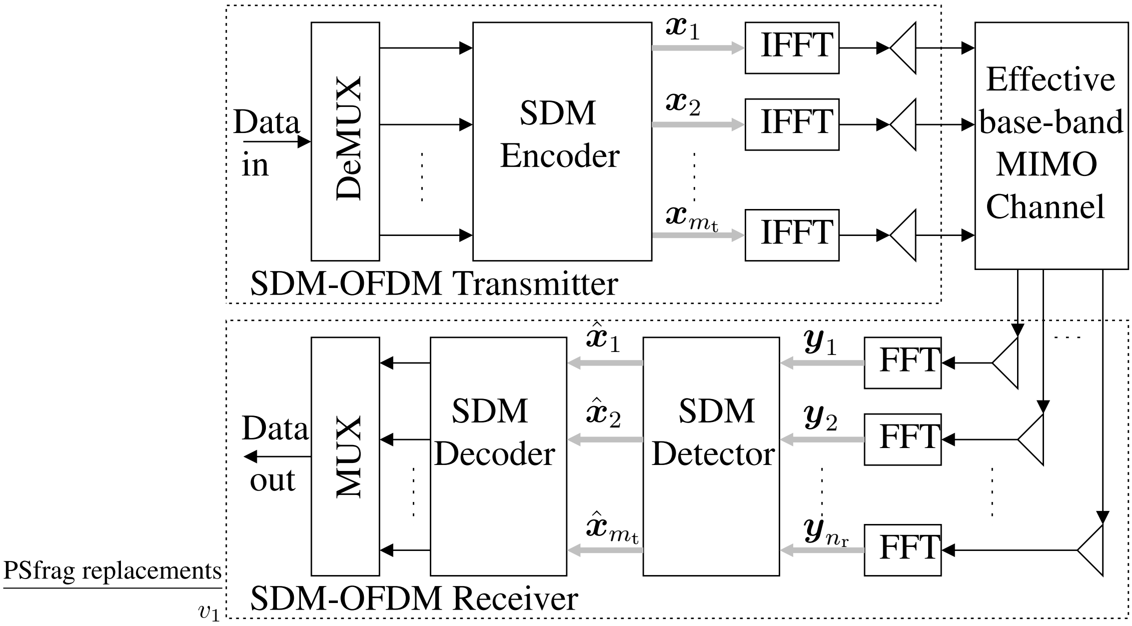

Figure 10.5: Schematic of a generic SDM-OFDM BLAST-type transceiver.

where we introduce the space-division-related vectors $\mathbf{y}[n,k]$, $\mathbf{x}[n,k]$ and $\mathbf{w}[n,k]$, as well as a space-division-related $(n_r \times m_t)$-dimensional matrix of CTF coefficients $\mathbf{H}[n,k]$. Note that similarly to the SISO case, the multi-carrier structure of the SDM-OFDM transceiver allows us to represent the broadband frequency-selective MIMO channel as a subcarrier-related vector of flat-fading MIMO-CTF matrices $\mathbf{H}[n,k]$.

10.4 Optimised Hierarchy Reduced Search Algorithm-aided SDM Detection

As it was pointed out in [90] , the "brute-force" ML detection method does not provide a feasible solution to the generic SDM detection problem as a result of its excessive computational complexity. Nevertheless, since typical wireless communication systems operate at moderate-to-high SNRs, Reduced Search Algorithms (RSA) may be employed, which are capable of obtaining the ML solution at a complexity which is considerably lower than that imposed by the ML detector of [90] . The most powerful of the RSA methods found in the literature is constituted by the Sphere Decoder (SD) [364]. The SD was first proposed for employment in the context of space-time processing in [365], where it is used for computing the ML estimates of the modulated symbols transmitted simultaneously from multiple transmit antennas. The complex-valued version of the sphere decoder was proposed by Hochwald and Brink in [176]. The subject was further investigated by Damen *et al.* in [366]. Subsequently, an improved version of the Complex Sphere Decoder (CSD) was advocated by Pham *et al.*

in [367].

Furthermore, CSD-aided detection was considered by Tellambura *et al.* in a joint channel estimation and data detection scheme considered in [368], while a revised version of the CSD method, namely the so-called Multistage Sphere Decoding (MSD) was introduced in [369]. The generalized version of the Sphere Decoder, which is suitable for employment in rank-defficient MIMO systems was introduced by Damen *et al.* in [370] and further refined by Cui and Tellambura in [371].

In this section we would like to introduce a novel Optimised Hierarchy (OH) RSA-aided SDM detection method, which may be regarded as an advanced extension of the CSD method portrayed in [367]. The algorithm proposed extends the potential range of applications of the CSD methods of [176] and [367], as well as reduces the associated computational complexity, rendering the algorithm attractive for employment in practical systems.

The method proposed, which we refer to as the Soft-output OPtimised HIErarchy (SOPHIE) algorithm exhibits the following attractive properties:

1) The method can be used in the so-called over-loaded scenario, where the number of transmit antenna elements exceeds that of the receive antenna elements. A particularly interesting potential application is found in a Multiple Input Single Output scenario, where the system employs multiple transmit antennas and a single receive antenna. Moreover, the associated computational complexity is only moderately increased even in heavily over-loaded scenarios and it is almost independent of the number of receive antennas.

2) As opposed to the conventional CSD schemes, the calculation of the sphere radius is not required and therefore the method proposed is robust to the particular choice of the initial parameters both in terms of the achievable performance and the associated computational complexity.

3) The method proposed allows a selected subset of the transmitted information-carrying symbols to be detected, while the interference imposed by the undetected signals is suppressed.

4) The overall computational complexity required is only slightly higher than that imposed by the linear MMSE multi-user detector designed for detecting a similar number of users.

5) Finally, the associated computational complexity is fairly independent of the channel conditions quantified in terms of the Signal-to-Noise Ratio encountered.

10.4.1 Optimised Hierarchy Reduced Search Algorithm-aided ML SDM Detection

We commence our discourse by deriving an OHRSA-aided ML SDM detection method for a constant-envelope modulation scheme, such as M-PSK, where the transmitted symbols s satisfy the condition of $|s|^2 = 1,\ \forall s \in \mathcal{M}$, and $\mathcal{M}$ denotes the set of M complex-valued constellation points. In the next section, we will then demonstrate that the method derived is equally applicable to arbitrary signal constellations, particularly for high-throughput multi-level modulation schemes, such as M-QAM.

Let us recall that our channel model described in detail in Section 10.3 is given by

$$\mathbf{y} = \mathbf{H}\mathbf{s} + \mathbf{w}, \tag{10.7}$$

where we omit the OFDM subcarrier and symbol indices k and n, respectively. As outlined in [90] , the ML SDM detector provides an m_t-antenna-based estimated signal vector candidate $\hat{\mathbf{s}}$, which maximises the objective function defined as the conditional *a posteriori* probability function $\mathtt{P}\{\check{\mathbf{s}}|\mathbf{y},\mathbf{H}\}$ over the set $\mathcal{M}^{m_\mathrm{t}}$ of legitimate solutions. More explicitly, we have

$$\hat{\mathbf{s}} = \arg \max_{\check{\mathbf{s}} \in \mathcal{M}^{m_\mathrm{t}}} \mathtt{P}\{\check{\mathbf{s}}|\mathbf{y},\mathbf{H}\}, \tag{10.8}$$

where $\mathcal{M}^{m_\mathrm{t}}$ is the set of *all possible* m_t-dimensional candidate symbol vectors of the m_t-antenna-based transmitted signal vector $\mathbf{s}$. More specifically, we have

$$\mathcal{M}^{m_\mathrm{t}} = \left\{\check{\mathbf{s}} = (\check{s}_1, \cdots, \check{s}_{m_\mathrm{t}})^\mathtt{T};\ \check{s}_i \in \mathcal{M}\right\}. \tag{10.9}$$

Furthermore, it was shown in [90] that we have

$$\mathtt{P}\{\check{\mathbf{s}}|\mathbf{y},\mathbf{H}\} = A \exp\left[-\frac{1}{\sigma_w^2}\|\mathbf{y} - \mathbf{H}\check{\mathbf{s}}\|^2\right], \tag{10.10}$$

where A is a constant, which is independent of any of the values $\{\check{s}_i\}_{i=1,\cdots,m_\mathrm{t}}$. Thus, it may be shown [90] that the probability maximisation problem of Equation (10.8) is equivalent to the corresponding Euclidean distance minimisation problem. Specifically, we have

$$\hat{\mathbf{s}} = \arg \min_{\check{\mathbf{s}} \in \mathcal{M}^{m_\mathrm{t}}} \|\mathbf{y} - \mathbf{H}\check{\mathbf{s}}\|^2, \tag{10.11}$$

where the probability-based objective function of Equation (10.8) is substituted by the objective function determined by the Euclidean distance between the received signal vector $\mathbf{y}$ and the corresponding product of the channel matrix $\mathbf{H}$ with the *a priori* candidate of the transmitted signal vector $\check{\mathbf{s}} \in \mathcal{M}^{m_\mathrm{t}}$.

Consequently, our detection method relies on the observation, which may be summarised in the following lemma.

Lemma 1 *The ML solution of Equation* (10.8) *of a noisy linear problem described by Equation* (10.7) *is given by*

$$\hat{\mathbf{s}} = \arg \min_{\check{\mathbf{s}} \in \mathcal{M}^{m_\mathrm{t}}} \left\{\|\mathbf{U}(\check{\mathbf{s}} - \hat{\mathbf{x}})\|^2\right\}, \tag{10.12}$$

where $\mathbf{U}$ *is an upper-triangular matrix having positive real-valued elements on the main diagonal and satisfying*

$$\mathbf{U}^\mathtt{H}\mathbf{U} = (\mathbf{H}^\mathtt{H}\mathbf{H} + \sigma_w^2\mathbf{I}), \tag{10.13}$$

while

$$\hat{\mathbf{x}} = (\mathbf{H}^\mathtt{H}\mathbf{H} + \sigma_w^2\mathbf{I})^{-1}\mathbf{H}^\mathtt{H}\mathbf{y} \tag{10.14}$$

is the unconstrained MMSE estimate of the transmitted signal vector $\mathbf{s}$*, which was derived in [90] .*

Note 1: Observe that Lemma 1 imposes no constraints on the dimensions, or rank of the matrix $\mathbf{H}$ of the linear system described by Equation (10.7). This property is particularly important, since it enables us to apply our proposed detection technique to the scenario of *over-loaded* systems, where the number of transmit antenna elements exceeds that of the receive antenna elements.

Note 2: As substantiated by Equation (10.11), it is sufficient to prove that the following minimisation problems are equivalent

$$\hat{\mathbf{s}} = \arg \min_{\check{\mathbf{s}} \in \mathcal{M}^{m_{\mathrm{t}}}} \|\mathbf{y} - \mathbf{H}\check{\mathbf{s}}\|^2 \tag{10.15}$$

$$\Leftrightarrow \quad \hat{\mathbf{s}} = \arg \min_{\check{\mathbf{s}} \in \mathcal{M}^{m_{\mathrm{t}}}} \|\mathbf{U}(\check{\mathbf{s}} - \hat{\mathbf{x}})\|^2. \tag{10.16}$$

Proof of Lemma 1: It is evident that in contrast to the matrix $\mathbf{H}^{\mathrm{H}}\mathbf{H}$, the matrix $(\mathbf{H}^{\mathrm{H}}\mathbf{H} + \sigma_w^2\mathbf{I})$ of Equation (10.12) is always Hermitian and positively definite, regardless of the rank of the channel matrix $\mathbf{H}$ associated with the particular MIMO channel realisation encountered. Consequently, it may be represented as the product of an upper-triangular matrix $\mathbf{U}$ and its Hermitian adjoint matrix $\mathbf{U}^{\mathrm{H}}$ using for example the Cholesky factorisation method [372].

Let $\mathbf{U}$ be the matrix generated by the Cholesky decomposition of the Hermitian positive definite matrix $(\mathbf{H}^{\mathrm{H}}\mathbf{H} + \sigma_w^2\mathbf{I})$ of Equation (10.13). More specifically, we have

$$\mathbf{U}^{\mathrm{H}}\mathbf{U} = (\mathbf{H}^{\mathrm{H}}\mathbf{H} + \sigma_w^2\mathbf{I}), \tag{10.17}$$

where $\mathbf{U}$ is an upper-triangular matrix having positive real-valued elements on its main diagonal.

Upon expanding the objective function of Equation (10.12) and subsequently invoking Equation (10.13) we obtain

$$\begin{aligned}
J(\check{\mathbf{s}}) &= \|\mathbf{U}(\check{\mathbf{s}} - \hat{\mathbf{x}})\|^2 \\
&= (\check{\mathbf{s}} - \hat{\mathbf{x}})^{\mathrm{H}}\mathbf{U}^{\mathrm{H}}\mathbf{U}(\check{\mathbf{s}} - \hat{\mathbf{x}}) \\
&= (\check{\mathbf{s}} - \hat{\mathbf{x}})^{\mathrm{H}}(\mathbf{H}^{\mathrm{H}}\mathbf{H} + \sigma_w^2\mathbf{I})(\check{\mathbf{s}} - \hat{\mathbf{x}}) \\
&= \check{\mathbf{s}}^{\mathrm{H}}(\mathbf{H}^{\mathrm{H}}\mathbf{H} + \sigma_w^2\mathbf{I})\check{\mathbf{s}} - \hat{\mathbf{x}}^{\mathrm{H}}(\mathbf{H}^{\mathrm{H}}\mathbf{H} + \sigma_w^2\mathbf{I})\check{\mathbf{s}} \\
&\quad - \check{\mathbf{s}}^{\mathrm{H}}(\mathbf{H}^{\mathrm{H}}\mathbf{H} + \sigma_w^2\mathbf{I})\hat{\mathbf{x}} + \hat{\mathbf{x}}^{\mathrm{H}}(\mathbf{H}^{\mathrm{H}}\mathbf{H} + \sigma_w^2\mathbf{I})\hat{\mathbf{x}}.
\end{aligned} \tag{10.18}$$

Furthermore, substituting Equation (10.14) into (10.18) yields

$$\begin{aligned} J(\check{\mathbf{s}}) &= \check{\mathbf{s}}^{\mathrm{H}}\mathbf{H}^{\mathrm{H}}\mathbf{H}\check{\mathbf{s}} - \mathbf{y}^{\mathrm{H}}\mathbf{H}\check{\mathbf{s}} - \check{\mathbf{s}}^{\mathrm{H}}\mathbf{H}^{\mathrm{H}}\mathbf{y} \\ &+ \sigma_w^2\check{\mathbf{s}}^{\mathrm{H}}\check{\mathbf{s}} + \mathbf{y}^{\mathrm{H}}\mathbf{H}(\mathbf{H}^{\mathrm{H}}\mathbf{H} + \sigma_w^2\mathbf{I})^{-1}\mathbf{H}^{\mathrm{H}}\mathbf{y} \\ &= \|\mathbf{y} - \mathbf{H}\check{\mathbf{s}}\|^2 + \underbrace{\sigma_w^2\check{\mathbf{s}}^{\mathrm{H}}\check{\mathbf{s}} + \mathbf{y}^{\mathrm{H}}(\mathbf{H}(\mathbf{H}^{\mathrm{H}}\mathbf{H} + \sigma_w^2\mathbf{I})^{-1}\mathbf{H}^{\mathrm{H}} - \mathbf{I})\mathbf{y}}_{\psi}. \end{aligned} \tag{10.19}$$

Observe that in the case of a system employing a constant-envelope modulation scheme, such as M-PSK, where we have $\check{\mathbf{s}}^{\mathrm{H}}\check{\mathbf{s}} = 1$, ψ constitutes a real-valued scalar and its value does not depend on the argument $\check{\mathbf{s}}$ of the minimisation problem formulated in Equation (10.12). Consequently, the minimisation of the objective function $J(sv\check{e}cs)$ of Equation (10.19) can be reduced to the minimisation of the term $\|\mathbf{y} - \mathbf{H}\mathbf{x})\|^2$, which renders it equivalent to the minimisation problem of Equation (10.15). This completes the proof.

Using Lemma 1, in particular the fact that the matrix $\mathbf{U}$ is an upper-triangular matrix, the objective function $J(\check{\mathbf{s}})$ of Equation (10.19) may be reformulated as follows

$$\begin{aligned} J(\check{\mathbf{s}}) &= \|\mathbf{U}(\check{\mathbf{s}} - \hat{\mathbf{x}})\|^2 \\ &= (\check{\mathbf{s}} - \hat{\mathbf{x}})^{\mathrm{H}}\mathbf{U}^{\mathrm{H}}\mathbf{U}(\check{\mathbf{s}} - \hat{\mathbf{x}}) \\ &= \sum_{i=1}^{m_{\mathrm{t}}}\Big|\sum_{j=i}^{m_{\mathrm{t}}} u_{ij}(\check{s}_j - \hat{x}_j)\Big|^2 = \sum_{i=1}^{m_{\mathrm{t}}}\phi_i(\check{\mathbf{s}}_i), \end{aligned} \tag{10.20}$$

where $J(\check{\mathbf{s}})$ and $\phi_i(\check{\mathbf{s}}_i)$ are positive real-valued cost and sub-cost functions, respectively. Elaborating a little further we have

$$\begin{aligned} \phi_i(\check{\mathbf{s}}_i) &= \Big|\sum_{j=i}^{m_{\mathrm{t}}} u_{ij}(\check{s}_j - \hat{x}_j)\Big|^2 \\ &= \Big|u_{ii}(\check{s}_i - \hat{x}_i) + \underbrace{\sum_{j=i+1}^{m_{\mathrm{t}}} u_{ij}(\check{s}_j - \hat{x}_j)}_{a_i}\Big|^2. \end{aligned} \tag{10.21}$$

Note that the term a_i is a complex-valued scalar, which is independent of the specific symbol value $\check{s}_i$ of the ith element of the *a priori* candidate signal vector $\check{\mathbf{s}}$.

Furthermore, let $J_i(\check{\mathbf{s}}_i)$ be a Cumulative Sub-Cost (CSC) function recursively defined as

$$J_{m_{\mathrm{t}}}(\check{s}_{m_{\mathrm{t}}}) = \phi_{m_{\mathrm{t}}}(\check{s}_{m_{\mathrm{t}}}) = |u_{m_{\mathrm{t}}m_{\mathrm{t}}}(\check{s}_{m_{\mathrm{t}}} - \hat{x}_{m_{\mathrm{t}}})|^2 \tag{10.22a}$$

$$J_i(\check{\mathbf{s}}_i) = J_{i+1}(\check{\mathbf{s}}_{i+1}) + \phi_i(\check{\mathbf{s}}_i), \quad i = 1, \cdots, m_{\mathrm{t}}{-}1, \tag{10.22b}$$

where we define the candidate subvector as $\check{\mathbf{s}}_i = [\check{s}_i, \cdots, \check{s}_{m_{\mathrm{t}}}]$. Clearly, $J_i(\check{\mathbf{s}}_i)$ exhibits the following properties

$$J(\check{\mathbf{s}}) = J_1(\check{\mathbf{s}}_1) > J_2(\check{\mathbf{s}}_2) > \cdots > J_{m_{\mathrm{t}}}(\check{s}_{m_{\mathrm{t}}}) > 0 \tag{10.23a}$$

$$J_i(\check{\mathbf{s}}_i) = J_i(\{\check{s}_j\},\ j = i, \cdots, m_{\mathrm{t}}) \tag{10.23b}$$

for all possible realisations of $\hat{\mathbf{x}} \in \mathbb{C}^{m_t}$ and $\check{\mathbf{s}} \in \mathcal{M}^{m_t}$, where the space $\mathbb{C}^{m_t}$ contains all possible unconstrained MMSE estimates $\hat{\mathbf{x}}$ of the transmitted signal vector $\mathbf{s}$.

Equations (10.23a) and (10.23b) enable us to employ a highly efficient reduced search algorithm, which decreases the number of objective function evaluations of the minimisation problem outlined in Equation (10.12) to a small fraction of the set $\mathcal{M}^{m_t}$. This reduced-complexity search algorithm is outlined in the next section.

10.4.2 Search Strategy

Example 1 (OHRSA-ML 3x3 BPSK)

Consider a BPSK system having $n_r = m_t = 3$ transmit and receive antennas, which is described by Equation (10.7). The transmitted signal $\mathbf{s}$, the received signal $\mathbf{y}$ as well as the channel matrix $\mathbf{H}$ of Equation (10.7) are exemplified by the following values

$$\mathbf{s} = \begin{bmatrix} 1 \\ -1 \\ 1 \end{bmatrix}, \quad \mathbf{y} = \begin{bmatrix} 0.2 \\ 0.8 \\ -1.2 \end{bmatrix}, \quad \mathbf{H} = \begin{bmatrix} 0.5 & 0.4 & -0.2 \\ 0.4 & -0.3 & 0.2 \\ 0.9 & 1.8 & -0.1 \end{bmatrix}. \tag{10.24}$$

Our task is to obtain the ML estimate of the transmitted signal vector $\mathbf{s}$. Firstly, we evaluate the triangular matrix $\mathbf{U}$ of Equation (10.13) as well as the unconstrained MMSE estimate $\hat{\mathbf{x}}$ of Equation (10.14). The resultant quantities are given by

$$\mathbf{U} = \begin{bmatrix} 1.15 & 1.48 & -0.10 \\ 0 & 1.18 & -0.15 \\ 0 & 0 & 0.40 \end{bmatrix}, \quad \hat{\mathbf{x}} = \begin{bmatrix} 0.85 \\ -1.05 \\ -0.01 \end{bmatrix}. \tag{10.25}$$

Observe that the direct slicing of the MMSE estimate $\hat{\mathbf{x}}$ will result in an erroneously decided signal $\hat{\mathbf{s}} = \begin{bmatrix} 1 & -1 & -1 \end{bmatrix}^T$. Subsequently, following the philosophy outlined in Section 10.4.1, for each legitimate candidate $\check{\mathbf{s}} \in \mathcal{M}^{m_t}$ of the m_t-antenna-based composite transmitted signal vector $\mathbf{s}$ we calculate the corresponding value of the cost function $J(\check{\mathbf{s}})$ of Equation (10.20) using the recursive method described by Equation (10.22). The search process performed is illustrated in Figure 10.6(a). Each evaluation step, namely each evaluation of the CSC function $J_i(\check{\mathbf{s}}_i)$ of Equation (10.22b) is indicated by an elliptic node in Figure 10.6(a). The label inside each node indicates the order of evaluation as well as the corresponding value $J_i(\check{\mathbf{s}}_i)$ of the CSC function inside the brackets. Furthermore, the branches corresponding to the two legitimate values of $\check{s}_i = -1$ and 1 are indicated using the dashed and solid edges and nodes, respectively.

More specifically, commencing from the top of Figure 10.6(a), at recursive step $i = 3$ we calculate the CSC function of Equation (10.22a) associated with all legitimate values of the last element of the signal vector $\mathbf{s}$, where we have

$$J_3(\check{s}_3 = -1) = |u_{33}(\check{s}_3 - \hat{x}_3)|^2 = (0.40(-1 - (-0.01)))^2 = 0.15 \tag{10.26}$$

and

$$J_3(\check{s}_3 = 1) = (0.40(1 - (-0.01)))^2 = 0.16. \tag{10.27}$$

The corresponding values of $J_3(\check{s}_3 = -1) = 0.15$ and $J_3(\check{s}_3 = 1) = 0.16$ are indicated by the nodes 1 and 8 in Figure 10.6(a). Observe that the *recursive* nature of the search process considered suggests that the latter value of $J_3(\check{s}_3 = 1)$ is not considered until the entire search branch originating from the more promising node 1 associated with the lower CSC value of 0.15 is completed. Consequently, the value $J_3(\check{s}_3 = 1)$ is the 8th value of the CSC function to be evaluated, which is indicated by the corresponding node's index 8.

Furthermore, at recursive step $i = 2$ for each hypothesised value $\check{s}_3$ we calculate both the quantity a_2 of Equation (10.21) as well as the sub-cost function of Equation (10.21) and the corresponding CSC function of Equation (10.22b) associated with all legitimate values of the last-but-one element of the signal vector $\mathbf{s}$. Explicitly, for $\check{s}_3 = -1$ we have

$$a_2 = u_{23}(\check{s}_3 - \hat{x}_3) = -0.15(-1 - (-0.01)) = 0.15 \tag{10.28}$$

and

$$\begin{aligned}
&J_2(\check{s}_2 = -1, \check{s}_3 = -1) = J_3(\check{s}_3 = -1) + \phi_2(\check{s}_2 = -1, \check{s}_3 = -1)\\
&\quad = J_3(\check{s}_3 = -1) + |u_{22}(\check{s}_2 - \hat{x}_2)) + a_2|^2\\
&\quad = 0.15 + (1.18(-1 - (-1.05)) + 0.15) = 0.20\\
&J_2(\check{s}_2 = 1, \check{s}_3 = -1) = J_3(\check{s}_3 = -1) + \phi_2(\check{s}_2 = 1, \check{s}_3 = -1)\\
&\quad = 0.15 + (1.18(1 - (-1.05)) + 0.15) = 6.79.
\end{aligned} \tag{10.29}$$

The corresponding values of $J_2(\check{\mathbf{s}}_2 = [-1, -1]) = 0.20$ and $J_2(\check{\mathbf{s}}_2 = [1, -1]) = 6.79$ are indicated by the nodes 2 and 5 in Figure 10.6(a).

Finally, at recursive index $i = 1$ we calculate the quantity $a_1(\check{\mathbf{s}}_2)$ for each hypothesised subvector $\check{\mathbf{s}}_2$ and the sub-cost function $\phi_1(\check{\mathbf{s}}_1)$ of Equation (10.21) as well as the corresponding *total* cost function $J(\check{s}_1 = -1, \check{\mathbf{s}}_2)$ and $J(\check{s}_1 = 1, \check{\mathbf{s}}_2)$ of Equation (10.20) associated with all legitimate values of the first element of the signal vector $\mathbf{s}$. Specifically, for the left-most search branch of Figure 10.6(a) corresponding to the *a priori* candidate $\check{\mathbf{s}}_2 = [-1, -1]$ we have

$$\begin{aligned}
a_1 &= u_{12}(\check{s}_2 - \hat{x}_2) + u_{13}(\check{s}_3 - \hat{x}_3)\\
&= 1.48(-1 - -1.05) + -0.10(-1 - -0.01) = 0.17
\end{aligned} \tag{10.30}$$

and

$$\begin{aligned}
&J_1(\check{s}_1 = -1, \check{s}_2 = -1, \check{s}_3 = -1)\\
&\quad = J_2(\check{s}_2 = -1, \check{s}_3 = -1) + \phi_1(\check{s}_1 = -1, \check{s}_2 = -1, \check{s}_3 = -1)\\
&\quad = J_2(\check{s}_2 = -1, \check{s}_3 = -1) + |u_{11}(\check{s}_1 - \hat{x}_1)) + a_1|^2\\
&\quad = 0.20 + (1.15(-1 - 0.85) + 0.17) = 4.03,\\
&J_1(\check{s}_1 = 1, \check{s}_2 = -1, \check{s}_3 = 1)\\
&\quad = J_2(\check{s}_2 = -1, \check{s}_3 = -1) + \phi_2(\check{s}_1 = 1, \check{s}_2 = -1, \check{s}_3 = -1)\\
&\quad = 0.20 + (1.15(1 - 0.85) + 0.17) = 0.31.
\end{aligned} \tag{10.31}$$

Upon completing the entire search process outlined above we arrive at eight different values of the total cost function $J(\check{\mathbf{s}})$ associated with the eight legitimate 3-bit solutions of the detection problem considered. The eight different candidate solutions are indicated by the eight bottom-most elliptic nodes in Figure 10.6(a). Clearly, the ML solution is constituted by the search branch terminating at node 11 of Figure 10.6(a) and having the minimum value $J(\check{\mathbf{s}}) = 0.19$ of the total cost function.

Observe that the difference between the values of $J_3(\check{s}_3 = -1)$ and $J_3(\check{s}_3 = 1)$ associated with nodes 1 and 8 in Figure 10.6(a) is quite small and thus the ML solution along either of the search branches commencing at nodes 1 and 8 in Figure 10.6(a) may not be recognised with a high degree of confidence. On the other hand, the difference between the values of the CSC function along two complementary search branches commencing at nodes 1 and 8 becomes substantially more evident, if we apply the *best-first* detection strategy suggested in [373]. More specifically, we sort the columns of the channel matrix $\mathbf{H}$ in the increasing order of their Euclidean or square norm. The resultant reordered channel matrix $\mathbf{H}'$ as well as the corresponding triangular matrix $\mathbf{U}$ and the unconstrained MMSE estimate $\hat{\mathbf{x}}'$ may be expressed as

$$\mathbf{H}' = \begin{bmatrix} -0.2 & 0.5 & 0.4 \\ 0.2 & 0.4 & -0.3 \\ -0.1 & 0.9 & 1.8 \end{bmatrix}, \; \mathbf{U}' = \begin{bmatrix} 0.44 & -0.25 & -0.73 \\ 0 & 1.12 & 1.35 \\ 0 & 0 & 1.11 \end{bmatrix}, \; \hat{\mathbf{x}}' = \begin{bmatrix} -0.01 \\ 0.85 \\ -1.05 \end{bmatrix}. \tag{10.32}$$

The search tree generated by applying the aforementioned search process and using the modified quantities $\mathbf{H}', \mathbf{U}'$ and $\hat{\mathbf{x}}'$ is depicted in Figure 10.6(b). Note the substantial difference between the values of the CSC function $J_3(\check{s}_3 = -1)$ and $J_3(\check{s}_3 = 1)$ associated with the nodes 1 and 8. Moreover, by comparing the value of the CSC function $J_3(\check{s}_3)$ of node 8 to that of the total cost function $J(\check{\mathbf{s}})$ of node 7 we can conclude that the search along the branch commencing at node 8 is in fact redundant.

In order to further optimise our search process, at recursive steps of $i = 3$ and 2 we first calculate the sub-cost functions $\phi_3(\check{s}_3 = \{-1, 1\})$ and $\phi_2(\check{s}_3, \check{s}_2 = \{-1, 1\})$ of Equation (10.21). We then compare the values obtained and continue with the processing of the specific search branch corresponding to the smaller value of the sub-cost function $\phi_i(\check{\mathbf{s}}_i)$ first. The resultant search tree is depicted in Figure 10.6(c). Observe that in Figure 10.6(c) the minimum value of the total cost function $J(\check{\mathbf{s}}) = 0.19$ is obtained faster, namely in three evaluation steps in comparison to seven steps required by the search tree of Figure 10.6(b).

Finally, we discard all the search branches commencing at nodes having an associated value of the CSC function, which is in excess of the minimum total cost function value obtained. Specifically, we discontinue the search branches commencing at nodes 5 and 8 having the CSC function values in excess of 0.19, namely 4.03 and 5.15, respectively. The resultant reduced search tree is depicted in Figure 10.6(d). Note that the ML solution is obtained in six evaluation steps in comparison to the 14 steps required in the case of the exhaustive search of Figure 10.6(a). In conclusion, upon performing the appropirte reordering of the obtained ML estimate, we arrive at the correct value of the transmitted signal vector $\hat{\mathbf{s}} = \begin{bmatrix} 1 & -1 & 1 \end{bmatrix}^{\mathrm{T}}$.

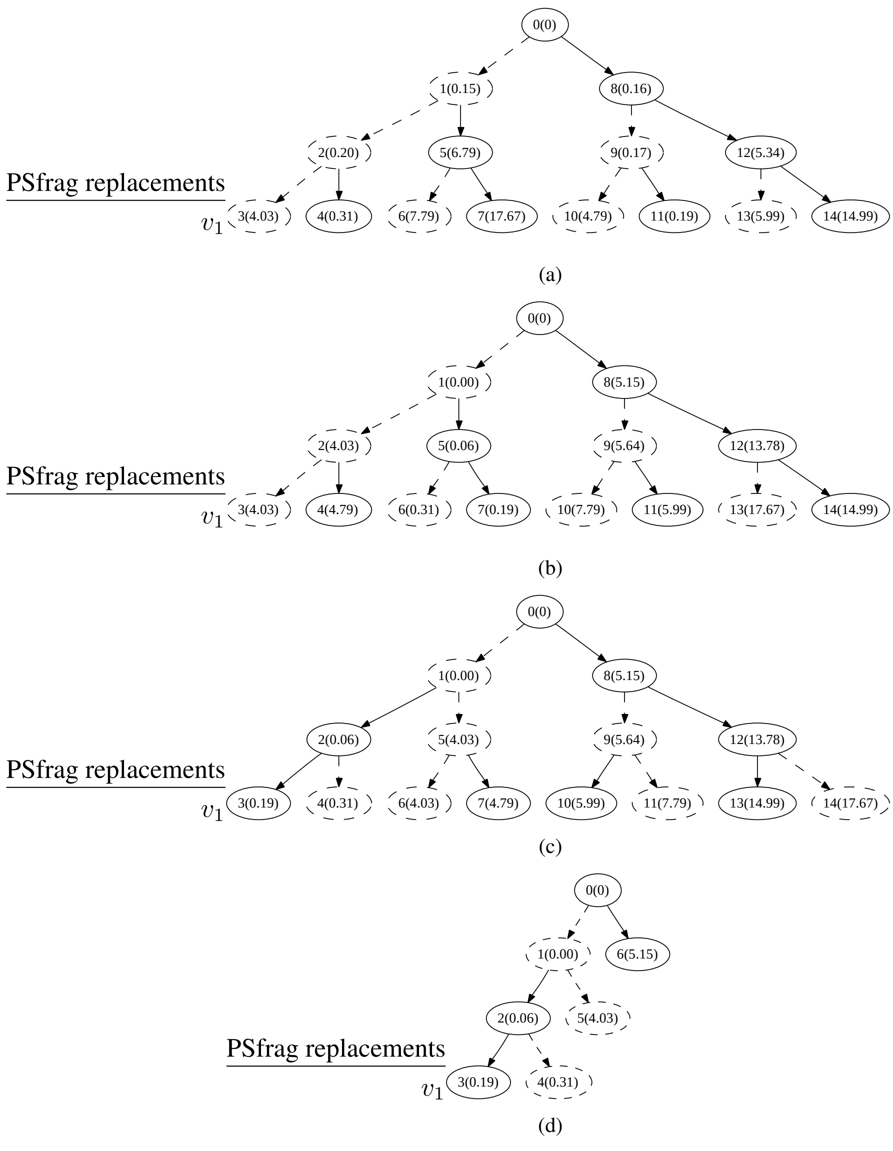

Figure 10.6: Examples of a search tree formed by the OHRSA-ML SDM detector in the scenario of a system employing BPSK modulation, $m_{\mathrm{t}} = n_{\mathrm{r}} = 3$ transmit and receive antennas and encountering average SNRs of 10dB. The labels indicate the order of evaluation, as well as the corresponding value $J_i(\check{\mathbf{s}}_i)$ of the CSC function of Equation (10.22), as seen in the brackets. The dashed and solid arrows indicate the values of $\check{s}_i = -1$ and 1, respectively.

10.4.2.1 Generalisation of the OHRSA-ML SDM Detector

Let us now generalise and substantiate further the detection paradigm derived in Example 1. Firstly, we commence the recursive search process with the evaluation of the CSC function value $J_{m_t}(\check{s}_{m_t})$ of Equation (10.22a). Secondly, at each recursive step i of the search algorithm proposed we stipulate a series of hypotheses concerning the value of the M-ary transmitted symbol s_i associated with the ith transmit antenna element and subsequently calculate the conditioned sub-cost function $J_i(\check{\mathbf{s}}_i)$ of Equation (10.22b), where $\check{\mathbf{s}}_i = (\check{s}_i, \cdots, \check{s}_{m_t})^{\mathrm{T}}$ denotes the subvector of the m_t-antenna-based candidate vector $\check{\mathbf{s}}$ comprising only the indices higher than or equal to i. Furthermore, for each tentatively assumed value of $\check{s}_i$ we execute a successive recursive search step $i-1$, which is conditioned on the hypotheses made in all preceding recursive steps $j = i, \cdots, m_t$. As substantiated by Equations (10.21) and (10.22b), the value of the CSC function $J_i(\check{\mathbf{s}}_i)$ is dependent only on the values of the elements $\{\check{s}_j\}_{j=i,\cdots,m_t}$ of the *a priori* candidate signal vector $\check{\mathbf{s}}$, which are hypothesised from from step $j = m_t$ up to the present step i of our recursive process. At each arrival at the step $i = 1$ of the recursive process, a complete candidate vector $\check{\mathbf{s}}$ is hypothesised and the corresponding value of the cost function $J(\check{\mathbf{s}})$ formulated in Equation (10.20) is evaluated.

Observe that the recursive hierarchical search procedure described above may be employed to perform an exhaustive search through all possible values of the transmitted signal vector $\check{\mathbf{s}}$, and the resultant search process is guaranteed to arrive at the ML solution $\check{\mathbf{s}}_{\mathrm{ML}}$, which minimises the value of the cost function $J(\check{\mathbf{s}})$ of Equation (10.20). Fortunately however, as opposed to other ML search schemes, the search process described above can be readily optimised, resulting in a dramatic reduction of the associated computational complexity. Specifically, the potential optimisation complexity gain originates from the fact that most of the hierarchical search branches can be discarded at an early stage of the recursive search process. The corresponding optimisation rules proposed may be outlined as follows.

Rule 1. We reorder the system model of Equation (10.7) as suggested in [373]. Specifically, we apply the *best-first* detection strategy outlined in [90, pp.754-756] , which implies that the transmitted signal vector components are detected in the decreasing order of the associated channel quality. As it was advocated in [90, pp.754-756] , the quality of the channel associated with the ith element of the transmitted signal vector $\mathbf{s}$ is determined by the norm of the ith column of the channel matrix $\mathbf{H}$. Consequently, for the sake of applying the *best-first* detection strategy, the columns of the channel matrix $\mathbf{H}$ are sorted in the increasing order of their norm. Thus, the resultant, column-reordered channel matrix $\mathbf{H}$ complies with the following criterion

$$\|(\mathbf{H})_1\|^2 \leq \|(\mathbf{H})_2\|^2 \leq \cdots \leq \|(\mathbf{H})_{m_t}\|^2, \tag{10.33}$$

where $(\mathbf{H})_i$ denotes the ith column of the channel matrix $\mathbf{H}$. Note that the elements of the transmitted signal vector $\mathbf{s}$ are reordered correspondingly, but their original order has to be reinstated in the final stage of the detection process.

Rule 2. At each recursive detection step $i = m_t, \cdot, 1$, the potential candidate values $\{c_m\}_{m=1,\cdots,M} \in \mathcal{M}$ of the transmitted signal component s_i are considered in the increasing order of the corresponding value of the sub-cost function $\phi_i(\check{\mathbf{s}}_i) = \phi_i(c_m, \check{\mathbf{s}}_{i+1})$ of Equation

(10.21), where we have

$$\phi_i(c_1, \check{\mathbf{s}}_{i+1}) < \cdots < \phi_i(c_m, \check{\mathbf{s}}_{i+1}) < \cdots \phi_i(c_M, \check{\mathbf{s}}_{i+1}),$$

and according to Equation (10.21)

$$\begin{aligned}\phi_i(c_m, \check{\mathbf{s}}_{i+1}) &= |u_{ii}(c_m - \hat{x}_i) + a_i|^2 \\ &= u_{ii}|c_m - \hat{x}_i + \frac{a_i}{u_{ii}^2}|^2. \end{aligned} \tag{10.34}$$

Consequently, the more likely candidates c_m of the ith element of the transmitted signal vector s are examined first. Observe that the sorting criterion of Equation (10.34) may also be interpreted as a biased Euclidean distance of the candidate constellation point c_m from the unconstrained MMSE estimate $\hat{x}_i$ of the transmitted signal component s_i.

Rule 3. We define a *cut-off* value of the cost fuction $J_{\min} = \min\{J(\check{\mathbf{s}})\}$ as the minimum value of the total cost function obtained up to the present point of the search process. Consequently, at each arrival at step $i = 1$ of the recursive search process, the *cut-off* value of the cost function is updated as follows

$$J_{\min} = \min\{J_{\min}, J(\check{\mathbf{s}})\} \tag{10.35}$$

Rule 4. Finally, at each recursive detection step i, only the high probability search branches corresponding to the highly likely symbol candidates c_m resulting in a value of the CSC function obeying $J_i(c_m) < J_{\min}$ are pursued. Furthermore, as follows from the sorting criterion of the optimisation Rule 2, as soon as the inequality $J_i(c_m) > J_{\min}$ is encountered, the search loop at the ith detection step is discontinued.

An example of the search tree generated by the algorithm invoking the Rules 1-4 described above is depicted in Figure 10.7. The search trees shown correspond to the scenario of using QPSK modulation and employing $m_{\mathrm{t}} = n_{\mathrm{r}} = 8$ antenna elements at both the transmitter and the receiver. Encountering the average SNRs of (a) 10 and (b) 20 dB was considered. Each step of the search procedure is depicted as an ellipsoidal-shaped node. The label associated with each node indicates the order of visitation, as well as the corresponding value of the CSC function $J_i(\check{\mathbf{s}}_i)$ formulated in Equation (10.22), as seen in the brackets. As suggested by the fact that QPSK modulation is considered, at each recursive step i, *four* legitimate search branches are possible. However, as can be seen in Figure 10.7(a), only a small fraction of the potential search branches are actually pursued. Observe that the rate of convergence of the algorithm proposed is particularly rapid at high values of SNR. In the case of encountering low SNR values, the convergence rate decreases. Nevertheless, the associated computational complexity is dramatically lower than that associated with an exhaustive ML search.

The pseudo-code summarising the recursive implementation of the OHRSA-based ML SDM detector proposed is depicted in Algorithm 3.

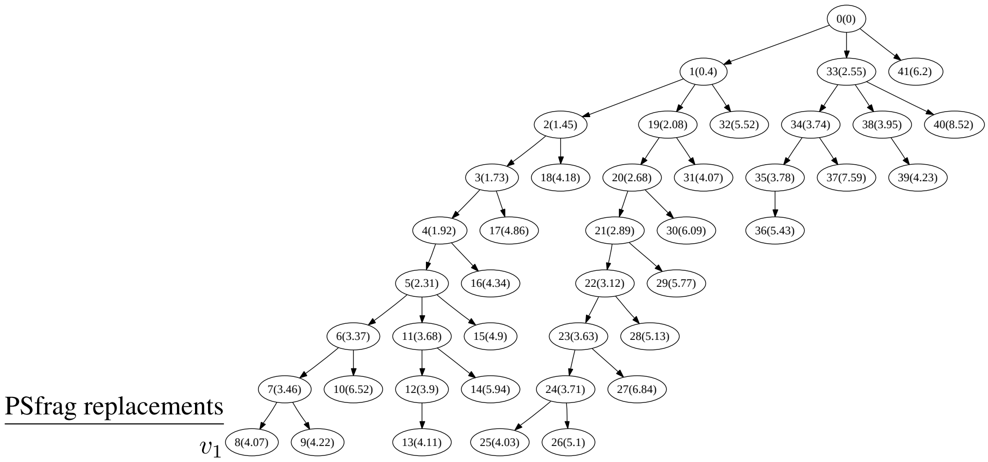

(a)

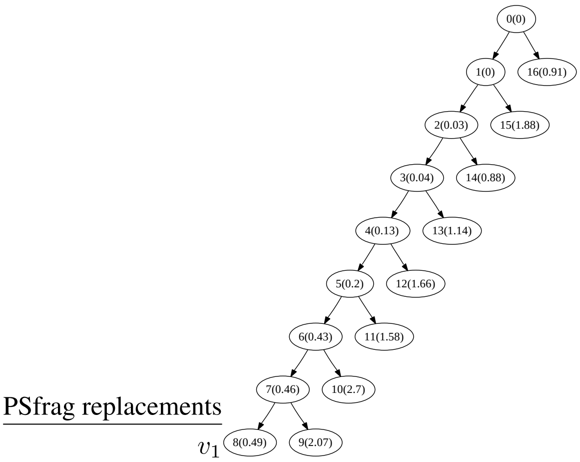

(b)

Figure 10.7: Examples of a search tree formed by the OHRSA-ML SDM detector in the scenario of a system employing QPSK modulation, $m_{\mathrm{t}} = n_{\mathrm{r}} = 8$ transmit and receive antennas and encountering average SNRs of (a) 10dB and (b) 20dB. The labels indicate the order of visitation, as well as the corresponding value $J_i(\check{\mathbf{s}}_i)$ of the CSC function of Equation (10.22), as seen in the brackets. The ML solution is attained in (a) 41 and (b) 16 evaluation steps in comparison to the $4^8 = 65536$ evaluation steps required in the case of the exhaustive ML search.

10.4.3 Bitwise OHRSA ML SDM Detection

Example 2 (OHRSA-ML QPSK 2x2)

Let us now consider a QPSK system having $n_{\mathrm{r}} = m_{\mathrm{t}} = 3$ transmit and receive antennas, which is described by Equation (10.7). The transmitted signal $\mathbf{s}$, the received signal $\mathbf{y}$ as

Algorithm 3 OH-RSA-aided ML SDM Detector

$$\texttt{Sort}\{\mathbf{H}\},\ \texttt{such that}\ \|(\mathbf{H})_1\|^2 \leq \cdots \leq \|(\mathbf{H})_{m_t}\|^2 \tag{10.36a}$$
$$\mathbf{G} = (\mathbf{H}^{\mathrm{H}}\mathbf{H} + \sigma_w^2\mathbf{I}) \tag{10.36b}$$
$$\mathbf{U} = \texttt{CholeskyDecomposition}(\mathbf{G}) \tag{10.36c}$$
$$\hat{\mathbf{x}} = \mathbf{G}^{-1}\mathbf{H}^{\mathrm{H}}\mathbf{y} \tag{10.36d}$$
$$\texttt{Calculate}\quad J_{m_t} \tag{10.36e}$$
$$\texttt{Unsort}\{\hat{\mathbf{s}}\} \tag{10.36f}$$

$$\texttt{function}\quad \texttt{Calculate}\quad J_i(\check{\mathbf{s}}_i) \tag{10.36g}$$
$$a_i = \sum_{j=i+1}^{m_t} u_{ij}(\check{s}_j - \hat{x}_j) \tag{10.36h}$$
$$\texttt{Sort}\{c_m\},\ \texttt{such that}\ \phi_i(c_1) < \cdots < \phi_i(c_M), \tag{10.36i}$$
$$\texttt{where}\quad \phi_i(c_m) = |u_{ii}(c_m - \hat{x}_i) + a_i|^2 \tag{10.36j}$$
$$\texttt{for}\quad m = 1, 2, \ldots, M \quad \texttt{do}$$
$$\check{s}_i = c_m \tag{10.36k}$$
$$J_i(\check{\mathbf{s}}_i) = J_{i+1}(\check{\mathbf{s}}_{i+1}) + \phi_i(\check{s}_i) \tag{10.36l}$$
$$\texttt{if}\quad J_i(\check{\mathbf{s}}_i) < J_{\min} \quad \texttt{then} \tag{10.36m}$$
$$\texttt{if}\quad i > 0 \quad \texttt{then}\quad \texttt{Calculate}\quad J_{i-1} \tag{10.36n}$$
$$\texttt{else}$$
$$J_{\min} = J(\check{\mathbf{s}}) \tag{10.36o}$$
$$\hat{\mathbf{s}} = \check{\mathbf{s}} \tag{10.36p}$$
$$\texttt{end}\quad \texttt{if}$$
$$\texttt{end}\quad \texttt{if}$$
$$\texttt{end}\quad \texttt{for}$$
$$\texttt{end}\quad \texttt{function}$$

well as the *best-first* reordered channel matrix $\mathbf{H}$ of Equation (10.7) are exemplified by the following values

$$\mathbf{s} = \begin{bmatrix} 1 - 1\jmath \\ -1 - 1\jmath \end{bmatrix}, \quad \mathbf{y} = \begin{bmatrix} 0.2 + 1.1\jmath \\ 1.4 + 1.7\jmath \end{bmatrix},$$
$$\mathbf{H} = \begin{bmatrix} 0.1 - 0.2\jmath & -0.7 - 0.6\jmath \\ 0.3 + 0.4\jmath & -1.3 - 0.5\jmath \end{bmatrix}. \tag{10.37}$$

As before, our task is to obtain the ML estimate of the transmitted signal vector $\mathbf{s}$. Firstly, we apply the OHRSA-ML method of Algorithm 3.

As suggested by Algorithm 3, we commence the detection process by evaluating the quantities $\mathbf{U}$ and $\hat{\mathbf{x}}$ of Equations (10.36c) and (10.36d) respectively, which yields

$$\mathbf{U} = \begin{bmatrix} 0.63 & -0.85 + 0.27\jmath \\ 0 & 1.45 \end{bmatrix}, \quad \hat{\mathbf{x}} = \begin{bmatrix} 0.43 - 0.34\jmath \\ -1.10 - 0.79\jmath \end{bmatrix}. \tag{10.38}$$

Furthermore, we proceed by calculating *four* values of the CSC function $J_2(\check{s}_2 = c_m),\ m = 1, \cdots, 4$ of Equation (10.36l) associated with the *four* different points c_m of the QPSK constellation. For instance, we have

$$\begin{aligned} J_2(\check{s}_2 = -1 - 1\jmath) &= \phi_2(\check{s}_2 = -1 - 1\jmath) = |u_{22}(\check{s}_2 - \hat{x}_2)|^2 \\ &= |1.45(-1 - 1\jmath - (-1.10 - 0.79\jmath))|^2 = 0.12. \end{aligned} \tag{10.39}$$

Subsequently, four QPSK symbol candidates c_m are sorted in the order of increasing sub-cost function $\phi_2(c_m)$, as described by Equation (10.36i) of Algorithm 3. For each hypothesised symbol value $\check{s}_2 = c_m$ we can now obtain *four* values of the total cost function $J(\check{\mathbf{s}}) = J_1(\check{s}_1, \check{s}_2)$ of Equation (10.36l) associated with *four* legitimate values of $\check{s}_1 = c_m$. For instance, we have

$$\begin{aligned} &J(\check{s}_1 = 1 - 1\jmath, \check{s}_2 = -1 - 1\jmath) \\ &\quad = J_2(\check{s}_2 = -1 - 1\jmath) + \phi_1(\check{s}_1 = 1 - 1\jmath, \check{s}_2 = -1 - 1\jmath) \\ &\quad = J_2(\check{s}_2 = -1 - 1\jmath) + |u_{11}(\check{s}_1 - \hat{x}_1)) + a_1|^2 \\ &\quad = 0.12 + |0.63[1 - 1\jmath - (0.43 - 0.34\jmath)] + (-0.03 + 0.21\jmath)|^2 = 0.27, \end{aligned} \tag{10.40}$$

where the quantity a_1 is given by Equation (10.36h) of Algorithm 3 as follows

$$\begin{aligned} a_1(\check{s}_2 = -1 - 1\jmath) &= u_{12}(\check{s}_2 - \hat{x}_2) \\ &= (-0.85 + 0.27\jmath)[-1 - 1\jmath - (-1.10 - 0.79\jmath)] = -0.03 + 0.21\jmath. \end{aligned} \tag{10.41}$$

As further detailed in Algorithm 3, we calculate the values of the total cost function $J(\check{s}_1, \check{s}_2)$ only for the specific hypothesis $\check{s}_2$, for which the value of the CSC function $J_2(\check{s}_2)$ is lower than the minimum value $J_{\min}$ obtained.

The resultant search tree is depicted in Figure 10.8(a), where as before, each evaluation step, namely each evaluation of the CSC function $J_i(\check{\mathbf{s}}_i)$ of Equation (10.36l) is indicated by an elliptic node. Moreover, the label inside each node indicates the order of evaluation as well as the corresponding value $J_i(\check{\mathbf{s}}_i)$ of the CSC function inside the brackets. The branches corresponding to *four* legitimate values of the QPSK symbol are indicated by the specific type of the edges and nodes. Specifically, the *gray* and *black* lines indicate the value of the real part of the QPSK symbol $\mathcal{R}\{\check{s}_i\} = -1$ and 1, while the *dashed* and *solid* lines indicate the value of the imaginary part $\mathcal{I}\{\check{s}_i\} = -1$ and 1.

Example 3 (Bitwise OHRSA-ML QPSK 2x2)

Let us consider a QPSK system identical to that described in Example 2 and attempt to derive an alternative way of finding the ML estimate of the transmitted signal vector s using the bit-based representation of the QPSK symbols. In order to describe this bit-based multi-user phasor constellation, let us develop a matrix- and vector-based mathematical model. Firstly, observe that each point of the QPSK constellation $c_m \in \mathcal{M}$ may be represented as the inner product $c_m = \boldsymbol{q}^{\mathrm{T}}\boldsymbol{d}_m$ of a unique bit-based vector $\boldsymbol{d}_m = [d_{m1}, d_{m2}]^{\mathrm{T}},\ d_{ml} = \{-1, 1\}$ and the vector $\boldsymbol{q} = [1, 1\jmath]^{\mathrm{T}}$. For instance we have

$$c_1 = -1 - 1\jmath = \boldsymbol{q}^{\mathrm{T}}\boldsymbol{d}_1 = \begin{bmatrix} 1 & 1\jmath \end{bmatrix} \cdot \begin{bmatrix} -1 \\ -1 \end{bmatrix}. \tag{10.42}$$

Furthermore, let us define a (4×2)-dimensional matrix

$$\mathbf{Q} = \mathbf{I} \otimes \boldsymbol{q} = \begin{bmatrix} 1 & 1\jmath & 0 & 0 \\ 0 & 0 & 1 & 1\jmath \end{bmatrix}, \tag{10.43}$$

where $\mathbf{I}$ is (2×2)-dimensional identity matrix, while $\otimes$ denotes the *matrix direct product* [374]. Consequently, the QPSK-modulated signal vector $\mathbf{s}$ may be represented as

$$\mathbf{s} = \begin{bmatrix} 1 - 1\jmath \\ -1 - 1\jmath \end{bmatrix} = \mathbf{Q}\mathbf{t} = \begin{bmatrix} 1 & 1\jmath & 0 & 0 \\ 0 & 0 & 1 & 1\jmath \end{bmatrix} \begin{bmatrix} 1 \\ -1 \\ -1 \\ -1 \end{bmatrix}, \tag{10.44}$$

where $\mathbf{t} = [\boldsymbol{t}_1^{\mathrm{T}}, \boldsymbol{t}_2^{\mathrm{T}}]^{\mathrm{T}}$ is a column supervector comprising the two bit-based vectors $\boldsymbol{t}_1$ and $\boldsymbol{t}_2$ associated with the QPSK-modulated symbols s_1 and s_2, respectively.

Substituting Equation (10.44) into the system model of Equation (10.7) yields

$$\mathbf{y} = \mathbf{H}\mathbf{Q}\mathbf{t} + \mathbf{w}. \tag{10.45}$$

Moreover, since $\mathbf{t}$ is a real-valued vector, we can elaborate a bit further and deduce a real-valued system model as follows

$$\begin{bmatrix} \mathcal{R}\{\mathbf{y}\} \\ \mathcal{I}\{\mathbf{y}\} \end{bmatrix} = \begin{bmatrix} \mathcal{R}\{\mathbf{HQ}\} \\ \mathcal{I}\{\mathbf{HQ}\} \end{bmatrix} \mathbf{t} + \begin{bmatrix} \mathcal{R}\{\mathbf{w}\} \\ \mathcal{I}\{\mathbf{w}\} \end{bmatrix} = \tilde{\mathbf{H}}\mathbf{t} + \tilde{\mathbf{w}}, \tag{10.46}$$

where $\tilde{\mathbf{H}}$ is a real-valued (4×4)-dimensional bitwise channel matrix, which may be expressed as

$$\tilde{\mathbf{H}} = \begin{bmatrix} \mathcal{R}\{\mathbf{HQ}\} \\ \mathcal{I}\{\mathbf{HQ}\} \end{bmatrix} = \begin{bmatrix} 0.1 & 0.2 & -0.7 & 0.6 \\ 0.3 & -0.4 & -1.3 & 0.5 \\ -0.2 & 0.1 & -0.6 & -0.7 \\ 0.4 & 0.3 & -0.5 & -1.3 \end{bmatrix}. \tag{10.47}$$

Thus, we arrive at the new system model of Equation (10.46), which may be interpreted as a (4×4)-dimensional BPSK-modulated SDM system. By applying the OHRSA-ML method of Algorithm 3 we have

$$\mathbf{U} = \begin{bmatrix} 0.63 & 0 & -0.85 & -0.27 \\ 0 & 0.63 & 0.27 & -0.85 \\ 0 & 0 & 1.45 & 0 \\ 0 & 0 & 0 & 1.45 \end{bmatrix}, \quad \hat{\mathbf{x}} = \begin{bmatrix} 0.43 \\ -0.34 \\ -1.10 \\ -0.79 \end{bmatrix}. \tag{10.48}$$

Furthermore, the first two steps of the recursive search process of Algorithm 3 are given by

$$\begin{aligned} J_4(\check{t}_4 = -1) &= |u_{44}(\check{t}_4 - \hat{x}_4)|^2 \\ &= |1.45(-1 - (-0.79))|^2 = 0.10 \end{aligned} \tag{10.49}$$

and

$$\begin{aligned} a_3(\check{t}_4 = -1) &= u_{34}(\check{t}_4 - \hat{x}_4) \\ &= 0(-1 - (-0.79)) = 0, \\ J_3(\check{t}_3 = -1, \check{t}_4 = -1) &= |u_{33}(\check{t}_3 - \hat{x}_3) + a_3|^2 \\ &= |1.45(-1 - (-1.10)) + (0)|^2 = 0.12. \end{aligned} \tag{10.50}$$

Upon completing the recursive search process of Algorithm 3 we arrive at the search tree depicted in Figure 10.8(b). As before, each evaluation step, namely each evaluation of the CSC function $J_i(\check{\mathbf{t}}_i)$ of Equation (10.36l) is indicated by an elliptic node. Moreover, the label inside each node indicates the order of evaluation as well as the corresponding value $J_i(\check{\mathbf{t}}_i)$ of the CSC function inside the brackets. The branches corresponding to two legitimate values $\check{t}_i = -1$ and 1 are indicated using the *dashed* and *solid* edges and nodes, respectively.

Observe that the ML estimates $\hat{\mathbf{s}}$ and $\hat{\mathbf{t}}$ of Figures 10.8 (a) and (b) are obtained within the same number of evaluation steps. Nevertheless, the latter search procedure is constituted by lower-complexity real-valued operations. Furthermore, in contrast to the detection method considered in Example 2, the search method outlined in this QPSK-based example can be readily generalised for the scenario of M-QAM SDM systems, as demonstrated in the forthcoming section.

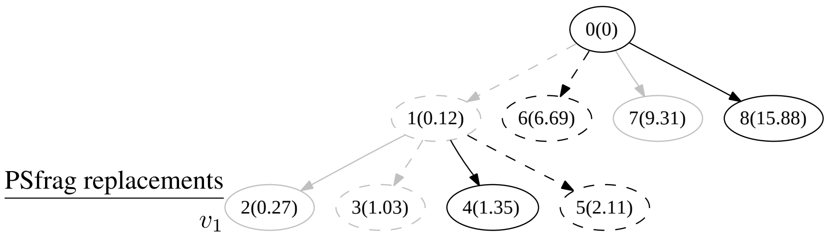

(a)

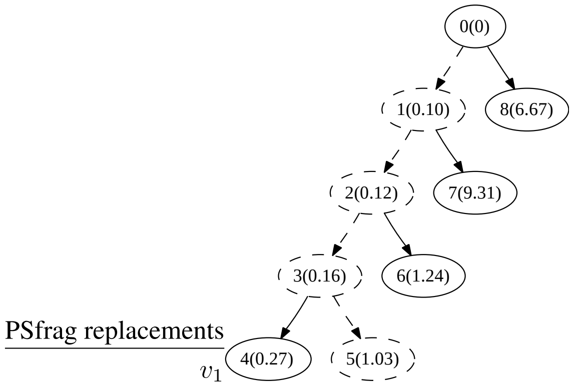

(b)

Figure 10.8: Examples of a search tree formed by the (a) OHRSA-ML and (b) BW-OHRSA-ML SDM detectors in the scenario of a system employing QPSK modulation, $m_{\rm t} = n_{\rm r} = 3$ transmit and receive antennas and encountering average SNRs of 10dB. The labels indicate the order of execution, as well as the corresponding value $J_i(\check{\mathbf{s}}_i)$ of the CSC function of Equation (10.22), as seen in the brackets.

10.4.3.1 Generalisation of the BW-OHRSA-ML SDM Detector

In this section we generalise the result obtained in Section 10.4.1 to the case of systems employing hyper-rectangular modulation schemes, namely M-QAM, where each modulated symbol belongs to a discrete phasor constellation $\mathcal{M} = \{c_m\}_{m=1,\cdots,M}$. It is evident that each phasor point c_m of an M-QAM constellation map may be represented as the inner product of a unique bit-based vector $\boldsymbol{d}_m = \{d_{ml} = -1, 1\}_{l=1,\cdots,b}$ and the corresponding *quantisation vector* $\boldsymbol{q}$. Specifically, we have

$$c_m = \boldsymbol{q}^{\mathrm{T}}\boldsymbol{d}_m. \tag{10.51}$$

Some examples of quantisation vectors corresponding to the modulation schemes of QPSK, 16-QAM and 64-QAM are portrayed in Table 10.2.

Table 10.2: Examples of quantization vectors.

Modulation scheme	$\boldsymbol{q}^{\mathrm{T}}$
BPSK	[1]
QPSK	$\frac{1}{\sqrt{2}}[1,\ \jmath]$
16QAM	$\frac{1}{\sqrt{10}}[1,\ 1\jmath,\ 2,\ 2\jmath]$
64QAM	$\frac{1}{\sqrt{42}}[1,\ 1\jmath,\ 2,\ 2\jmath,\ 4,\ 4\jmath]$

Furthermore, we define a $(bm_{\mathrm{t}} \times m_{\mathrm{t}})$-dimensional *quantisation matrix* $\mathbf{Q} = \mathbf{I} \otimes \boldsymbol{q}$, where $\mathbf{I}$ is an $(m_{\mathrm{t}} \times m_{\mathrm{t}})$-dimensional identity matrix and $\boldsymbol{q}$ is the aforementioned *quantisation vector*, while $\otimes$ denotes the *matrix direct product* [374]. Consequently the M-QAM-modulated signal vector s may be represented as

$$\mathbf{s} = \mathbf{Qt}, \tag{10.52}$$

where $\mathbf{t} = [\boldsymbol{t}_1^{\mathrm{T}}, \cdots, \boldsymbol{t}_{m_{\mathrm{t}}}^{\mathrm{T}}]^{\mathrm{T}}$ is a column supervector comprising the bit-based vectors $\boldsymbol{t}_i$ associated with each transmitted signal vector component s_i. Substituting Equation (10.52) into the system model of Equation (10.7) yields

$$\mathbf{y} = \mathbf{HQt} + \mathbf{w} = \tilde{\mathbf{H}}\mathbf{t} + \mathbf{w}, \tag{10.53}$$

where $\tilde{\mathbf{H}}$ is a $(n_{\mathrm{r}} \times bm_{\mathrm{t}})$-dimensional bitwise channel matrix. Observe in Equation (10.53) the requirement of having constant-envelope symbols is satisfied by the modified system model of Equation (10.53), since we have $|t_i|^2 = 1$ and thus the method described in Section 10.4.1 and summarised in Algorithm 3 is applicable to the evaluation of the bitwise ML estimate $\hat{\mathbf{t}}$ of Equation (10.53). Consequently, we apply the following changes to Algorithm 3:

1) Include the evaluation of the bitwise channel matrix $\tilde{\mathbf{H}}$ in (10.54a) and

2) Adjust the number of candidate bit values of t_i to $d_m = \{-1, 1\}$ in (10.54l).

Algorithm 4 Bit-Wise OHRSA-aided ML SDM Detector

$$\tilde{\mathbf{H}} = \begin{bmatrix} \mathcal{R}\{\mathbf{HQ}\} \\ \mathcal{I}\{\mathbf{HQ}\} \end{bmatrix} \tag{10.54a}$$

$$\texttt{Sort}\{\tilde{\mathbf{H}}\}, \ \texttt{such that} \ \|(\tilde{\mathbf{H}})_1\|^2 \leq \cdots \leq \|(\tilde{\mathbf{H}})_{m_\mathrm{t}}\|^2 \tag{10.54b}$$

$$\mathbf{G} = (\tilde{\mathbf{H}}^{\mathrm{H}}\tilde{\mathbf{H}} + \sigma_w^2\mathbf{I}) \tag{10.54c}$$

$$\mathbf{U} = \texttt{CholeskyDecomposition}(\mathbf{G}) \tag{10.54d}$$

$$\hat{\mathbf{x}} = \mathbf{G}^{-1}\tilde{\mathbf{H}}^{\mathrm{H}}\tilde{\mathbf{y}} \tag{10.54e}$$

$$\texttt{Calculate} \quad J_r \tag{10.54f}$$

$$\texttt{Unsort}\{\hat{\mathbf{t}}\} \tag{10.54g}$$

$$\texttt{function} \quad \texttt{Calculate} \quad J_i \tag{10.54h}$$

$$a_i = \sum_{j=i+1}^{m_\mathrm{t}} u_{ij}(\check{t}_j - \hat{x}_j) \tag{10.54i}$$

$$\texttt{Sort}\{d_m\}, \ \texttt{such that} \ \phi_i(d_0) < \phi_i(d_1), \tag{10.54j}$$

$$\texttt{where} \quad \phi_i(b_m) = |u_{ii}(d_m - \hat{x}_i) + a_i|^2 \tag{10.54k}$$

$$\texttt{for} \quad m = 0, 1 \quad \texttt{do} \tag{10.54l}$$

$$\check{t}_i = d_m \tag{10.54m}$$

$$J_i = J_{i+1} + \phi_i(\check{t}_i) \tag{10.54n}$$

$$\texttt{if} \quad J_i < J_{\min} \quad \texttt{then} \tag{10.54o}$$

$$\texttt{if} \quad i > 0 \quad \texttt{then} \quad \texttt{Calculate} \quad J_{i-1} \tag{10.54p}$$

$$\texttt{else}$$

$$J_{\min} = J_0 \tag{10.54q}$$

$$\hat{\mathbf{t}} = \check{\mathbf{t}} \tag{10.54r}$$

$$\texttt{end} \quad \texttt{if}$$

$$\texttt{end} \quad \texttt{if}$$

$$\texttt{end} \quad \texttt{for}$$

$$\texttt{end} \quad \texttt{function}$$

Hence we arrive at a new detection technique, namely the Bitwise OHRSA-aided ML SDM detector, which is summarised in Algorithm 4

The operation of Algorithm 4 is illustrated by the search tree diagram depicted in Figure 10.9. Each circular node in the diagram represents a subvector candidate $\check{\mathbf{t}}_i = \{\check{t}_j\}_{j=i,\cdots,r}$ of the transmitted bit-based signal vector $\mathbf{t}$. The bold and hollow nodes denote the binary values of the bit $\check{t}_i = \{-1, 1\}$ assumed in the current step of the recursive search process.

The corresponding values of the CSC function $J_i(\check{\mathbf{t}}_i)$ are indicated by both the colour and thickness of the transitions connecting each *child* or *descendant* node $\check{\mathbf{t}}_i$ with the corresponding *parent* node $\check{\mathbf{t}}_{i+1}$. The search-tree diagram depicted in Figure 10.9 corresponds to the system scenario employing QPSK modulation, $m_{\rm t}$=$n_{\rm r}$=8 operating at the average SNR of 6 dB. Observe that the ML solution is attained in 139 evaluation steps in comparison to the 2^{16} = 65536 evaluation steps required by the exhaustive ML search.

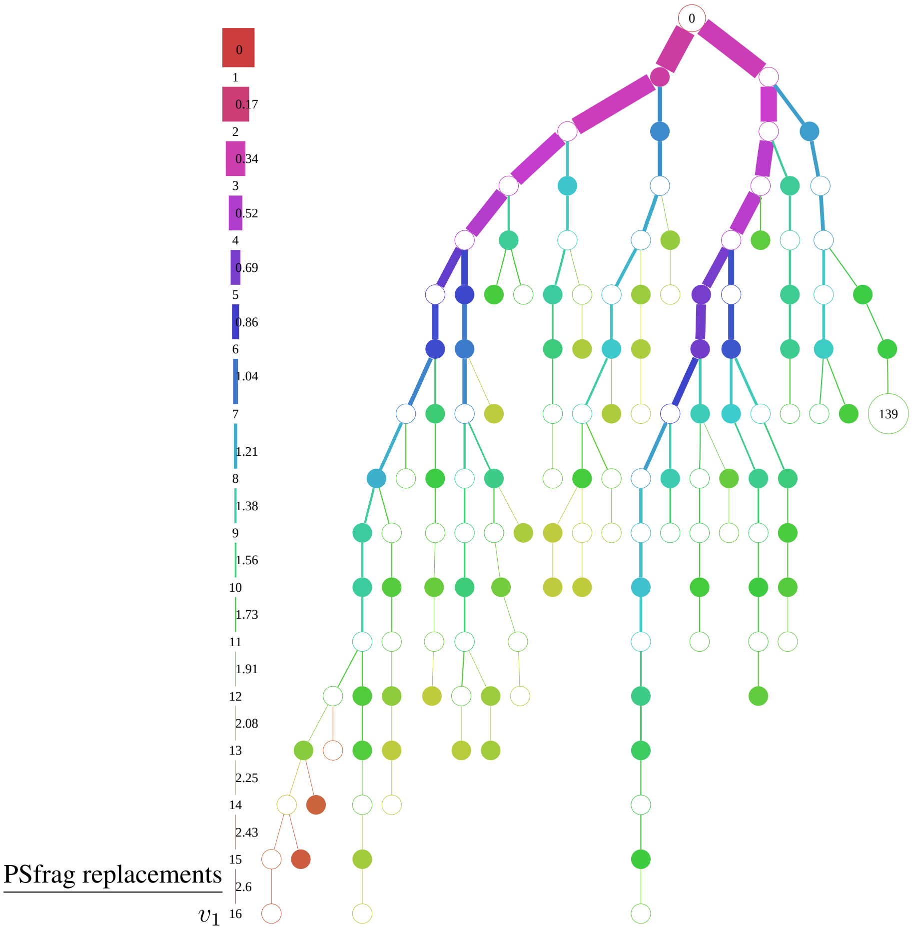

Figure 10.9: Example of a search tree formed by the BW-OHRSA method of Algorithm 4 in the scenario of QPSK, $m_{\rm t}$=$n_{\rm r}$=8 and an average SNR of 6 dB. Each circular node in the diagram represents a subvector candidate $\check{\mathbf{t}}_i = \{\check{t}_j\}_{j=i,\cdots,r}$ of the transmitted bit-based signal vector $\mathbf{t}$. The bold and hollow nodes denote the duo-binary values of the bit $\check{t}_i = \{-1, 1\}$ assumed. The corresponding value of the CSC function $J_i(\check{\mathbf{t}}_i)$ quantified in Equation (10.23b) is indicated by both the color and the thickness of the transitions connecting each child node $\check{\mathbf{t}}_i$ with the corresponding parent node $\check{\mathbf{t}}_{i+1}$. The ML solution is attained in 139 evaluation steps in comparison to the 2^{16} = 65536 evaluation steps required by the exhaustive ML search.

10.4.4 OHRSA-aided Log-MAP SDM Detection

It is evident [90] that the BER associated with the process of communicating over a fading noisy MIMO channel can be dramatically reduced by means of channel coding. A particularly effective channel coding scheme is constituted by the *soft-input soft-output* turbo coding method [216]. Turbo coding, however, requires *soft* information concerning the bit decisions at the output of the SDM detector, in other words, the *a posteriori* soft information regarding the confidence of the bit-decision is required.

The derivation of an expression for the low-complexity evaluation of the soft-bit information associated with the bit estimates of the SDM detector's output characterised by Equation (10.11) is given in [90]. Here, we present a brief summary of the results deduced in [90].

The soft-bit value associated with the mth bit of the QAM symbol transmitted from the ith transmit antenna element is determined by the log-likelihood function defined in [109] as

$$L_{im} = \log \frac{\sum_{\check{\mathbf{s}} \in \mathcal{M}_{im}^{1;m_t}} \mathrm{P}\left\{\mathbf{y}|\check{\mathbf{s}}, \mathbf{H}\right\}}{\sum_{\check{\mathbf{s}} \in \mathcal{M}_{im}^{0;m_t}} \mathrm{P}\left\{\mathbf{y}|\check{\mathbf{s}}, \mathbf{H}\right\}}, \tag{10.55}$$

where we define

$$\mathcal{M}_{im}^{b;m_t} = \left\{\check{\mathbf{s}} = (\check{s}_1, \cdots, \check{s}_{m_t})^{\mathrm{T}};\ \check{s}_j \in \mathcal{M} \text{ for } j \neq i,\ \check{s}_i \in \mathcal{M}_m^b\right\} \tag{10.56}$$

and $\mathcal{M}_m^b$ denotes the specific subset of the entire set $\mathcal{M}$ of modulation constellation points, which comprises the bit value $b = \{0, 1\}$ at the mth bit position.

However, the direct calculation of the accumulated *a posteriori* conditional probabilities in nominator and denominator of Equation (10.55) may have an excessive complexity in practice. Fortunately, as advocated in [90], the expression in Equation (10.55) can be closely approximated as follows

$$L_{im} \approx \log \frac{\mathrm{P}\left\{\mathbf{y}|\check{\mathbf{s}}_{im}^1, \mathbf{H}\right\}}{\mathrm{P}\left\{\mathbf{y}|\check{\mathbf{s}}_{im}^0, \mathbf{H}\right\}}, \tag{10.57}$$

where we define

$$\check{\mathbf{s}}_{im}^b = \arg \max_{\check{\mathbf{s}} \in \mathcal{M}_{im}^{b;m_t}} \mathrm{P}\left\{\mathbf{y}|\check{\mathbf{s}}, \mathbf{H}\right\}, \quad b = 0, 1. \tag{10.58}$$

As suggested by the nature of Equation (10.57), the detection process employing the objective function determined by Equations (10.57) and (10.58) is usually referred to as Logarithmic Maximum *A Posteriori* (Log-MAP) probability detector.

A practical version of the Log-MAP detector may be derived as follows. Substituting Equation (10.10) into (10.55) yields

$$L_{im} = \log \frac{\sum_{\check{\mathbf{s}} \in \mathcal{M}_{im}^{1;m_t}} \exp\left(-\frac{1}{\sigma_w^2}\|\mathbf{y} - \mathbf{H}\check{\mathbf{s}}\|^2\right)}{\sum_{\check{\mathbf{s}} \in \mathcal{M}_{im}^{0;m_t}} \exp\left(-\frac{1}{\sigma_w^2}\|\mathbf{y} - \mathbf{H}\check{\mathbf{s}}\|^2\right)}. \tag{10.59}$$

Note that Equation (10.59) involves summation over $2^{rm_t - 1}$ exponential functions. This operation may potentially impose an excessive computational complexity for large values of

m_t and/or r. However, as demonstrated in [90], the expression in (10.59) may be closely approximated by a substantially simpler expression, namely by

$$L_{im} \approx \frac{1}{\sigma_w^2}\left[\|\mathbf{y}-\mathbf{H}\check{\mathbf{s}}_{im}^0\|^2 - \|\mathbf{y}-\mathbf{H}\check{\mathbf{s}}_{im}^1\|^2\right], \tag{10.60}$$

where we have

$$\check{\mathbf{s}}_{im}^b = \arg\min_{\check{\mathbf{s}}\in\mathcal{M}_{im}^{b;m_\mathrm{t}}} \|\mathbf{y}-\mathbf{H}\check{\mathbf{s}}\|^2, \quad b=0,1, \tag{10.61}$$

and again, $\mathcal{M}_{im}^{b;m_\mathrm{t}}$ denotes the specific subset of the entire set $\mathcal{M}^{m_\mathrm{t}}$ of signal vector candidates associated with the modulation scheme employed, which comprises the bit value $b=\{0,1\}$ at the mth bit position of the ith signal vector component.

The Log-MAP detector defined by Equations (10.60) and (10.61) may be applied for the sake of obtaining the soft-bit information associated with the bitwise OHRSA ML SDM detector derived in Section 10.4.3. Consequently, substituting the bitwise system model of Equation (10.53) into (10.60) and (10.61) yields

$$L_i \approx \frac{1}{\sigma_w^2}\left[\|\mathbf{y}-\tilde{\mathbf{H}}\check{\mathbf{t}}_{i;\min}^0\|^2 - \|\mathbf{y}-\tilde{\mathbf{H}}\check{\mathbf{t}}_{i;min}^1\|^2\right], \tag{10.62}$$

where we have

$$\check{\mathbf{t}}_{i;\min}^m = \arg\min_{\check{\mathbf{t}}\in\mathcal{D}_i^{m;r}} \|\mathbf{y}-\tilde{\mathbf{H}}\check{\mathbf{t}}\|^2, \quad b=0,1 \tag{10.63}$$

and $\mathcal{D}_i^{m;r}$ denotes the subset of the entire set $\mathcal{D}^r$ of $(r=m_\mathrm{t}\log_2 M)$-dimensional bitwise vectors, which comprise the binary value $\check{t}_i = d_m = \{-1,1\}$ at the ith bit position.

Furthermore, substituting the bitwise objective function of Equation (10.60) into (10.62) yields

$$\begin{aligned} L_i \approx& \frac{1}{\sigma_w^2}\left[J(\check{\mathbf{t}}_{i;\min}^0)+\phi - J(\check{\mathbf{t}}_{i;\min}^1)-\phi\right] \\ =& \frac{1}{\sigma_w^2}\left[J(\check{\mathbf{t}}_{i;\min}^0) - J(\check{\mathbf{t}}_{i;\min}^1)\right], \end{aligned} \tag{10.64}$$

where $\check{\mathbf{t}}_{i;\min}^m$ and the corresponding cost function value $J(\check{\mathbf{t}}_{i;\min}^m)$ may be obtained by applying the constrained OHRSA-aided ML detection method derived in Section 10.4.3.

Consequently, the evaluation of the bitwise Log-MAP estimates of the transmitted bitwise signal vector $\mathbf{t}$ involves repetitive evaluation of $2r$ constrained ML estimates $\check{\mathbf{t}}_{i;\min}^m$ along with the associated $2r$ values of the objective function $J(\check{\mathbf{t}}_{i;\min}^m)$.

The pseudo-code describing the implementation of the bitwise OHRSA-aided Log-MAP SDM detector is summarised in Algorithm 5.

Clearly, the repetitive nature of the search process entailing Equations (10.65f,i-r) in Algorithm 5 imposes a substantial increase in the associated computational complexity. Hence, in the next section we derive an OHRSA-aided approximate Log-MAP method, which is capable of approaching the optimum Log-MAP performance, while avoiding the repetitive evaluation of Equation (10.65f) in Algorithm 5 and therefore imposes considerably reduced complexity requirements.

Example 4 (OHRSA-Log-MAP BPSK 3x3)

Consider a BPSK system having $n_{\mathrm{r}} = m_{\mathrm{t}} = 3$ transmit and receive antennas, which is described by Equation (10.7). The transmitted signal $\mathbf{s}$, received signal $\mathbf{y}$ as well as the channel matrix $\mathbf{H}$ of Equation (10.7) are exemplified by the following values

$$\mathbf{s} = \begin{bmatrix} -1 \\ 1 \\ 1 \end{bmatrix}, \quad \mathbf{y} = \begin{bmatrix} 0.2 \\ 0.3 \\ -0.5 \end{bmatrix}, \quad \mathbf{H} = \begin{bmatrix} 0.1 & -1 & 1.1 \\ -0.2 & 0.7 & -0.7 \\ 0.4 & 0.5 & -0.5 \end{bmatrix}. \tag{10.66}$$

Observe that the channel matrix $\mathbf{H}$ of Equation (10.66) happens to be *best-first* ordered and does not require any further reordering. Furthermore, in our scenario of BPSK modulation the channel matrix $\mathbf{H}$ of Equation (10.66) is equivalent to the bitwise channel matrix $\tilde{\mathbf{H}}$ of Algorithm 5.

Subsequently, our task is to obtain the Log-MAP estimate of the transmitted signal vector $\mathbf{t} = \mathbf{s}$. We apply the OHRSA-Log-MAP method of Algorithm 5. Firstly, we evaluate the triangular matrix $\mathbf{U}$ of Equation (10.65d) as well as the unconstrained MMSE estimate $\hat{\mathbf{x}}$ of Equation (10.65e). The resultant quantities are given by

$$\mathbf{U} = \begin{bmatrix} 0.56 & -0.07 & 0.09 \\ 0 & 1.35 & -1.35 \\ 0 & 0 & 0.46 \end{bmatrix}, \quad \hat{\mathbf{x}} = \begin{bmatrix} -0.80 \\ -0.01 \\ 0.13 \end{bmatrix}. \tag{10.67}$$

Secondly, as further suggested by Algorithm 5, for each transmitted bitwise symbol t_i we calculate the quantities $J(\check{\mathbf{t}}^{-1}_{i;\min})$ and $J(\check{\mathbf{t}}^{1}_{i;\min})$ corresponding to the values of the cost function $J(\check{\mathbf{t}})$ of Equation (10.65o) associated with the constrained ML estimates of the transmitted bitwise vector $\mathbf{t}$ with the ith bit-component assuming values of -1 and 1, respectively.

For instance, the cost function value $J(\check{\mathbf{t}}^{-1}_{1;\min})$ associated with the ML estimate of the bitwise signal vector $\mathbf{t}$ constrained by bit-component value $\check{t}_1 = -1$ may be calculated as follows

$$\begin{aligned} J_3(\check{t}_3 = 1) &= |u_{33}(\check{t}_3 - \hat{x}_3)|^2 = (0.46(1 - (0.13)))^2 = 0.16, \\ a_2(\check{t}_3 = 1) &= u_{23}(\check{t}_3 - \hat{x}_3) = -1.35(1 - (0.13)) = -1.17, \\ J_2(\check{t}_2 = 1, \check{t}_3 = 1) &= J_3(\check{t}_3 = 1) + |u_{22}(\check{t}_2 - \hat{x}_2) + a_2|^2 \\ &= 0.16 + |1.35(1 - (-0.01)) + (-1.17)|^2 = 0.20. \end{aligned} \tag{10.68}$$

Algorithm 5 BW-OHRSA-aided LogMAP SDM Detector

$$\tilde{\mathbf{H}} = \begin{bmatrix} \mathcal{R}\{\mathbf{HQ}\} \\ \mathcal{I}\{\mathbf{HQ}\} \end{bmatrix} \tag{10.65a}$$

$$\texttt{Sort}\{\tilde{\mathbf{H}}\},\ \texttt{such that}\ \|(\tilde{\mathbf{H}})_1\|^2 \leq \cdots \leq \|(\tilde{\mathbf{H}})_{m_t}\|^2 \tag{10.65b}$$

$$\mathbf{G} = (\tilde{\mathbf{H}}^{\mathrm{H}}\tilde{\mathbf{H}} + \sigma_w^2\mathbf{I}) \tag{10.65c}$$

$$\mathbf{U} = \texttt{CholeskyDecomposition}(\mathbf{G}) \tag{10.65d}$$

$$\hat{\mathbf{x}} = \mathbf{G}^{-1}\tilde{\mathbf{H}}^{\mathrm{H}}\tilde{\mathbf{y}} \tag{10.65e}$$

`for` $i = 1, \cdots, r$

$$L_{im} = \frac{1}{\sigma_w^2}\left[J^0_{i;\min} - J^1_{i;\min}\right] \tag{10.65f}$$

`end for`

$$\texttt{Unsort}\{L_i\}_{i=1,\cdots,r} \tag{10.65g}$$

`function Calculate` $J^b_{k;i}$ (10.65h)

$$a_i = \sum_{j=i+1}^{m_t} u_{ij}(\check{t}_j - \hat{x}_j) \tag{10.65i}$$

`if` $i = k$ `then`

$$d_0 = \{-1, 1\}_b \tag{10.65j}$$

`else`

`Sort`$\{d_m = -1, 1\}$, (10.65k)

`such that` $\phi_i(d_0) < \phi_i(d_1)$, (10.65l)

`where` $\phi_i(d_m) = |u_{ii}(d_m - \hat{x}_i) + a_i|^2$ (10.65m)

`end if`

`for` $m = 0, 1$ `do`

$$\check{t}_i = d_m \tag{10.65n}$$

$$J_{k;i} = J_{k;i+1} + \phi_i(d_m) \tag{10.65o}$$

`if` $J_i < J_{\min}$ `then` (10.65p)

`if` $i > 0$ `then Calculate` $J^b_{k;i-1}$ (10.65q)

`else`

$$J_{\min} = J^b_{k;\min} = J^b_{k;0} \tag{10.65r}$$

`end if`

`end if`

`if` $i = k$ `then break for loop`

`end for`

`end function`

Furthermore, we have

$$\begin{aligned}
&a_1(\check{t}_2 = 1, \check{t}_3 = 1) = u_{12}(\check{t}_2 - \hat{x}_2) + u_{13}(\check{t}_3 - \hat{x}_3) \\
&\quad = -0.07(1 - (-0.01)) + 0.09(1 - (0.13)) = 0.00, \\
&J(\check{\mathbf{t}}^{-1}_{1;\min}) = J_1(\check{t}_1 = -1, \check{t}_2 = 1, \check{t}_3 = 1) \\
&\quad = J_2(\check{t}_2 = 1, \check{t}_3 = 1) + |u_{11}(\check{t}_1 - \hat{x}_1) + a_1|^2 \\
&\quad = 0.20 + |0.56(-1 - (-0.80)) + (0.00)|^2 = 0.21.
\end{aligned} \tag{10.69}$$

Observe that for the sake of brevity we omit the calculation of the CSC values outside the major search branch of Algorithm 5, *i. e.* outside the search branch leading to the constrained ML estimate. The corresponding search tree formed by the evaluation of the value of $J(\check{\mathbf{s}}^{-1}_{1;\min})$ using Algorithm 5 is depicted in Figure 10.10(a). Furthermore, Figures 10.10 (b)-(f) illustrate the search trees formed by the search sub-processes of Algorithm 5 corresponding to the remaining *five* values $\left\{J(\check{\mathbf{s}}^{b}_{i;\min})\right\}^{b=-1,1}_{i=1,\cdots,3}$.

Finally, upon completing the calculation of all *six* values $\left\{J(\check{\mathbf{s}}^{b}_{i;\min})\right\}^{b=-1,1}_{i=1,\cdots,3}$ we arrive at the following matrix

$$\hat{\mathbf{J}} = \left\{J(\check{\mathbf{s}}^{b}_{i;\min})\right\}^{b=-1,1}_{i=1,\cdots,3} = \begin{bmatrix} 0.21 & 1.21 \\ 0.33 & 0.21 \\ 0.33 & 0.21 \end{bmatrix}, \tag{10.70}$$

where the elements of the matrix $\hat{\mathbf{J}}$, which we refer to as Minimum Cost Function (MCF) matrix, are defined as $\hat{J}_{ij} = J(\check{\mathbf{s}}^{b_j}_{i;\min})$. Consequently, the *soft-bit* vector representing the Log-MAP estimate of the transmitted bitwise signal vector $\mathbf{t}$ may be expressed as

$$\mathbf{L} = \frac{1}{\sigma_w^2}\left[(\hat{\mathbf{J}})_1 - (\hat{\mathbf{J}})_2\right] = \begin{bmatrix} -9 \\ 1.2 \\ 1.2 \end{bmatrix}, \tag{10.71}$$

where $(\hat{\mathbf{J}})_j$ denotes the jth column of the MCF matrix $\hat{\mathbf{J}}$ defined in Equation (10.70).

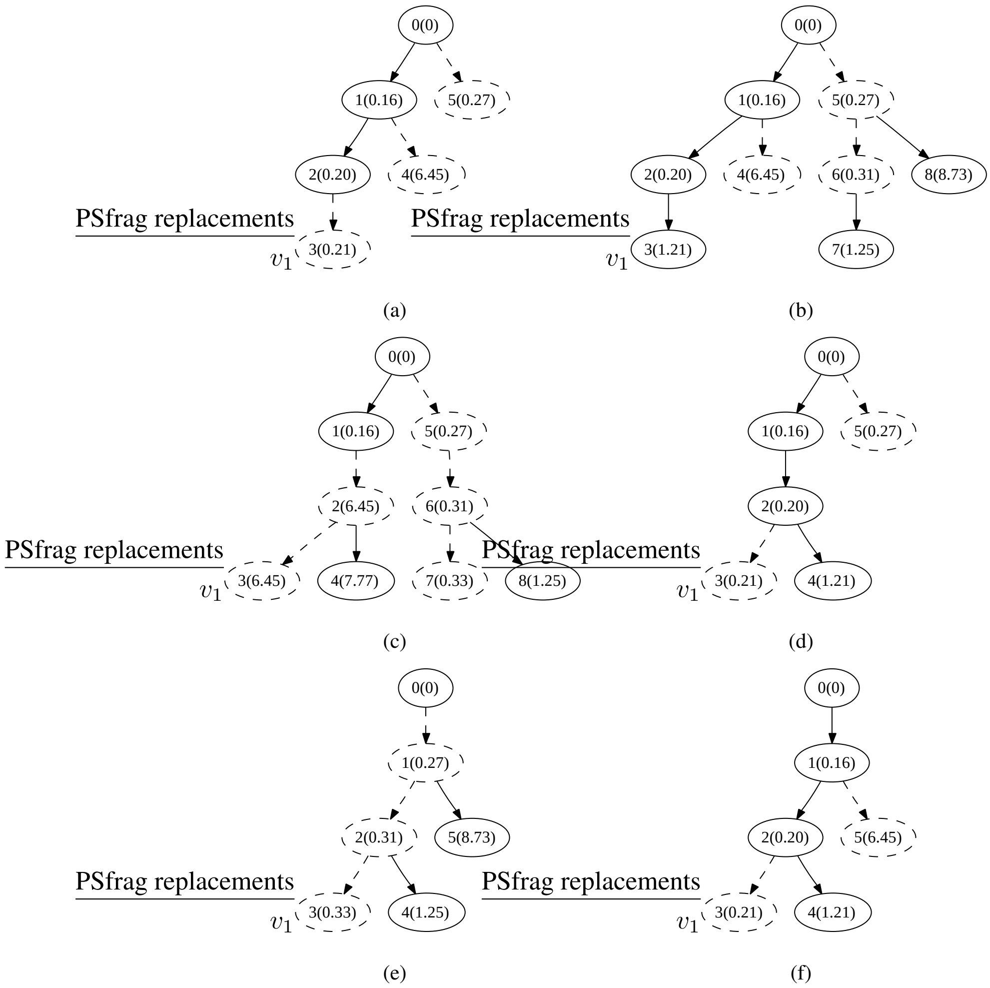

Figure 10.10: Example of search trees formed by the OHRSA-Log-MAP SDM detector of Algorithm 5 in the scenario of a system employing BPSK modulation, $m_{\mathrm{t}} = n_{\mathrm{r}} = 3$ transmit and receive antennas and encountering average SNRs of 10dB. The labels indicate the order of visitation, as well as the corresponding value $J_i(\check{\mathbf{t}}_i)$ of the CSC function of Equation (10.65o), as seen in the brackets.

Example 5 (OHRSA Approximate Log-MAP BPSK 3x3)

Again, consider a BPSK system identical to that described in Example 4. Specifically, we have a (3×3)-dimensional real-valued linear system described by Equation (10.7) with the corresponding transmitted signal $\mathbf{s}$, the received signal $\mathbf{y}$ and the channel matrix $\mathbf{H}$ described in Equation (10.66). In this example we would like to demonstrate an alternative search paradigm, which avoids the repetitive process characterised by Algorithm 5 and exemplified in Figure 10.10 of Example 4, while obtaining a similar result.

Firstly, we apply the OHRSA-ML method of Algorithm 4. The triangular matrix $\mathbf{U}$ of Equation (10.54d) as well as the unconstrained MMSE estimate $\hat{\mathbf{x}}$ of Equation (10.54e) are similar to those evaluated in Example 4 and are characterised by Equation (10.67). The resultant search process is characterised by the search tree diagram portrayed in Figure 10.11(a).

Additionally, however, we define a (3×2)-dimensional Minimum Cost Function (MCF) matrix $\hat{\mathbf{J}}$, which will be used for the evaluation of the soft-bit information, and we assign an initial value of $\hat{\mathbf{J}} = J_0\, \mathbf{1}$, where $\mathbf{1}$ is a (3×2)-dimensional matrix of ones and $J_0 \gg \gamma$ is some large constant, which should be greater than the average SNR of $\gamma = 10$ encountered. For instance let us assume $J_0 = 100$. Subsequently, the cost-function-related matrix $\hat{\mathbf{J}}$ is updated according to a procedure to be outlined below each time when the search branch forming the search tree portrayed in Figure 10.11(a) is terminated, regardless whether its termination occured due to reaching the final recursive index value of $i = 1$, or owing to exceeding the minimum value of the cost function $J_{\min}$. More specifically, we update the elements of the matrix $\hat{\mathbf{J}}$ corresponding to the bitwise symbols $\check{t}_j,\ j = i, \cdots, 3$ constituting the bitwise subvector candidate $\check{\mathbf{t}}_i$ associated with the particular search branch, as outlined below

$$\hat{J}_{jb_j} = \min\left\{\hat{J}_{jb_j}, J_i(\check{\mathbf{t}}_i)\right\}, \quad j = i, \cdots, 3, \quad \check{t}_j = \{-1, 1\}_{b_j}. \tag{10.72}$$

For instance, upon completing the first, left-most search branch depicted in Figure 10.11(a) and associated with the transmitted signal candidate $\check{\mathbf{t}} = \begin{bmatrix} -1 & 1 & 1 \end{bmatrix}^{\mathrm{T}}$, namely upon reaching node 3 of the search tree, the following update of the MCF matrix $\hat{\mathbf{J}}$ is performed

$$\begin{aligned} \hat{J}_{11} &= \min\left\{\hat{J}_{11}, J(\check{\mathbf{t}})\right\} = \min\{100, 0.21\} = 0.21 \\ \hat{J}_{22} &= \hat{J}_{32} = \min\{100, 0.21\} = 0.21. \end{aligned} \tag{10.73}$$

Consequently, the matrix $\hat{\mathbf{J}}$ becomes

$$\hat{\mathbf{J}}(3) = \begin{bmatrix} 0.21 & 100 \\ 100 & 0.21 \\ 100 & 0.21 \end{bmatrix}. \tag{10.74}$$

Furthermore, the states of the MCF matrix corresponding to the search steps 4, 5 and 6 of Figure 10.11(a) are

$$\hat{\mathbf{J}}(4) = \begin{bmatrix} 0.21 & 1.21 \\ 100 & 0.21 \\ 100 & 0.21 \end{bmatrix}, \quad \hat{\mathbf{J}}(5) = \begin{bmatrix} 0.21 & 1.21 \\ 6.45 & 0.21 \\ 100 & 0.21 \end{bmatrix}, \quad \hat{\mathbf{J}}(6) = \begin{bmatrix} 0.21 & 1.21 \\ 6.45 & 0.21 \\ 0.27 & 0.21 \end{bmatrix}. \tag{10.75}$$

Finally, by substituting the resultant value of the MCF matrix $\hat{\mathbf{J}}(6)$ of Equation (10.75) into

(10.71) we obtain the following soft-bit estimate of the transmitted bitwise signal vector $\mathbf{t}$

$$\mathbf{L}_a = \begin{bmatrix} -9 \\ 62.39 \\ 0.60 \end{bmatrix}. \tag{10.76}$$

Observe that the soft-bit estimate $\mathbf{L}_a$ of Equation (10.76) appears to be considerably more reliable than the MMSE estimate $\hat{\mathbf{x}}$ of Equation (10.67). Specifically, as opposed to the MMSE estimate $\hat{\mathbf{x}}$ in Equation (10.25) the direct slicing of the soft-bit estimate $\mathbf{L}_a$ results in the correct signal vector $\mathbf{s}$ of Equation (10.66). Moreover, the soft-bit estimate $\mathbf{L}_a$ provides further information concerning the reliability of each estimated bit, albeit the resultant soft-bit information of Equation (10.76) substantially deviates from the more reliable exact Log-MAP estimate $\mathbf{L}$ given by Equation (10.71).

Fortunately, however, the precision of the soft-bit estimate $\mathbf{L}_a$ may be readily improved. Specifically, we introduce an additional parameter ρ, which will allow us to control the rate of convergence in the search process of Algorithm 4 by increasing the threshold value of the CSC function, which controls the passage of the recursive search process through *low-likelihood* search branches having CSC function values $J_i(\check{\mathbf{t}}_i)$ in excess of $\rho J_{\min}$, as opposed to $J_{\min}$ of Equation (10.54o) in Algorithm 4. Let us now execute the modified OHRSA-ML method of Algorithm 4, where the condition $J_i < J_{\min}$ of Equation (10.54o) is replaced by the corresponding condition of $J_i < \rho J_{\min}$.

The search trees formed by the execution of the modified Algorithm 4 in the scenarios of setting (b) $\rho = 1.3$ and (c) $\rho = 2.0$ are depicted in Figures 10.10 (b) and (c), respectively. Furthermore, the convergence of the MCF matrix $\hat{\mathbf{J}}$ as well as the resultant soft-bit estimate $\mathbf{L}$ of both scenarious may be characterised as follows

$$(b) \quad \hat{\mathbf{J}}(7) = \begin{bmatrix} 0.21 & 1.21 \\ 0.31 & 0.21 \\ 0.31 & 0.21 \end{bmatrix}, \hat{\mathbf{J}}(8) = \begin{bmatrix} 0.21 & 1.21 \\ 0.31 & 0.21 \\ 0.31 & 0.21 \end{bmatrix}, \mathbf{L}_b = \begin{bmatrix} -9 \\ 0.99 \\ 0.99 \end{bmatrix} \tag{10.77}$$

and

$$(c) \quad \hat{\mathbf{J}}(8) = \begin{bmatrix} 0.21 & 1.21 \\ 0.33 & 0.21 \\ 0.33 & 0.21 \end{bmatrix}, \hat{\mathbf{J}}(10) = \begin{bmatrix} 0.21 & 1.21 \\ 0.33 & 0.21 \\ 0.33 & 0.21 \end{bmatrix}, \mathbf{L}_c = \begin{bmatrix} -9 \\ 1.2 \\ 1.2 \end{bmatrix}, \tag{10.78}$$

where as before, $\hat{\mathbf{J}}(n)$ denotes the state of the MCF matrix at search step n corresponding to the nth node of the search tree in Figures 10.10 (b) and (c). Note that the search processes characterised by Figures 10.10 (b) and (c) merely expand the search process portrayed in Figure 10.10(a). Consequently, for the sake of brevity, the corresponding Equations (10.77) and (10.78) depict only the extra states of the MCF matrix introduced by the expanded search procedure. For instance, the states $\hat{\mathbf{J}}(10)$ and $\hat{\mathbf{J}}(8)$ of Equation (10.78) complement the state $\hat{\mathbf{J}}(7)$ of Equation (10.77), as well as the states $\hat{\mathbf{J}}(6), \hat{\mathbf{J}}(5), \hat{\mathbf{J}}(4)$ and $\hat{\mathbf{J}}(3)$ of Equations (10.74) and (10.75), respectively.

Finally, by comparing the resultant soft-bit estimates $\mathbf{L}_a, \mathbf{L}_b$ and $\mathbf{L}_c$ of Equations (10.76), (10.77) and (10.78) corresponding to the scaling values of $\rho = 1.0, 1.3$ and 2.0 to the corresponding Log-MAP estimate $\mathbf{L}$ of Equation (10.71), we may hypothesise that the value of the soft-bit estimate obtained by the modified OHRSA-ML method of Algorithm 4 rapidly converges to the Log-MAP estimate of the OHRSA-Log-MAP method of Algorithm 5 upon increasing the value of the parameter ρ. As expected, there is a tradeoff between the accuracy of the soft-bit information obtained and the corresponding computational complexity associated with the particular choice of ρ. In the next section we will generalise the results obtained in this example and substantiate the aforementioned convergence-related hypothesis, as well as deduce the optimal value of the associated scaling parameter ρ.

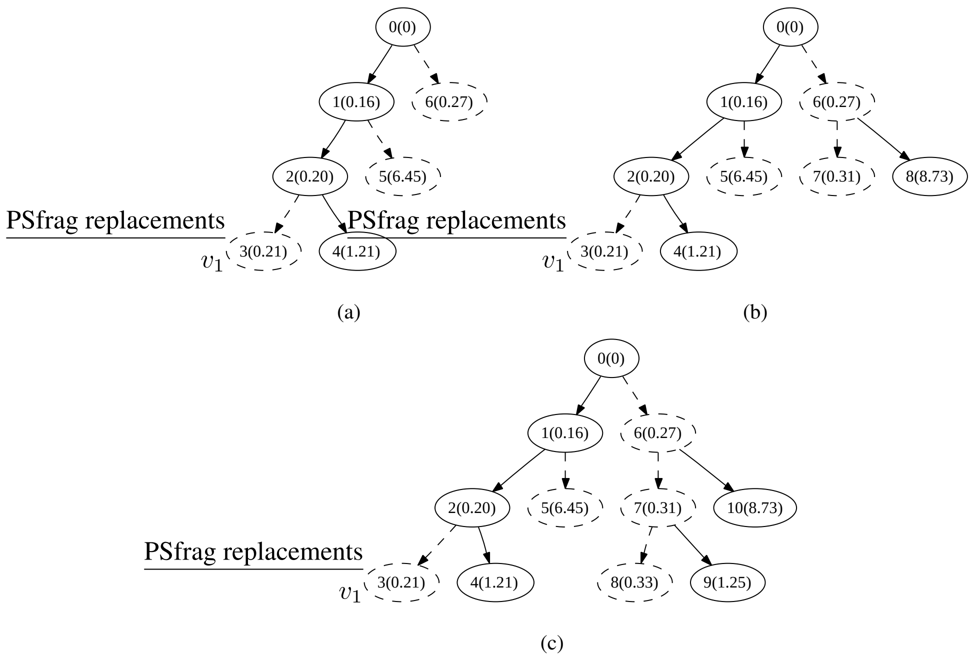

Figure 10.11: Example of the search trees formed by the modified OHRSA-ML SDM detector of Algorithm 4 using different values of the parameter ρ, namely, (a) $\rho = 1.0$, (b) 1.3 and (c) 2.0. We consider a system employing BPSK modulation, $m_{\mathrm{t}} = n_{\mathrm{r}} = 3$ transmit and receive antennas and encountering an average SNR of 10dB. The labels indicate the order of evaluation, as well as the corresponding value $J_i(\check{\mathbf{s}}_i)$ of the CSC function of Equation (10.22), as seen in the brackets.

Clearly, the repetitive nature of the search process entailing Equations (10.65f,i-r) in Algorithm 5 and exemplified by Example 4 imposes a substantial increase in the associated computational complexity. Hence, in the next section we derive an OHRSA-aided approximate Log-MAP method, which is capable of approaching the optimum Log-MAP performance, while avoiding the repetitive evaluation of Equation (10.65f) in Algorithm 5 and therefore imposes considerably reduced complexity requirements.

10.4.5 Soft-Output OHRSA-aided Approximate Log-MAP Detection

Let us define the $(r\times 2)$-dimensional Bitwise Minimum Cost (BMC) function matrix $\hat{\mathbf{J}}$ having elements as follows

$$\hat{J}_{ib} = J(\hat{\mathbf{t}}_i^b),\ i = 1, \cdots, r,\ b = -1, 1, \tag{10.79}$$

where $\hat{\mathbf{t}}_i^b$ is defined by Equation (10.61). Using the BMC matrix of Equation (10.79), Equation (10.64) may also be expressed in a vectorial form as

$$\mathbf{L} = \frac{1}{\sigma_w^2}\left[(\hat{\mathbf{J}})_1 - (\hat{\mathbf{J}})_2\right], \tag{10.80}$$

where, as before, $(\hat{\mathbf{J}})_b$ denotes the bth column of the matrix $\hat{\mathbf{J}}$ having elements defined by Equation (10.79).

Consequently, in order to evaluate the bit-related soft information we have to populate the BMC matrix $\hat{\mathbf{J}}$ of Equation (10.79) with the corresponding values of the cost function of Equation (10.79). Observe, that the evaluation of the ML estimate $\hat{\mathbf{t}}$ will situate half elements of the cost matrix $\hat{\mathbf{J}}$ with the corresponing minimum value of the cost function associated with the ML estimate, such that we have

$$J_{ib} = J(\hat{\mathbf{t}}),\ i = 1, \cdots, r,\ b = \hat{t}_i. \tag{10.81}$$

Subsequently, let us introduce the following adjustments to Algorithm 4. Firstly, we introduce an additional parameter ρ, which we refer to as the *search radius factor*. More specifically, the parameter ρ allows us to control the rate of convergence for the tree search process of Algorithm 4 and affects the cut-off value of a CSC function, which limits the passage of the recursive search process through *low-likelihood* search branches having the a CSC function value $J_i(\check{\mathbf{t}}_i)$ in excess of $\rho J_{\min}$, as opposed to $J_{\min}$. Thus, the following rule replaces Rule 4 of Section 10.4.2.

Rule 4a At each recursive detection level i, only the high-probability search branches corresponding to the highly likely symbol candidates c_m resulting in low values of the CSC function obeying $J_i(c_m) < \rho J_{\min}$ are pursued. Furthermore, as follows from the sorting criterion of the optimisation Rule 2, as soon as the inequality $J_i(c_m) > \rho J_{\min}$ is sutisfied, the search loop at the ith recursive detection level is discontinued.

Secondly, we introduce an additional rule, which facilitates the evaluation of the elements of the BMC matrix $\hat{\mathbf{J}}$ of Equation (10.79). Explicitly, we postulate Rule 5.

Rule 5 At each arrival at the bottom of the search tree, which corresponds to search level 1, the resultant value of the branch cost function $J(\check{\mathbf{t}})$ is utilized to populate the elements of the BMC matrix $\hat{\mathbf{J}}$, which correspond to the bitwise signal components $\check{t}_i$ comprising the obtained signal candidate $\check{\mathbf{t}}$. Namely, we have

$$\hat{J}_{ib} = \min\{\hat{J}_{ib}, J(\check{\mathbf{t}})\},\ i = 1, \cdots, r,\ b = \check{t}_i. \tag{10.82}$$

Subsequently, we suggest that the evaluation of the BMC matrix $\hat{\mathbf{J}}$, which is performed in the process of the ML search of Algorithm 4 extended by Rule 4a and using Rule 5 will allow us to provide reliable soft-bit information, while imposing a relatively low computational complexity. The main rationale of this assumption will be outlined in our quantitative complexity and performance analysis portrayed in Section 10.4.5.1.

As we will further demonstrate in Section 10.4.5.1, the resultant approximate Log-MAP SDM detector exhibits a particularly low complexity at high SNR values. On the other hand, at low SNR values the associated complexity substantially increases. Consequently, in order to control the computational complexity at low SNR values, we indroduce the additional complexity-control parameter γ. Our aim is to avoid the computationally demanding and yet inefficient detection of the specific signal components, which have their signal energy well below the noise floor. More specifically, we modify Equation (10.54p) of Algorithm 4 according to Rule 6.

Rule 6 The branching of the tree search described by Algorithm 4 is truncated, if the SNR associated with the corresponding signal component is lower than the value of the complexity-control parameter γ. In other words, the search along a given branch is truncated if we have $\frac{\|\mathbf{H}_i\|^2}{\sigma_w^2} < \gamma$.

Upon applying Rules 4, 5 and 6 in the context of the OHRSA-ML method of Algorithm 4, we arrive at an *approximate* OHRSA-Log-MAP SDM detector, which avoids the repetitive search required by the OHRSA-Log-MAP SDM detector of Section 10.4.4.

The resultant OHRSA-aided approximate Log-MAP SDM detector, which we refer to as the Soft-output OPtimised HIErarchy (SOPHIE) SDM detector is summarised in Algorithm 6.

Algorithm 6 SOPHIE Approximate Log-MAP SDM Detector

$$\tilde{\mathbf{H}} = \begin{bmatrix} \mathcal{R}\{\mathbf{HQ}\} \\ \mathcal{I}\{\mathbf{HQ}\} \end{bmatrix} \tag{10.83a}$$

$$\texttt{Sort}\{\tilde{\mathbf{H}}\},\ \text{such that } \|(\tilde{\mathbf{H}})_1\|^2 \leq \cdots \leq \|(\tilde{\mathbf{H}})_r\|^2 \tag{10.83b}$$

$$\mathbf{G} = (\tilde{\mathbf{H}}^{\mathrm{H}}\tilde{\mathbf{H}} + \sigma_w^2\mathbf{I}) \tag{10.83c}$$

$$\mathbf{U} = \texttt{CholeskyDecomposition}(\mathbf{G}) \tag{10.83d}$$

$$\hat{\mathbf{x}} = \mathbf{G}^{-1}\tilde{\mathbf{H}}^{\mathrm{H}}\tilde{\mathbf{y}} \tag{10.83e}$$

$$\texttt{Calculate}\quad J_r \tag{10.83f}$$

$$\mathbf{L} = \frac{1}{\sigma_w^2}\left[(\hat{\mathbf{J}})_0 - (\hat{\mathbf{J}})_1\right] \tag{10.83g}$$

$$\texttt{Unsort}\{L_i\}_{i=1,\cdots,r} \tag{10.83h}$$

$$\texttt{function}\quad \texttt{Calculate}\quad J_i \tag{10.83i}$$

$$\quad a_i = \sum_{j=i+1}^{m_t} u_{ij}(\check{t}_j - \hat{x}_j) \tag{10.83j}$$

$$\quad \texttt{Sort}\{\boldsymbol{b}\},\ \text{such that } \phi_i(b_1) < \phi_i(b_2), \tag{10.83k}$$

$$\quad \texttt{where}\quad \phi_i(b) = |u_{ii}(b - \hat{x}_i) + a_i|^2 \tag{10.83l}$$

$$\quad \texttt{for}\quad m = 1, 2\quad \texttt{do} \tag{10.83m}$$

$$\qquad \check{t}_i = b_m \tag{10.83n}$$

$$\qquad J_i = J_{i+1} + \phi_i(\check{t}_i) \tag{10.83o}$$

$$\qquad \texttt{if}\quad J_i < \rho J_{\min}\quad \texttt{then} \tag{10.83p}$$

$$\qquad\quad \texttt{if}\quad i > 0 \text{ and } \frac{\|(\tilde{\mathbf{H}})_i\|^2}{\sigma_w^2} > \gamma\quad \texttt{then} \tag{10.83q}$$

$$\qquad\qquad \texttt{Calculate}\quad J_{i-1} \tag{10.83r}$$

```
      else
```

$$\qquad\qquad J_{\min} = \min(J_i, J_{\min}) \tag{10.83s}$$

$$\qquad\qquad \texttt{for}\quad j = 1, \cdots, r \tag{10.83t}$$

$$\qquad\qquad\quad \hat{J}_{j\check{t}_j} = \min\{\hat{J}_{j\check{t}_j}, J(\check{\mathbf{t}})\},\ j = 1, \cdots, r \tag{10.83u}$$

$$\qquad\qquad \texttt{end}\quad \texttt{for} \tag{10.83v}$$

```
      end  if
    end  if
  end  for
end  function
```

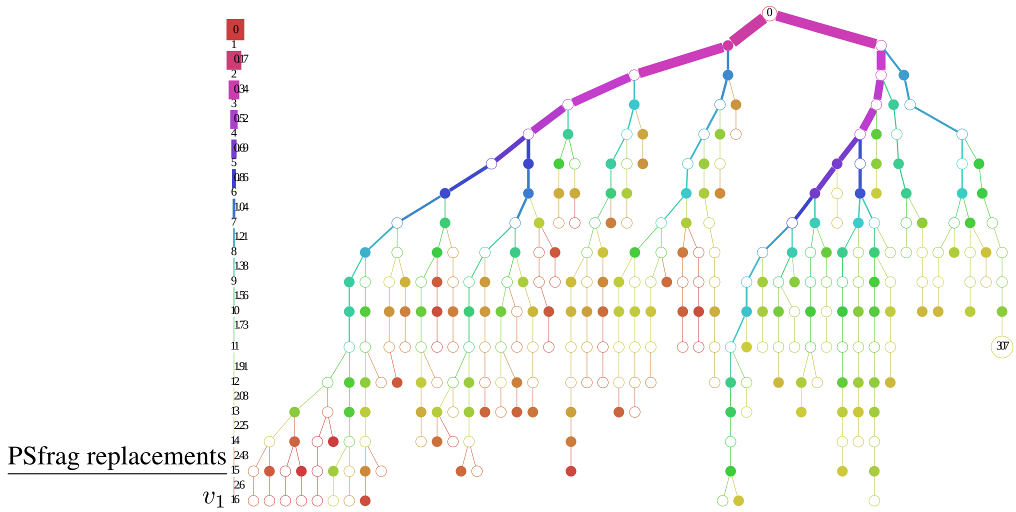

Figure 10.12: Example of a search tree formed by the SOPHIE SDM detector of Algorithm 4 in the scenario of QPSK, $m_\mathrm{t} = n_\mathrm{r} = 8$ and an average SNR of 6 dB. The approximate Log-MAP solution is attained in 307 evaluation steps in comparison to $32 \cdot 2^{15} = 1,048,576$ evaluation steps required by the exhaustive Log-MAP search. For more details on the notations employed in the diagram see the caption of Figure 10.9.

Example 6 (SOPHIE 16QAM 1x1)

In this example we would like to demonstrate two major points, namely

1) the applicability of the SOPHIE detection method of Algorithm 6 in the context of systems employing high-throughput modulation schemes, such as M-QAM, as well as

2) the advantage of employing SOPHIE detection in the SISO M-QAM scenario.

Consider a 16-QAM SISO-OFDM system. Specifically, we have a scalar complex-valued linear system described by Equation (10.7), where the corresponding transmitted signal $\mathbf{s}$, the received signal $\mathbf{y}$ and the (1×1)-dimensional channel matrix $\mathbf{H}$ are exemplified by the values

$$\mathbf{s} = -3 + 1\jmath, \quad \mathbf{y} = -0.57 + 4.08\jmath \quad \text{and} \quad \mathbf{H} = [0.8 - 1.2\jmath]. \tag{10.84}$$

Observe that the transmitted symbol s belongs to the unnormalised 16-QAM constellation obtained by multiplying the transmitted bit-vector $\mathbf{t}$ to the corresponding quantisation vector $\mathbf{q}$ depicted in Table 10.2. Firstly, we apply the brute-force Log-MAP QAM demodulation technique. Namely, for each transmitted bit t_i we calculate the log-likelihood ratio (LLR) value

$$\log\left(\frac{p(t_i = 0|y, H)}{p(t_i = 0|y, H)}\right) = \log\left(\frac{\sum_{\check{s}\in\mathcal{M}_0}\left(\frac{|y-H\check{s}|^2}{\sigma_w^2}\right)}{\sum_{\check{s}\in\mathcal{M}_1}\left(\frac{|y-H\check{s}|^2}{\sigma_w^2}\right)}\right) \tag{10.85}$$

for each of the 16 legitimate signal candidates $\check{s}$. Then we calculate the corresponding value of the objective function as follows

$$J(\check{s}) = \|y - H\check{s}\|^2. \tag{10.86}$$

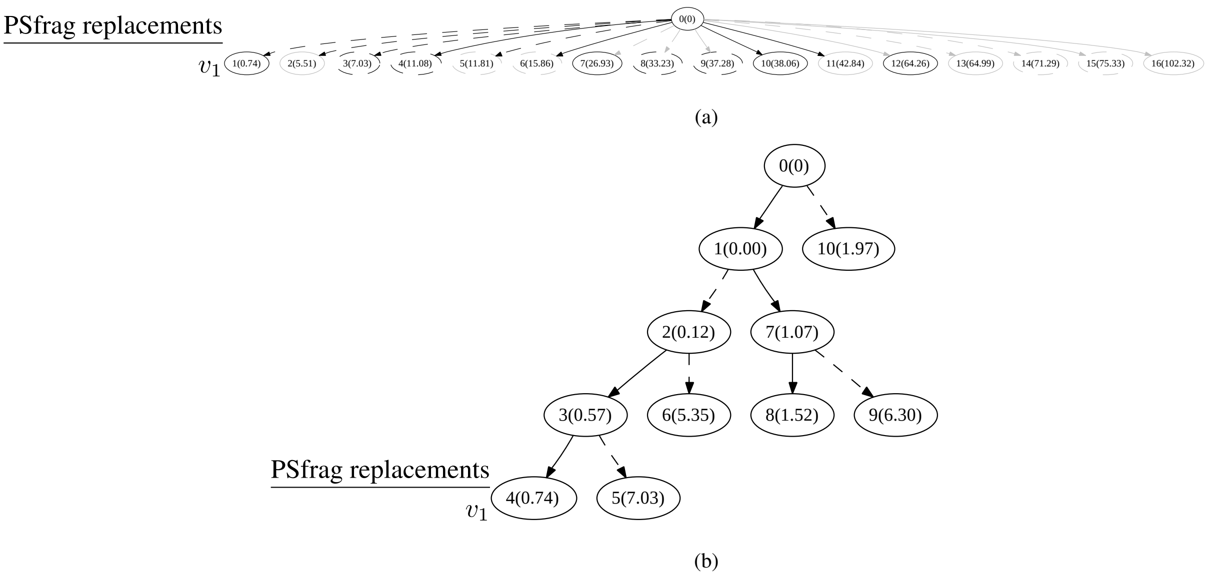

Figure 10.13: Examples of a search tree formed by the (a) OHRSA-ML and (b) BW-OHRSA-ML SDM detectors in the scenario of a system employing QPSK modulation, $m_{\rm t} = n_{\rm r} = 3$ transmit and receive antennas and encountering average SNRs of 10dB. The labels indicate the order of execution, as well as the corresponding value $J_i(\check{\mathbf{s}}_i)$ of the CSC function of Equation (10.22), as seen in the brackets.

10.4.5.1 Complexity Analysis.

As pointed out in [90] , "the brute-force" ML SDM detection method does not provide a feasible solution to the generic SDM detection problem, as a result of the excessive associated computational complexity. More explicitly, the ML SDM detector advocated in [90] has a computational complexity, which is of the order of

$$\mathcal{C}_{\rm ML} = O\{M^{m_{\rm t}} \cdot (3n_{\rm r} + 2n_{\rm r}m_{\rm t})\}, \tag{10.87}$$

where $3n_{\rm r} + 2n_{\rm r}m_{\rm t}$ is the complexity associated with a single search step, namely the evaluation of the objective function value $\|\mathbf{H}\check{\mathbf{s}} - \mathbf{y}\|^2$, while $M^{m_{\rm t}}$ is the number of legitimate candidates of the transmitted signal vector $\mathbf{s}$. Clearly, the order of complexity imposed by Equation (10.87) becomes excessive for a large number of transmit antennas, for example in the case of employing 16QAM and $m_{\rm t} = n_{\rm r} = 8$ transmit and receive antennas, where the computational complexity associated with ML detection is of the order of 10^7 complex operations per channel use, or 10^9 complex operations per OFDM symbol formed by $K = 128$ subcarriers. Furthermore, the evaluation of the soft-bit information required by an efficient turbo-decoder implementation imposes a further substantial increase of the associated computational complexity. Specifically, the soft-output Log-MAP SDM detector advocated in [90] has a computational complexity, which is of the order of

$$\mathcal{C}_{\mathrm{LM}} = O\{m_{\mathrm{t}} \log_2 M \cdot 2^{m_{\mathrm{t}} \log_2 M-1} \cdot (3n_{\mathrm{r}} + 2n_{\mathrm{r}} m_{\mathrm{t}})\}. \tag{10.88}$$

On the other hand, the MMSE SDM detector derived in [90] constitutes the low-complexity SDM detector. The complexity imposed by the MMSE SDM detector of [90] may be shown to be of the order of

$$\mathcal{C}_{\mathrm{MMSE}} = O\{m_{\mathrm{t}}^3 + m_{\mathrm{t}} n_{\mathrm{r}}^2 + m_{\mathrm{t}}^2 n_{\mathrm{r}} + m_{\mathrm{t}} n_{\mathrm{r}}\}. \tag{10.89}$$

Clearly, the MMSE SDM detector's complexity is substantially lower than that associated with the ML or Log-MAP SDM detectors. Specifically, for example only 1600 complex operations are required for detecting 16QAM signals transmitted and received by $m_{\mathrm{t}} = n_{\mathrm{r}} = 8$ transmit and receive antennas. Unfortunately, however, as demonstrated in [90] , the achievable performance exhibited by the linear MMSE SDM detector is considerably lower than that attained by the optimal Log-MAP SDM detector advocated in [90] . Moreover, linear SDM detectors, such as the MMSE detector do not allow the high-integrity detection of signals in the over-loaded scenario, where the number of the transmit antennas exceeds that of the receive antennas.

Consequently, in Sections 10.4.3, 10.4.4 and 10.4.5 we derived a family of methods which combine the advantageous properties of the ML and Log-MAP detection, while imposing a substantially lower complexity. In this section we demonstrate that the computational complexity associated with the SOPHIE-aided Log-MAP SDM detector of Algorithm 6 is in fact only slightly higher than that imposed by the low-complexity MMSE SDM detector advocated in [90] , while its performance is virtually identical to the performance of the Log-MAP SDM detector [90] .

The direct calculation of the complexity associated with the OHRSA methods of Algorithms 4, 5 and 6 is infeasible, since the complexity is not a constant, but rather a random variable, which is a function of several parameters, such as the number m_{t} and n_{r} of transmit and receive antennas, the average SNR encountered as well as the value of the parameter ρ in Algorithm 6. Therefore, we perform the corresponding complexity analysis using computer simulations. Figure 10.14(a) illustrates our comparison between the computational complexity required by different SDM detection methods, namely the linear MMSE detector advocated in [90] , the SIC detector of [90, pp.754-756] , the exhaustive search-based ML and Log-MAP detectors of [90] as well as the OHRSA-aided ML, Log-MAP and SOPHIE SDM detectors of Algorithms 4, 5 and 6, respectively. The results depicted in Figure 10.14(a) correspond to the *fully-loaded* scenario, where we have $m_{\mathrm{t}} = n_{\mathrm{r}}$ transmit and receive antennas. Observe that the complexity associated with both the OHRSA-ML and SOPHIE SDM detectors is only slightly higher than that imposed by the MMSE SDM detector and is in fact lower than the complexity imposed by the SIC SDM detector.

Furthermore, the achievable performance of the SDM-OFDM system employing the different SDM detection methods considered is depicted in Figure 10.14(b). Observe that both the OHRSA-Log-MAP and SOPHIE SDM detectors considerably outperform the linear MMSE detector. Moreover, the associated BER decreases upon increasing the number of transmit and receive antennas $m_{\mathrm{t}} = n_{\mathrm{r}}$, which suggests that as opposed to both the MMSE and the SIC SDM detectors, the OHRSA-Log-MAP SDM detector is capable of achieving spatial diversity even in the *fully-loaded* system. In other words, it is capable of achieving

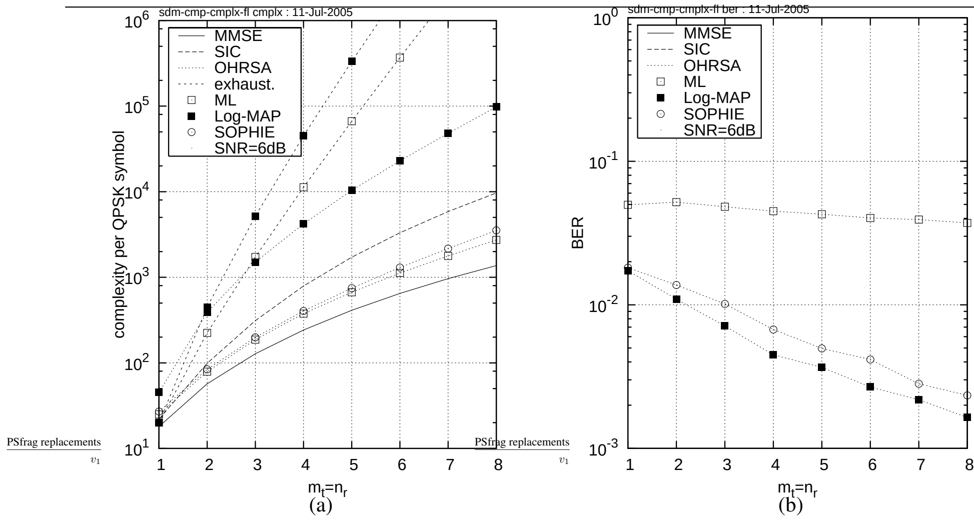

Figure 10.14: (a) **Computational complexity** quantified in terms of the total number of real multiplications and additions per detected QPSK symbol and (b) the corresponding **BER** exhibited by the rate half turbo-coded **SDM-QPSK-OFDM** system employing the different SDM detection methods considered at SNR=6dB. The abscissa represents the number $m_{\mathrm{t}} = n_{\mathrm{r}} = 1, \cdots, 8$ of transmit and receive antenna elements. The corresponding system parameters are summarized in Table 10.3.

both multiplexing and diversity gains simultaneously, while maintaining a low computational complexity.

The relatively low performance of the OHRSA-ML SDM detector may be attributed to the fact that it produces no soft-bit information and therefore the efficiency of the turbo code employed is substantially degraded. Moreover, observe that while the SIC SDM detector outperforms its MMSE counterpart at high SNR values [90], the achievable performance of the two methods is fairly similar at low SNR values, such as 6dB.

Additionally, Figure 10.15 illustrates the complexity imposed by the OHRSA methods of Algorithms 4, 5 and 6 as a function of the average SNR encountered. Figures 10.15 (a) and (b) portray the average complexity encountered in the scenatios of $m_{\mathrm{t}} = n_{\mathrm{r}} = 8$ and $m_{\mathrm{t}} = 8, n_{\mathrm{r}} = 4$ transmit and receive antennas, respectively. Observe that the complexity associated with both the OHRSA-ML and SOPHIE methods of Algorithms 5 and 6 is mainly determined by the number m_{t} of transmit antennas employed. Furthermore, the complexity associated with the SOPHIE method closely matches that exhibited by the OHRSA-ML method at high SNR values and the complexity exhibited by both methods is only slightly higher than the complexity exhibited by the low-complexity MMSE SDM detector.

10.4.5.2 Performance Analysis

In this section we present our simulation results characterising the SDM-OFDM system employing the OHRSA-aided SDM detection schemes described in Section 10.4. Our simulations were performed in the base-band frequency domain and the system configuration characterised in Table 10.3 is to a large extent similar to that used in [361]. We assume having

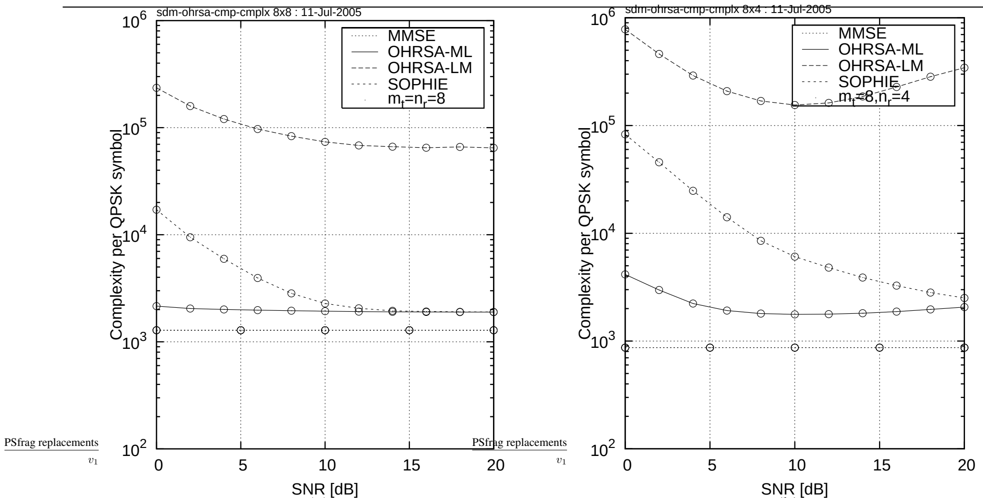

(a) (b)

Figure 10.15: Computational complexity quantified in terms of the total number of real multiplications and additions per detected QPSK symbol. We consider the **OHRSA-ML, OHRSA-Log-MAP** and **SOPHIE** SDM detection methods of Algorithms 4, 5 and 6, respectively. Additionally, we show the corresponding computational complexity required by the low-complexity linear MMSE SDM detector. The abscissa represents the average SNR encountered.

Table 10.3: System parameters.

Parameter	OFDM	MC-CDMA
Channel bandwidth	800 kHz	
Number of carriers K	128	
Symbol duration T	160 μs	
Max. delay spread τ_{max}	40 μs	
Channel interleaver	WCDMA [375] 248 bit	–
Modulation	QPSK	
Spreading scheme	–	WH
FEC component codes code interleaver	Turbo code [216] , rate 1/2 RSC, K=3(7,5) WCDMA (124 bit)	

a total bandwidth of 800kHz. The OFDM system utilises 128 orthogonal subcarriers. For forward error correction (FEC) we use 1/2-rate turbo coding [216] employing two constraint-length $K = 3$ Recursive Systematic Convolutional (RSC) component codes [375]. The octally represented RCS generator polynomials of (7,5) were used. Finally, throughout this chapter we stipulate the assumption of perfect channel knowledge, where the knowledge of the frequency-domain subcarrier-related coefficients $H[n, k]$ is deemed to be available in the receiver. Figure 10.16 characterises the achievable performance as well as the associated

PSfrag replacements
v_1

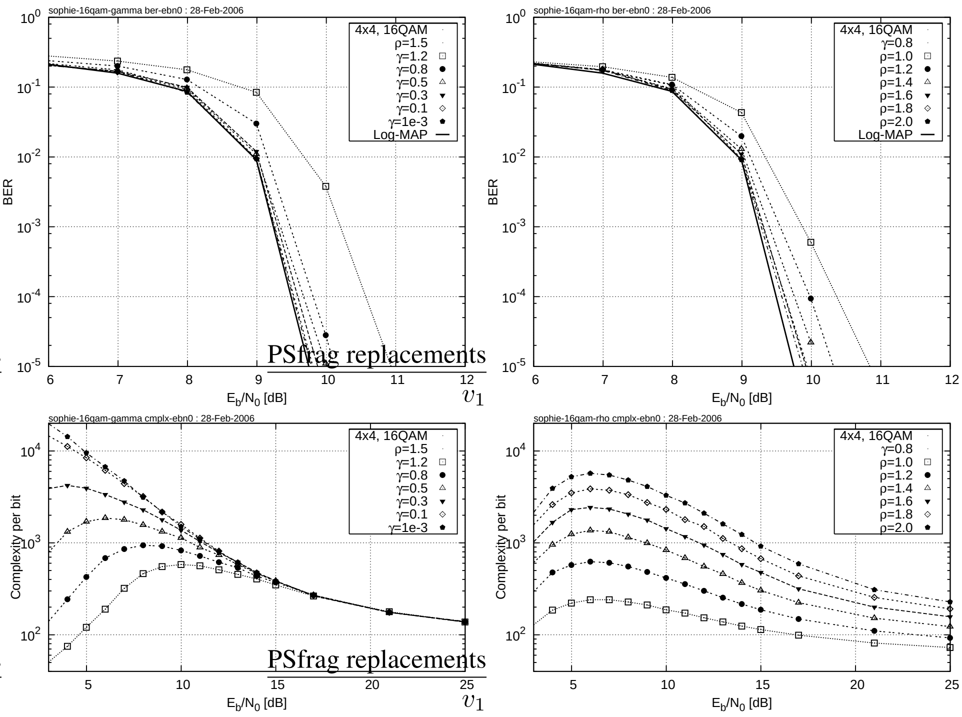

PSfrag replacements
v_1

(a) (b)

Figure 10.16: Bit Error Rate (top) and the associated **computational complexity per detected bit** (bottom) exhibited by the 4×4 **16QAM-SDM-OFDM** system employing a **SOPHIE** SDM detector of Algorithm 6. (a) assuming different values of parameters (a) γ and (b) ρ. The abscissa represents the average E_b/N_0 recorded at the receive antenna elements.

computational complexity exhibited by the 4×4 16QAM-SDM-OFDM system employing the SOPHIE SDM detector of Algorithm 6. More specifically, we analyse the associated performance versus complexity trade-offs of using various values of the complexity-control parameters ρ and γ. In Figure 10.16(a) we can observe how the achievable BER performance (top) and the corresponding computational complexity depend on the value of the parameter γ. Using the results depicted in Figure 10.16(a) we may conclude that the optimum choice of the complexity-control parameter γ lies in the range $0.5 - 0.8$, where we have a minor BER performance degradation of less than 0.5 dB, while achieving up to two orders of magnitude complexity reduction at low SNR values, when compared to the full-complexity SOPHIE algorithm assuming $\gamma = 0$.

On the other hand, Figure 10.16(b) portrays both the achievable BER performance and the associated compexity of the 4×4 16QAM-SDM-OFDM system for different values of the complexity-control parameter ρ. We may conclude that the optimum trade-off between the attainable BER performance and the associated complexity is achieved, when the value of the complexity-control parameter ρ lies in the range of $1.3 - 1.5$, where the BER performance degradation imposed does not exceed 0.5 dB, while the associated computational complexity is reduced by more than an order of magnitude, when compared to large values of ρ, such as for instance $\rho = 2.0$.

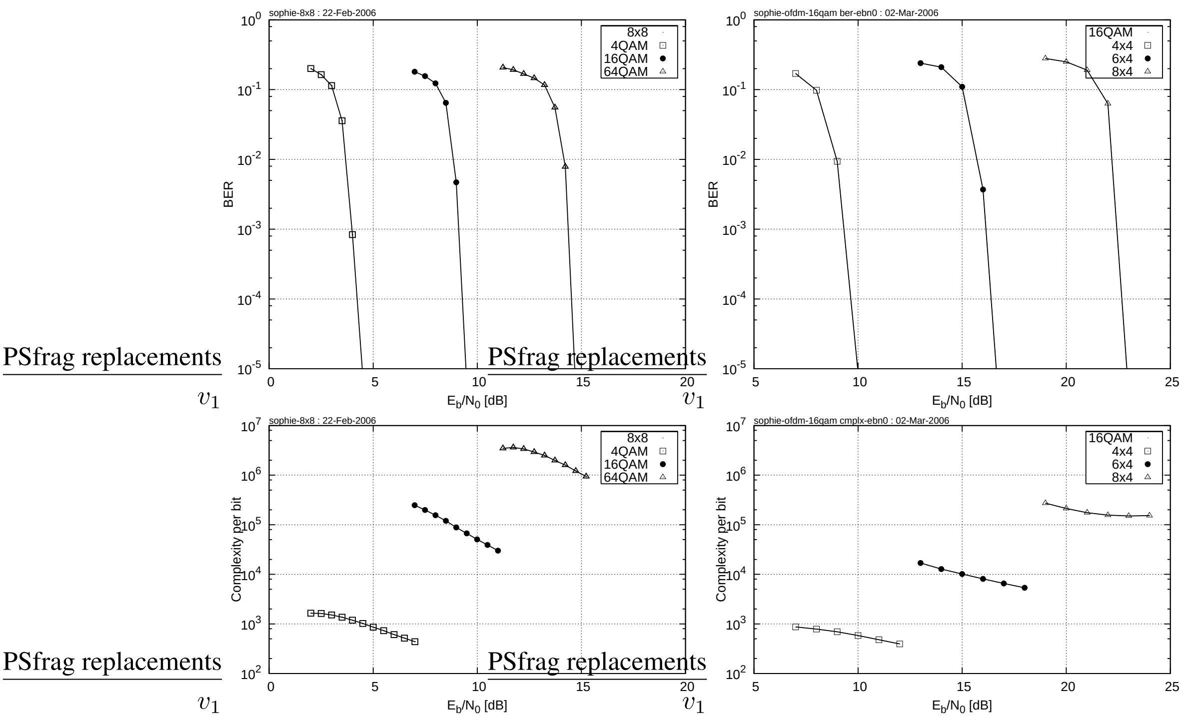

(a) (b)

Figure 10.17: Bit Error Rate (top) and the associated **computational complexity per detected bit** (botom) exhibited by the **SDM-OFDM** system employing a **SOPHIE** SDM detector of Algorithm 6assuming different values of parameters (a) γ and (b) ρ. The abscissa represents the average E_b/N_0 recorded at the receive antenna elements.

Furthermore, Figure 10.17(a) demonstrates both the BER performance (top) and the associated computational complexity exhibited by the (8×8) 4, 16 and 64QAM SDM-OFDM systems employing the SOPHIE SDM detector of Algorithm 6. Figure 10.17(b) characterises the 16QAM-SDM-OFDM system employing the SOPHIE SDM detector of Algorithm 6 and having a constant number of $n_{\mathrm{r}} = 4$ receive antenna elements in terms of its ability to detect the multiplexed signals arriving from various numbers of transmit antenna elements. Specifically, we aim for exploring the performance of the SOPHIE SDM detector in the overloaded system scenario, where the number of transmit antenna elements exceeds that of the receiver elements and thus we have $m_{\mathrm{t}} > n_{\mathrm{r}}$. Indeed, the BER curves portrayed in Figure 10.17 (top) confirm the near-Log-MAP performance of the SOPHIE SDM detector of Algorithm 6 in both systems employing high-throughput modulation schemes as well as in the overloaded system scenario.

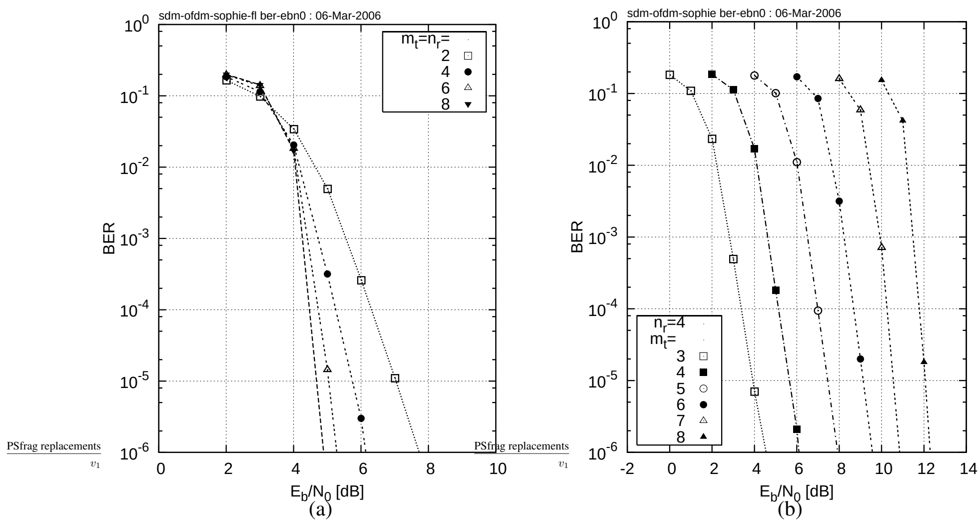

Figure 10.18: Bit Error Rate exhibited by the **SDM-QPSK-OFDM** system employing **SOPHIE** SDM detector of Algorithm 6 in (a) fully-loaded scenario with $m_{\mathrm{t}} = n_{\mathrm{r}} = 2, 4, 6$ and 8 transmit and receive antennas, as well as (b) overloaded scenario with fixed number of $n_{\mathrm{r}} = 4$ receive antennas and $m_{\mathrm{t}} = 3, 4, \cdots, 8$ transmit antennas. The abscissa represents the average value of E_b/N_0 recorded at the receive antenna elements and.

Figure 10.18(a) demonstrates that the SDM-OFDM system employing the SOPHIE SDM detector of Algorithm 6 is capable of exploiting the available MIMO channel's multiplexing gain in the fully loaded system scenario, when the number of the transmit antenna elements m_{t} is equal to that of the receiver antenna elements n_{r}. More specifically, the results depicted in Figure 10.18(a) suggest that the SDM-OFDM SOPHIE SDM detector having $m_{\mathrm{t}} = n_{\mathrm{r}} = 8$ transmit and receive antennas exhibits an SNR-related diversity gain of 2dB at the target BER of 10^{-4}, as well as a factor four higher throughput, when compared to the same system employing two antennas at both the transmitter and receiver.

Additionally, Figure 10.18(b) characterises the SDM-OFDM system employing the SOPHIE SDM detector of Algorithm 6 and having a constant number of $n_{\mathrm{r}} = 4$ receive antenna elements in terms of its ability to detect the multiplexed signals arriving from various numbers of transmit antenna elements. Specifically, we aim for exploring the performance of the SOPHIE SDM detector in the over-loaded system scenario, where the number of transmit antenna elements exceeds that of the receiver elements and thus we have $m_{\mathrm{t}} > n_{\mathrm{r}}$. We can see that as opposed to the MMSE SDM detector [90] , the SOPHIE SDM detector exhibits a good performance both when we have $m_{\mathrm{t}} \leq n_{\mathrm{r}}$, as well as in the over-loaded system scenario, when the number of transmit antenna elements exceeds the number of the receive antenna elements, i.e. when we have $m_{\mathrm{t}} > n_{\mathrm{r}}$.

10.5 Chapter Summary and Conclusion

In this chapter we proposed a novel OHRSA-aided SDM detection method, which may be regarded as an advanced extension of the CSD method. The algorithm proposed extends the potential range of applications of the CSD methods, as well as reducing the associated computational complexity, rendering the algorithm proposed a feasible solution for implementation in high-throughput practical systems.

Furthermore, we have shown that the OHRSA-aided SDM detector proposed combines the advantageous properties of both the optimum-performance Log-MAP SDM detector and that of the low-complexity linear MMSE SDM detector, which renders it an attractive alternative for implementation in practical systems. More specifically, we have shown that the OHRSA-aided SDM detector proposed exhibits the following advantageous properties.

The method can be employed in the over-loaded scenario, where the number of transmit antenna elements exceeds that of the receive antenna elements, while the associated computational complexity increases only moderately even in heavily over-loaded scenarios and is almost independent of the number of receive antennas. Furthermore, as opposed to standard CSD schemes [176], no calculation of the sphere radius is required and therefore the method proposed is robust to the particular choice of the initial parameters both in terms of the achievable performance and the associated computational complexity. The overall computational complexity required is only slightly higher than that imposed by the linear MMSE multi-user detector designed for detecting a similar number of users. Specifically, the computational complexity per detected QAM symbol associated with both the MMSE and SOPHIE SDM detectors is of the order of $O\{m_{\rm t}^3\}$, where $m_{\rm t}$ is the number of transmit antennas. Finally, the associated computational complexity is fairly independent of the channel conditions quantified in terms of the SNR encountered.

In our future work the achievable performance of the SDM detection schemes proposed will be explored in the presence of imperfect channel state information. More explicitly, we will characterise and analyse the performance of a range of channel estimation methods suitable for employment in the SDM-OFDM system considered in this chapter. Subsequently, we will analyse the achievable performance of the SDM detection methods portrayed in this chapter in the context of the SDM-OFDM system employing our channel estimation schemes.

Additionally, an iterative joint SDM detection and decoding scheme, which can potentially approach the information-theoretic capacity bound will be designed. Furthermore, joint iterative turbo-structured SDM detection, decoding and channel estimation methods will be explored.

Chapter 13

Conclusion and Further Research Problems [1]

13.1 Summary and Conclusions of Part I

13.1.1 Summary of Part I

In Chapters 2 - 4 we discussed the basic implementational, algorithmic and performance aspects of orthogonal frequency division multiplexing in predominantly duplex mobile communications environments. Specifically, following a rudimentary introduction to OFDM in Chapter 2, in Chapter 3 we further studied the structure of an OFDM modem and we investigated the problem of the high peak-to-mean power ratio observed for OFDM signals, and that of clipping amplification caused by insufficient amplifier back-off. We investigated the BER performance and the spectrum of the OFDM signal in the presence of clipping, and we have seen that for an amplifier back-off of 6 dB the BER performance was indistinguishable from the perfectly amplified case. We investigated the effects of quantisation of the time domain OFDM signal. The effects of phase noise on the OFDM transmission were studied, and two-phase noise models were suggested. One model was based on white phase noise, only relying on the integrated phase jitter, while a second model used coloured noise, which was generated from the phase noise mask.

In Chapter 4 we studied OFDM transmissions over time-dispersive channels. The spectrum of the transmitted frequency domain symbols is multiplied with the channel's frequency domain channel transfer function, hence the amplitude and phase of the received subcarriers are distorted. If the channel is varying significantly during each OFDM symbol's duration, then additional inter-subcarrier interference occurs, affecting the modem's performance. We have seen the importance of channel estimation on the performance of coherently detected OFDM, and we have studied two simple pilot-based channel estimation schemes. Differentially detected modulation can operate without channel estimation, but exhibits lower BER performance than coherent detection. We have seen that the signal-to-noise ratio is not con-

OFDM and MC-CDMA: A Primer. L.Hanzo, T. Keller, ©2006 John Wiley & Sons, Ltd. ISBN 0-470-03007-0

stant across the OFDM symbol's subcarriers, and that this translates into a varying bit error probability across the different subcarriers.

The effects of timing and frequency errors between transmitter and receiver were studied in Chapter 5. We saw that a timing error results in a phase rotation of the frequency domain symbols, and possibly inter-OFDM-symbol interference, while a carrier frequency error leads to inter-subcarrier interference. We suggested the introduction of a cyclic postamble, in order to suppress inter-OFDM-symbol interference for small timing errors, but we saw that frequency errors higher than 5% of the subcarrier separation lead to severe performance losses. In order to combat this, we investigated a set of frequency- and timing-error estimation algorithms. We suggested a time domain-based joint time and frequency error acquisition algorithm, and studied the performance of the resulting system over fading time-dispersive channels.

Based on the findings of Chapter 4 we investigated adaptive modulation techniques to exploit the frequency diversity of the channel. Specifically, in Chapter 6, three adaptive modulation algorithms were proposed and their performance was investigated. The issue of signalling was discussed, and we saw that adaptive OFDM systems require a significantly higher amount of signalling information than adaptive serial systems. In order to limit the amount of signalling overhead, a sub-band adaptive scheme was suggested, and the performance trade-offs against a subcarrier-by-subcarrier adaptive scheme were discussed. Blind modulation mode detection schemes were investigated, and combined with an error correction decoder. We saw that by combining adaptive modulation techniques with a strong convolutional turbo channel codec significant system throughput improvements were achieved for low SNR values. Finally, frequency domain pre-distortion techniques were investigated in order to pre-equalise the time-dispersive channel's transfer function. We saw that by incorporating pre-distortion in adaptive modulation, significant throughput performance gains were achieved compared to adaptive modems without pre-equalisation.

13.1.2 Conclusions of Part I

(1) Based on the implementation-oriented characterisation of OFDM modems, leading to a real-time testbed implementation and demonstration at 34 Mbps we concluded that OFDM is amenable to the implementation of high bit rate wireless ATM networks, which is underlined by the recent ratification of the HIPERLAN II standard.

(2) The range of proposed joint time and frequency synchronisation algorithms efficiently supported the operation of OFDM modems in a variety of propagation environments, resulting in virtually no BER degradation in comparison to the perfectly synchronised modems. For implementation in the above-mentioned 34 Mbps, real-time testbed simplified versions of these algorithms were invoked.

(3) Symbol-by-symbol adaptive OFDM substantially increases the BPS throughput of the system at the cost of moderately increased complexity. It was demonstrated in the context of an adaptive real-time audio system that this increased modem throughput can be translated into improved audio quality at a given channel quality.

(4) The proposed blind symbol-by-symbol adaptive OFDM modem mode detection algorithms were shown to be robust against channel impairments in conjunction with

twin-mode AOFDM. However, it was necessary to combine it with higher-complexity channel coding based mode detection techniques, in order to maintain sufficient robustness, when using quadruple-mode AOFDM.

(5) The combination of frequency domain pre-equalisation with AOFDM resulted in further performance benefits at the cost of a moderate increase in the peak-to-mean envelope flluctuation and system complexity.

13.2 Summary and Conclusions of Part II

13.2.1 Summary of Part II

Since their initial introduction in 1993 [70, 73, 263, 264], multi-carrier spread-spectrum systems have attracted significant research interest. Existing advanced techniques originally developed for DS-CDMA and OFDM have also been applied to MC-CDMA, while a range of new unique techniques have been proposed for solving various problems specific to multi-carrier CDMA systems. The first two chapters of Part II, namely Chapters 7 and 8, reviewed the basic concepts of MC-CDMA and the various spreading sequences applicable to MC-CDMA transmissions. Chapter 9 characterised the achievable performance of MC-CDMA schemes employing various detectors. A number of further topics closely related to MC-CDMA based communications were also investigated in depth.

Part II of the book concentrated on investigating the MC-CDMA scheme of [70, 71, 73], which constitutes a specific family of the three different multi-carrier CDMA types often used in the literature [90]. This technique was advocated, because MC-CDMA results in the lowest BER among the three schemes investigated in a similar scenario [312]. Our investigations concentrated on the downlink, because in the uplink stringent synchronisation of the mobile terminals has to be met. Future research should extend the results of Chapter 6 to both multi-carrier DS-CDMA [263] and to multi-tone (MT) CDMA [264], as well as to the family of more sophisticated adaptive MC-CDMA schemes [300].

13.2.2 Conclusions of Part II

The main contributions and conclusions of Part II of the book emerge from Section 9.4.3, where the performance of Space-Time (ST) block coded constant-power adaptive multi-carrier modems employing the optimum SNR-dependent modem mode switching levels derived in Chapter 12 of [90] were investigated [334, 466]. As expected, it was found that ST block coding reduces the relative performance advantage of adaptive modulation, since it increases the diversity order and eventually reduces the channel quality variations, as it can be observed in Figure 13.1(a).*Having observed that 1-Tx aided AOFDM and 2-Tx ST coding aided fixed-mode MC-CDMA resulted in a similar BPS throughput performance, we concluded that fixed-mode MC-CDMA in conjunction with 2-Tx ST coding could be employed, provided that we could afford the associated complexity. By contrast, AOFDM could be a low complexity alternative of counteracting the near-instantaneous channel quality variations.* When turbo convolutional coding was concatenated to the ST block codes, near-error-free transmission was achieved at the expense of halving the average throughput, as seen in Figure 13.1(b) . Compared to the uncoded system, the turbo coded system was capable

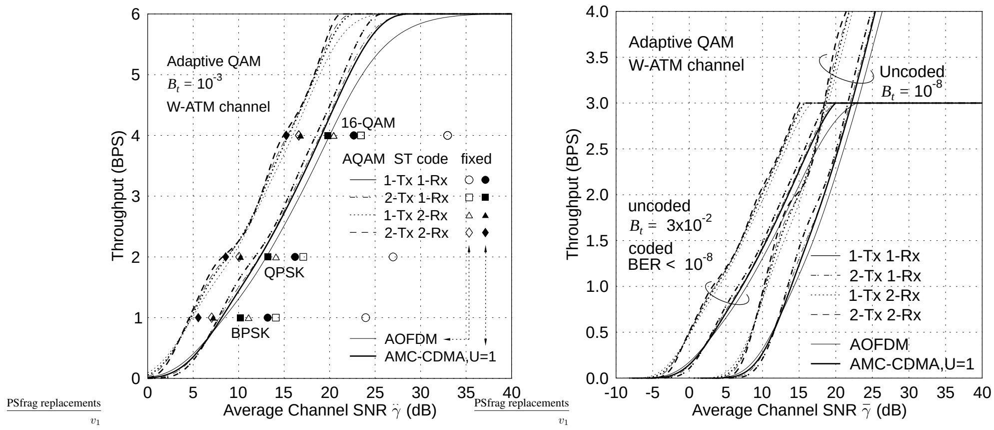

(a) With ST coding

(b) With ST and turbo coding

Figure 13.1: The BPS throughput performance of five-mode AOFDM and AMC-CDMA for communicating over the W-ATM channel [2, pp.474]. (a) The SNR gain of the adaptive modems decreases, as the diversity of the ST coding increases. The BPS curves appear in pairs, corresponding to AOFDM and AMC-CDMA - indicated by the thin and thick lines, respectively - for each of the four different ST code configurations. The markers represent the SNRs required by the fixed-mode OFDM and MC-CDMA schemes for maintaining the target BER of 10^{-3} in conjunction with the four ST-coded schemes considered. (b) The turbo convolutional coding assisted adaptive modems have SNR gains up to 7dB compared to their uncoded counterparts achieving a comparable average BER.

of achieving a higher throughput in the low SNR region at the cost of a higher complexity. Our study of the relationship between the uncoded BER and the corresponding coded BER showed that adaptive modems obtain higher coding gains, than that of fixed modems. This was due to the fact that the adaptive modem avoids burst errors even in deep channel fades by reducing the number of bits per modulated symbol eventually to zero.

13.3 Summary and Conclusions of Part III

13.3.1 Near-ML Enhanced Sphere Detection of MIMO-OFDM

In Chapter 10 we proposed a novel OHRSA-aided SDM detection method, which may be regarded as an advanced extension of the Complex Sphere Detector. The algorithm proposed extends the potential range of applications of the CSD methods, as well as reducing the associated computational complexity, rendering the algorithm proposed a feasible solution for implementation in practical systems.

Furthermore, we demonstrated that the OHRSA-aided SDM detector proposed combines the advantageous properties of both the optimum-performance Log-MAP SDM detector and the minimum-complexity linear MMSE SDM detector, which renders it an attractive alternative for implementation in practical systems. More specifically, we have shown that the OHRSA-aided SDM detector proposed exhibits the following advantageous properties.

The method can be employed in the over-loaded scenario, where the number of transmit antenna elements exceeds that of the receive antenna elements, while the associated computational complexity increases only moderately even in heavily overloaded scenarios and is almost independent of the number of receive antennas. Furthermore, as opposed to standard CSD schemes [176], no calculation of the sphere radius is required and therefore the method proposed is robust to the particular choice of the initial parameters both in terms of the achievable performance and the associated computational complexity. The overall computational complexity required is only slightly higher than that imposed by the linear MMSE multiuser detector designed for detecting a similar number of users. Specifically, the computational complexity per detected QAM symbol associated with both the MMSE and SOPHIE SDM detectors is of the order of $O\{m_\mathrm{t}^3\}$, where m_t is the number of transmit antennas. Finally, the associated computational complexity is fairly independent of the channel conditions quantified in terms of the SNR encountered.

In our future work the achievable performance of the SDM detection schemes proposed will be explored in the presence of imperfect channel state information. More explicitly, we will characterize and analyse the performance of a range of channel estimation methods suitable for employment in the SDM-OFDM system considered in this chapter. Subsequently, we will analyse the achievable performance of the SDM detection methods portrayed in this chapter in the context of the SDM-OFDM system employing our channel estimation schemes.

Additionally, an iterative joint SDM detection and decoding scheme, which can potentially approach the information-theoretic capacity bound will be designed. Furthermore, joint iterative turbo-structured SDM detection, decoding and channel estimation methods will be explored.

13.3.2 GA-Aided Joint MUD and Channel Estimation

From the investigations and discussions conducted in Chapter 11 we conclude that the proposed GA-aided iterative joint channel estimation and multi-user detection scheme generating soft outputs constitutes an effective solution to the channel estimation problem in multi-user MIMO SDMA-OFDM systems. Furthermore, the GA-JCEMUD is capable of exhibiting a robust performance in overloaded scenarios, where the number of users is higher than the number of receiver antenna elements, either with or without FEC coding. This attractive property enables the SDMA-OFDM system to potentially support an increased number of users. Our future research will consider the design of similar downlink systems.

13.3.3 GA-Aided MBER MUD

In Chapter 12 we demonstrated that GAs may be applied in the context of an SDMA-OFDM system for determining the MBER MUD's weight vectors. The GA-aided system has an edge over the conjugate gradient algorithm based system, because it does not require an initial SDMA array weight solution. Unlike the MMSE MUD of Chapter 12 in [90], the MBER MUD is capable of supporting more users than the number of receiver antennas. It was also shown that the GA is capable of approaching the exact MBER solution at a lower complexity than the conjugate gradient algorithm. Our future work will aim for finding more efficient adaptive weight optimisation algorithms in the context of LDPC-coded SDMA-OFDM systems.

13.4 Closing Remarks

This monograph has considered a range of OFDM and MC-CDMA-related topics applicable to both single-user and multi-user communications. However, a whole host of further recent advances in the field of communications research are applicable also to OFDM. Specifically, the family of classification and learning-based neural network-assisted receivers investigated in the context of conventional single-carrier systems provides a rich set of further research topics. Partial response modulation techniques also promise performance advantages in OFDM schemes. The joint optimisation of adaptive subcarrier bit-allocation and crest-factor reduction techniques constitutes a further research challange in the context of multi-user OFDM and MC-CDMA systems. All the above-mentioned techniques have the potential of improving the complexity versus performance balance of the system. The design of joint coding and modulation schemes is particularly promising in the context of OFDM and MC-CDMA. Finally, the use of OFDM in ultra-wide band systems invoking various frequency-hopping and multiple access techniques is likely to grow in popularity as an exciting research area.

These enabling techniques along with those detailed in the book are expected to find their way into future standards, such as the successors of the 802.11, the High Performance Local Area Network standard known as HiPerLAN, the European Digital Audio Broadcast (DAB) and Digital Video Broadcast (DVB) arrangements and their descendants. They are also likely to be adopted by the standardisation bodies in future generations of personal communications systems.

It is expected that wireless systems of the near future are likely to witness the co-existence of space-time-coded transmit diversity arrangements and near-instantaneously adaptive OFDM as well as MC-CDMA schemes for years to come. Intelligent learning algorithms will configure the transceivers in the appropriate mode that ultimately provides the best trade-off in terms of satisfying the user's preference in the context of the service requested [7, 215, 217].

A further advantage of the near-instantaneously adaptive OFDM and MC-CDMA transceivers is that they allow the system to instantaneously drop its transmission rate, when the channel quality is reduced, for example, as a consequence of the instantaneously peaking co-channel interference. By contrast, a conventional fixed-mode transceiver would drop the call and hence degrade both the quality of service and the network's teletraffic capacity. The achievable teletraffic performance of adaptive CDMA systems was documented in depth in conjunction with adaptive antenna-assisted dynamic channel allocation schemes in [217].[2]

∗ ∗

Throughout this monograph we endeavoured to depict the range of contradictory system design trade-offs associated with the conception of OFDM and MC-CDMA systems. Our

[2] A range of related research papers and book chapters can be found at http://www-mobile.ecs.soton.ac.uk.

intention was to present the material in an unbiased fashion and sufficiently richly illustrated in terms of the associated design trade-offs so that readers will be able to find recipes and examples for solving their own particular wireless communications problems. In this rapidly evolving field it is a challenge to complete a timely, yet self-contained treatise, since new advances are being discovered at an accelerating pace, which the authors would like to report on. Our sincere hope is that you, dear readers, have found the book a useful source of information, but above all a catalyst for further research.

Glossary

ACF	Auto-correlation Function
ACTS	Advanced Communications Technologies and Services - a European research programme
ADSL	Asynchronous Digital Subscriber Loop
AOFDM	Adaptive Orthogonal Frequency Division Multiplexing
APR	A Priori
APT	A Posteriori
AWGN	Additive White Gaussian Noise
BER	Bit-Error Ratio
BLAST	Bell Labs Space-Time architecture
BPOS	Bit Per OFDM Symbol
BPSK	Binary Phase-Shift Keying
BS	Base Station
CDF	Cumulative Distribution Function
CDMA	Code-Division Multiple Access
CE	Channel Estimation
CIR	Channel Impulse Response
DAB	Digital Audio Broadcasting
DDCE	Decision-Directed Channel Estimation

DDCP	Decision-Directed Channel Prediction
DFT	Discrete Fourier Transform
DMUX	Demultiplexer
DTTB	Digital Terrestrial Television Broadcast
D-BLAST	Diagonal BLAST
EM	Expectation Maximisation
EVD	EigenValue Decomposition
FDM	Frequency Division Multiplexing
FDMA	Frequency Division Multiple Access
FEC	Forward Error Correction
FFT	Fast Fourier Transform
FIR	Finite Impulse Response
HF	High-Frequency
ICI	Inter-subCarrier Interference
IDFT	Inverse Discrete Fourier Transform
IFFT	Inverse Fast Fourier Transform
IIR	Infinite Impulse Response
ISI	Inter-Symbol Interference
IWHT	Inverse Walsh Hadamard Transform
KLT	Karhunen-Loeve Transform
LLR	Log-Likelihood Ratio
LS	Least-Squares
LSE	Least-Squares Error
MA	Multiple Access
MC	Multi-Carrier
MIMO	Multiple-Input Multiple-Output
ML	Maximum Likelihood

MLSE	Maximum Likelihood Sequence Estimation
MMSE	Minimum Mean-Square Error
MSE	Mean-Square Error
MU	Multi-User
MUD	Multi-User Detection
MUI	Multi-User Interference
MUX	Multiplexer
MV	Minimum Variance
MVDR	Minimum Variance Distortionless Response
OFDM	Orthogonal Frequency Division Multiplexing
PAPR	Peak-to-Average Power Ratio
PDF	Probability Density Function
PIC	Parallel Interference Cancellation
PSAM	Pilot Symbol Aided Modulation
PSD	Power Spectral Density
PSK	Phase-Shift Keying
QAM	Quadrature Amplitude Modulation
QPSK	Quadrature Phase-Shift Keying
RLS	Recursive Least-Squares
RNS	Residue Number System
SB	Subband
SDM	Space Division Multiplexing
SDMA	Space Division Multiple Access
SDI	Selective Decision Insertion
SER	Symbol Error Ratio
SIC	Successive Interference Cancellation
SINR	Signal-to-Interference-plus-Noise Ratio

SIR	Signal-to-Interference Ratio
SMI	Sample Matrix Inversion
SNR	Signal-to-Noise Ratio
STC	Space-Time Coding
SVD	Singular-Value Decomposition
TCM	Trellis-Coded Modulation
TDD	Time-Division Duplexing
TDMA	Time-Division Multiple Access
TTCM	Turbo-Trellis Coded Modulation
V-BLAST	Vertical BLAST
WATM	Wireless Asynchronous Transfer Mode
WHT	Walsh-Hadamard Transform
WHTS	Walsh-Hadamard Transform Spreading
ZF	Zero-Forcing
1D	One-Dimensional
2D	Two-Dimensional

Bibliography

[1] R. W. Chang, "Synthesis of band-limited orthogonal signals for multichannel data transmission," *Bell Systems Technical Journal*, vol. 46, pp. 1775–1796, December 1966.

[2] L. Hanzo, W. Webb, and T. Keller, *Single- and Multi-carrier Quadrature Amplitude Modulation*. New York, USA: John Wiley and IEEE Press, April 2000.

[3] W. Webb and R. Steele, "Variable rate QAM for mobile radio," *IEEE Transactions on Communications*, vol. 43, pp. 2223–2230, July 1995.

[4] L. Hanzo, "Bandwidth-efficient wireless multimedia communications," *Proceedings of the IEEE*, vol. 86, pp. 1342–1382, July 1998.

[5] S. Nanda, K. Balachandran, and S. Kumar, "Adaptation techniques in wireless packet data services," *IEEE Communications Magazine*, vol. 38, pp. 54–64, January 2000.

[6] L. Hanzo, F. Somerville, and J. Woodard, *Voice Compression and Communications: Principles and Applications for Fixed and Wireless Channels*. IEEE Press and John Wiley, 2001. (For detailed contents and sample chapters please refer to http://www-mobile.ecs.soton.ac.uk.).

[7] L. Hanzo, P. Cherriman, and J. Streit, *Wireless Video Communications: From Second to Third Generation Systems, WLANs and Beyond*. IEEE Press and John Wiley, 2001. (For detailed contents please refer to http://www-mobile.ecs.soton.ac.uk.).

[8] M. Zimmermann and A. Kirsch, "The AN/GSC-10/KATHRYN/variable rate data modem for HF radio," *IEEE Transactions on Communication Technology*, vol. CCM–15, pp. 197–205, April 1967.

[9] S. B. Weinstein and P. M. Ebert, "Data transmission by frequency division multiplexing using the discrete Fourier transform," *IEEE Transactions on Communication Technology*, vol. COM–19, pp. 628–634, October 1971.

[10] L. Cimini, "Analysis and simulation of a digital mobile channel using orthogonal frequency division multiplexing," *IEEE Transactions on Communications*, vol. 33, pp. 665–675, July 1985.

[11] M. Alard and R. Lassalle, "Principles of modulation and channel coding for digital broadcasting for mobile receivers," *EBU Review, Technical No. 224*, pp. 47–69, August 1987.

[12] *Proceedings of 1st International Symposium,DAB*, (Montreux, Switzerland), June 1992.

[13] A. Peled and A. Ruiz, "Frequency domain data transmission using reduced computational complexity algorithms," in *Proceedings of International Conference on Acoustics, Speech, and Signal Processing, ICASSP'80*, vol. 3, (Denver, CO, USA), pp. 964–967, IEEE, 9–11 April 1980.

[14] B. Hirosaki, "An orthogonally multiplexed QAM system using the discrete Fourier transform," *IEEE Transactions on Communications*, vol. COM-29, pp. 983–989, July 1981.

[15] H. Kolb, "Untersuchungen über ein digitales Mehrfrequenzverfahren zur Datenübertragung," in *Ausgewählte Arbeiten über Nachrichtensysteme*, no. 50, Universität Erlangen-Nürnberg, 1982.

[16] H. Schüssler, "Ein digitales Mehrfrequenzverfahren zur Datenübertragung," in *Professoren-Konferenz, Stand und Entwicklungsaussichten der Daten und Telekommunikation*, (Darmstadt, Germany), pp. 179–196, 1983.

[17] K. Preuss, "Ein Parallelverfahren zur schnellen Datenübertragung im Ortsnetz," in *Ausgewählte Arbeiten über Nachrichtensysteme*, no. 56, Universität Erlangen-Nürnberg, 1984.

[18] R. Rückriem, "Realisierung und messtechnische Untersuchung an einem digitalen Parallelverfahren zur Datenübertragung im Fernsprechkanal," in *Ausgewählte Arbeiten über Nachrichtensysteme*, no. 59, Universität Erlangen-Nürnberg, 1985.

[19] I. Kalet, "The multitone channel," *IEEE Transactions on Communications*, vol. 37, pp. 119–124, February 1989.

[20] B. Hirosaki, "An analysis of automatic equalizers for orthogonally multiplexed QAM systems," *IEEE Transactions on Communications*, vol. COM-28, pp. 73–83, January 1980.

[21] P. Bello, "Selective fading limitations of the KATHRYN modem and some system design considerations," *IEEE Transactions on Communications Technology*, vol. COM–13, pp. 320–333, September 1965.

[22] E. Powers and M. Zimmermann, "A digital implementation of a multichannel data modem," in *Proceedings of the IEEE International Conference on Communications*, (Philadelphia, USA), 1968.

[23] R. Chang and R. Gibby, "A theoretical study of performance of an orthogonal multiplexing data transmission scheme," *IEEE Transactions on Communication Technology*, vol. COM–16, pp. 529–540, August 1968.

[24] B. R. Saltzberg, "Performance of an efficient parallel data transmission system," *IEEE Transactions on Communication Technology*, pp. 805–813, December 1967.

[25] K. Fazel and G. Fettweis, eds., *Multi-Carrier Spread-Spectrum*. Dordrecht: Kluwer, 1997. ISBN 0-7923-9973-0.

[26] F. Classen and H. Meyr, "Synchronisation algorithms for an OFDM system for mobile communications," in *Codierung für Quelle, Kanal und Übertragung*, no. 130 in ITG Fachbericht, (Berlin), pp. 105–113, VDE–Verlag, 1994.

[27] F. Classen and H. Meyr, "Frequency synchronisation algorithms for OFDM systems suitable for communication over frequency selective fading channels," in *Proceedings of IEEE VTC '94*, (Stockholm, Sweden), pp. 1655–1659, IEEE, 8–10 June 1994.

[28] R. van Nee and R. Prasad, *OFDM for Wireless Multimedia Communications*. London: Artech House Publishers, 2000.

[29] P. Vandenameele, L. van der Perre, and M. Engels, *Space Division Multiple Access for Wireless Local Area Networks*. Kluwer, 2001.

[30] R. W. Chang, *U.S. Patent No. 3,488,445: Orthogonal Frequency Division Multiplexing*, filed November 14, 1966, issued January 6, 1970.

[31] W. E. Keasler, D. L. Bitzer, and P. T. Tucker, *U.S. Patent No. 4,206,320: High-speed Modem Suitable for Operating with a Switched Network*, filed August 21, 1978, issued June 3, 1980.

[32] M. Alard and R. Lassalle, "Principles of modulation and channel coding for digital broadcasting for mobile receivers," *EBU Technical Review*, pp. 168–190, August 1987.

[33] J. M. Cioffi, *A Multicarrier Primer*, November 1991. ANSI T1E1.4/91-157.

[34] ANSI Committee T1-Telecommunications, *A Technical Report on High-Bit-Rate Digital Subscriber Lines (HDSL)*, February 1994. Technical Report No. 28.

[35] European Telecommunication Standard Institute, *Digital Audio Broadcasting (DAB);DAB to mobile, portable and fixed Receivers*, February 1995. ETSI ETS 300 401 ed.1.

[36] European Telecommunication Standard Institute, *Radio Equipment and Systems (RES);HIgh PErformance Radio Local Area Network (HIPERLAN) Type 1;Functional specification*, October 1996. ETSI ETS 300 652 ed.1.

[37] European Telecommunication Standard Institute, *Digital Video Broadcasting (DVB);Framing structure, channel coding and modulation for digital terrestrial television (DVB-T)*, March 1997. ETSI ETS 300 744 ed.1.

[38] *Very-high-speed Digital Subscriber Lines: System Requirements*, September 1998. ANSI T1E1.4 VDSL SR: 98-043R5.

[39] European Telecommunication Standard Institute, *Transmission and Multiplexing (TM);Access transmission systems on metallic access cables;Very high speed Digital Subscriber Line (VDSL);Part 1: Functional requirements*, June 1998. ETSI TS 101 270-1 V1.1.2.

[40] European Telecommunication Standard Institute, *Broadband Radio Access Networks (BRAN);Inventory of broadband radio technologies and techniques*, May 1998. ETSI TR 101 173 V1.1.1.

[41] Institute of Electrical and Electronics Engineers, *IEEE Standard 802.11a: Wireless LAN Medium Access Control (MAC) and Physical Layer (PHY) specifications: high-speed physical layer in the 5 GHz band*, 1999.

[42] Institute of Electrical and Electronics Engineers, *IEEE Standard 802.11g: Wireless LAN Medium Access Control (MAC) and Physical Layer (PHY) specifications*, 2003.

[43] European Telecommunication Standard Institute, *Digital Video Broadcasting (DVB);Transmission System for Handheld Terminals (DVB-H)*, November 2004. ETSI EN 302 304 V1.1.1.

[44] Institute of Electrical and Electronics Engineers, *IEEE Standard 802.16: Air Interface for Fixed Broadband Wireless Access Systems*, 2004.

[45] Institute of Electrical and Electronics Engineers, *IEEE Candidate Standard 802.11n: Wireless LAN Medium Access Control (MAC) and Physical Layer (PHY) specifications*, 2004. http://grouper.ieee.org/groups/802/11/Reports/tgn_update.htm.

[46] Institute of Electrical and Electronics Engineers, *IEEE Candidate Standard 802.15.3a: Wireless Medium Access Control (MAC) and Physical Layer (PHY) specifications for high rate Wireless Personal Area Networks (WPANs) involving imaging and multimedia*, 2004. http://www.ieee802.org/15/pub/TG3a.html.

[47] M. Yabusaki, "Asia Pacific Viewpoint and Activities: Introduction." 4G Forum, 27 May 2003.

[48] S. Shepherd, P. van Eetvelt, C. Wyatt-Millington, and S. Barton, "Simple coding scheme to reduce peak factor in QPSK multicarrier modulation," *Electronics Letters*, vol. 31, pp. 1131–1132, July 1995.

[49] A. E. Jones, T. A. Wilkinson, and S. K. Barton, "Block coding scheme for reduction of peak to mean envelope power ratio of multicarrier transmission schemes," *Electronics Letters*, vol. 30, pp. 2098–2099, December 1994.

[50] D. Wulich, "Reduction of peak to mean ratio of multicarrier modulation by cyclic coding," *Electronics Letters*, vol. 32, pp. 432–433, 1996.

[51] S. Müller and J. Huber, "Vergleich von OFDM–Verfahren mit reduzierter Spitzenleistung," in *2. OFDM–Fachgespräch in Braunschweig*, 1997.

[52] M. Pauli and H.-P. Kuchenbecker, "Neue Aspekte zur Reduzierung der durch Nicht-linearitäten hervorgerufenen Außerbandstrahlung eines OFDM–Signals," in *2. OFDM–Fachgespräch in Braunschweig*, 1997.

[53] T. May and H. Rohling, "Reduktion von Nachbarkanalstörungen in OFDM–Funkübertragungssystemen," in *2. OFDM–Fachgespräch in Braunschweig*, 1997.

[54] D. Wulich, "Peak factor in orthogonal multicarrier modulation with variable levels," *Electronics Letters*, vol. 32, no. 20, pp. 1859–1861, 1996.

[55] H. Schmidt and K. Kammeyer, "Adaptive Subträgerselektion zur Reduktion des Crest faktors bei OFDM," in *3. OFDM Fachgespräch in Braunschweig*, 1998.

[56] R. Dinis and A. Gusmao, "Performance evaluation of OFDM transmission with conventional and 2-branch combining power amplification schemes," in *Proceeding of IEEE Global Telecommunications Conference, Globecom 96*, (London, UK), pp. 734–739, IEEE, 18–22 November 1996.

[57] R. Dinis, P. Montezuma, and A. Gusmao, "Performance trade-offs with quasi-linearly amplified OFDM through a 2-branch combining technique," in *Proceedings of IEEE VTC'96*, (Atlanta, GA, USA), pp. 899–903, IEEE, 28 April–1 May 1996.

[58] R. Dinis, A. Gusmao, and J. Fernandes, "Adaptive transmission techniques for the mobile broadband system," in *Proceeding of ACTS Mobile Communication Summit '97*, (Aalborg, Denmark), pp. 757–762, ACTS, 7–10 October 1997.

[59] B. Daneshrad, L. Cimini Jr., and M. Carloni, "Clustered-OFDM transmitter implementation," in *Proceedings of IEEE International Symposium on Personal, Indoor, and Mobile Radio Communications (PIMRC'96)*, (Taipei, Taiwan), pp. 1064–1068, IEEE, 15–18 October 1996.

[60] M. Okada, H. Nishijima, and S. Komaki, "A maximum likelihood decision based nonlinear distortion compensator for multi-carrier modulated signals," *IEICE Transactions on Communications*, vol. E81B, no. 4, pp. 737–744, 1998.

[61] R. Dinis and A. Gusmao, "Performance evaluation of a multicarrier modulation technique allowing strongly nonlinear amplification," in *Proceedings of ICC 1998*, pp. 791–796, IEEE, 1998.

[62] T. Pollet, M. van Bladel, and M. Moeneclaey, "BER sensitivity of OFDM systems to carrier frequency offset and wiener phase noise," *IEEE Transactions on Communications*, vol. 43, pp. 191–193, February/March/April 1995.

[63] H. Nikookar and R. Prasad, "On the sensitivity of multicarrier transmission over multipath channels to phase noise and frequency offset," in *Proceedings of IEEE International Symposium on Personal, Indoor, and Mobile Radio Communications (PIMRC'96)*, (Taipei, Taiwan), pp. 68–72, IEEE, 15–18 October 1996.

[64] W. Warner and C. Leung, "OFDM/FM frame synchronization for mobile radio data communication," *IEEE Transactions on Vehicular Technology*, vol. 42, pp. 302–313, August 1993.

[65] H. Sari, G. Karam, and I. Jeanclaude, "Transmission techniques for digital terrestrial TV broadcasting," *IEEE Communications Magazine*, pp. 100–109, February 1995.

[66] P. Moose, "A technique for orthogonal frequency division multiplexing frequency offset correction," *IEEE Transactions on Communications*, vol. 42, pp. 2908–2914, October 1994.

[67] K. Brüninghaus and H. Rohling, "Verfahren zur Rahmensynchronisation in einem OFDM-System," in *3. OFDM Fachgespräch in Braunschweig*, 1998.

[68] F. Daffara and O. Adami, "A new frequency detector for orthogonal multicarrier transmission techniques," in *Proceedings of IEEE Vehicular Technology Conference (VTC'95)*, (Chicago, USA), pp. 804–809, IEEE, 15–28 July 1995.

[69] M. Sandell, J.-J. van de Beek, and P. Börjesson, "Timing and frequency synchronisation in OFDM systems using the cyclic prefix," in *Proceedings of International Symposium on Synchronisation*, (Essen, Germany), pp. 16–19, 14–15 December 1995.

[70] N. Yee, J.-P. Linnartz, and G. Fettweis, "Multicarrier CDMA in indoor wireless radio networks," in *PIMRC'93*, pp. 109–113, 1993.

[71] A. Chouly, A. Brajal, and S. Jourdan, "Orthogonal multicarrier techniques applied to direct sequence spread spectrum CDMA systems," in *Proceedings of the IEEE Global Telecommunications Conference 1993*, (Houston, TX, USA), pp. 1723–1728, 29 November - 2 December 1993.

[72] G. Fettweis, A. Bahai, and K. Anvari, "On multi-carrier code division multiple access (MC-CDMA) modem design," in *Proceedings of IEEE VTC '94*, (Stockholm, Sweden), pp. 1670–1674, IEEE, 8–10 June 1994.

[73] K. Fazel and L. Papke, "On the performance of convolutionally-coded CDMA/OFDM for mobile communication system," in *PIMRC'93*, pp. 468–472, 1993.

[74] R. Prasad and S. Hara, "Overview of multicarrier CDMA," *IEEE Communications Magazine*, pp. 126–133, December 1997.

[75] B.-J. Choi, E.-L. Kuan, and L. Hanzo, "Crest–factor study of MC-CDMA and OFDM," in *Proceeding of VTC'99 (Fall)*, vol. 1, (Amsterdam, Netherlands), pp. 233–237, IEEE, 19–22 September 1999.

[76] P. Höher, "TCM on frequency-selective land-mobile fading channels," in *International Workshop on Digital Communications*, (Tirrenia, Italy), pp. 317–328, September 1991.

[77] J. Chow, J. Cioffi, and J. Bingham, "Equalizer training algorithms for multicarrier modulation systems.," in *International Conference on Communications*, (Geneva, Switzerland), pp. 761–765, IEEE, May 1993.

[78] S. Wilson, R. E. Khayata, and J. Cioffi, "16QAM Modulation with Orthogonal Frequency Division Multiplexing in a Rayleigh-Fading Environment," in *Vehicular Technology Conference*, vol. 3, (Stockholm, Sweden), pp. 1660–1664, IEEE, June 1994.

[79] J.-J. van de Beek, O. Edfors, M. Sandell, S. Wilson, and P. Börjesson, "On channel estimation in OFDM systems," in *Proceedings of Vehicular Technology Conference*, vol. 2, (Chicago, IL USA), pp. 815–819, IEEE, July 1995.

[80] O. Edfors, M. Sandell, J. van den Beek, S. K. Wilson, and P. Börjesson, "OFDM Channel Estimation by Singular Value Decomposition," in *Proceedings of Vehicular Technology Conference*, vol. 2, (Atlanta, GA USA), pp. 923–927, IEEE, April 28 - May 1 1996.

[81] P. Frenger and A. Svensson, "A Decision Directed Coherent Detector for OFDM," in *Proceedings of Vehicular Technology Conference*, vol. 3, (Atlanta, GA USA), pp. 1584–1588, IEEE, April 28 - May 1 1996.

[82] V. Mignone and A. Morello, "CD3-OFDM: A Novel Demodulation Scheme for Fixed and Mobile Receivers," *IEEE Transactions on Communications*, vol. 44, pp. 1144–1151, September 1996.

[83] F. Tufvesson and T. Maseng, "Pilot Assisted Channel Estimation for OFDM in Mobile Cellular Systems," in *Proceedings of Vehicular Technology Conference*, vol. 3, (Phoenix, Arizona), pp. 1639–1643, IEEE, May 4-7 1997.

[84] P. Höher, S. Kaiser, and P. Robertson, "Two-dimensional pilot-symbol-aided channel estimation by Wiener filtering," in *International Conference on Acoustics, Speech and Signal Processing*, (Munich, Germany), pp. 1845–1848, IEEE, April 1997.

[85] P. Höher, S. Kaiser, and P. Robertson, "Pilot–symbol–aided channel estimation in time and frequency," in *Proceedings of Global Telecommunications Conference: The Mini–Conf.*, (Phoenix, AZ), pp. 90–96, IEEE, November 1997.

[86] Y. Li, L. Cimini, and N. Sollenberger, "Robust Channel Estimation for OFDM Systems with Rapid Dispersive Fading Channels," *IEEE Transactions on Communications*, vol. 46, pp. 902–915, April 1998.

[87] O. Edfors, M. Sandell, J.-J. van den Beek, S. Wilson, and P. Börjesson, "OFDM Channel Estimation by Singular Value Decomposition," *IEEE Transactions on Communications*, vol. 46, pp. 931–939, July 1998.

[88] F. Tufvesson, M. Faulkner, and T. Maseng, “Pre-Compensation for Rayleigh Fading Channels in Time Division Duplex OFDM Systems,” in *Proceedings of 6th International Workshop on Intelligent Signal Processing and Communications Systems*, (Melbourne, Australia), pp. 57–33, IEEE, November 5-6 1998.

[89] M. Itami, M. Kuwabara, M. Yamashita, H. Ohta, and K. Itoh, “Equalization of Orthogonal Frequency Division Multiplexed Signal by Pilot Symbol Assisted Multipath Estimation,” in *Proceedings of Global Telecommunications Conference*, vol. 1, (Sydney, Australia), pp. 225–230, IEEE, November 8-12 1998.

[90] L. Hanzo, M. Münster, B. Choi, and T. Keller, *OFDM and MC-CDMA for Broadband Multi-user Communications, WLANs and Broadcasting*. John Wiley and IEEE Press, 2003. 992 pages.

[91] E. Al-Susa and R. Ormondroyd, “A Predictor-Based Decision Feedback Channel Estimation Method for COFDM with High Resilience to Rapid Time-Variations,” in *Proceedings of Vehicular Technology Conference*, vol. 1, (Amsterdam, Netherlands), pp. 273–278, IEEE, September 19-22 1999.

[92] B. Yang, K. Letaief, R. Cheng, and Z. Cao, “Robust and Improved Channel Estimation for OFDM Systems in Frequency Selective Fading Channels,” in *Proceedings of Global Telecommunications Conference*, vol. 5, (Rio de Janeiro, Brazil), pp. 2499–2503, IEEE, December 5-9 1999.

[93] Y. Li, “Pilot-Symbol-Aided Channel Estimation for OFDM in Wireless Systems,” *IEEE Transactions on Vehicular Technology*, vol. 49, pp. 1207–1215, July 2000.

[94] B. Yang, K. Letaief, R. Cheng, and Z. Cao, “Channel Estimation for OFDM Transmission in Multipath Fading Channels Based on Parametric Channel Modeling,” *IEEE Transactions on Communications*, vol. 49, pp. 467–479, March 2001.

[95] S. Zhou and G. Giannakis, “Finite-Alphabet Based Channel Estimation for OFDM and Related Multicarrier Systems,” *IEEE Transactions on Communications*, vol. 49, pp. 1402–1414, August 2001.

[96] X. Wang and K. Liu, “OFDM Channel Estimation Based on Time-Frequency Polynomial Model of Fading Multipath Channel,” in *Proceedings of Vehicular Technology Conference*, vol. 1, (Atlantic City, NJ USA), pp. 460–464, IEEE, October 7-11 2001.

[97] B. Yang, Z. Cao, and K. Letaief, “Analysis of Low-Complexity Windowed DFT-Based MMSE Channel Estimator for OFDM Systems,” *IEEE Transactions on Communications*, vol. 49, pp. 1977–1987, November 2001.

[98] B. Lu and X. Wang, “Bayesian Blind Turbo Receiver for Coded OFDM Systems with Frequency Offset and Frequency-Selective Fading,” *IEEE Journal on Selected Areas in Communications*, vol. 19, pp. 2516–2527, December 2001.

[99] Y. Li and N. Sollenberger, “Clustered OFDM with Channel Estimation for High Rate Wireless Data,” *IEEE Transactions on Communications*, vol. 49, pp. 2071–2076, December 2001.

[100] M. Morelli and U. Mengali, “A Comparison of Pilot-Aided Channel Estimation Methods for OFDM Systems,” *IEEE Transactions on Signal Processing*, vol. 49, pp. 3065–3073, December 2001.

[101] M.-X. Chang and Y. Su, "Model-Based Channel Estimation for OFDM Signals in Rayleigh Fading," *IEEE Transactions on Communications*, vol. 50, pp. 540–544, April 2002.

[102] M. Necker and G. Stüber, "Totally Blind Channel Estimation for OFDM over Fast Varying Mobile Channels," in *Proceedings of International Conference on Communications*, (New York, NY USA), IEEE, April 28 - May 2 2002.

[103] B. Yang, Z. Cao, and K. Letaief, "Low Complexity Channel Estimator Based on Windowed DFT and Scalar Wiener Filter for OFDM Systems," in *Proceedings of International Conference on Communications*, vol. 6, (Helsinki, Finland), pp. 1643–1647, IEEE, June 11-14 2001.

[104] J. Deller, J. Proakis, and J. Hansen, *Discrete-Time Processing of Speech Signals*. Macmillan Publishing Company, 1993.

[105] L. Hanzo, F. Somerville, and J. Woodard, *Voice Compression and Communications*. IEEE Press Wiley Inter-Science, 2001.

[106] A. Duel-Hallen, S. Hu, and H. Hallen, "Long Range Prediction of Fading Signals," *IEEE Signal Processing Magazine*, vol. 17, pp. 62–75, May 2000.

[107] F. Tufvesson, *Design of Wireless Communication Systems - Issues on Synchronization, Channel Estimation and Multi-Carrier Systems,*. Department of Applied Electronics, Lund University, Sweden, 2000.

[108] W. Press, S. Teukolshy, W. Vetterling, and B. Flannery, *Numerical Recipes in C*. Cambridge University Press, 1992.

[109] T. Moon and W. Stirling, *Mathematical Methods and Algorithms for Signal Processing*. Prentice Hall, 2000.

[110] Y. Li, N. Seshadri, and S. Ariyavisitakul, "Channel Estimation for OFDM Systems with Transmitter Diversity in Mobile Wireless Channels," *IEEE Journal on Selected Areas in Communications*, vol. 17, pp. 461–471, March 1999.

[111] W. Jeon, K. Paik, and Y. Cho, "An Efficient Channel Estimation Technique for OFDM Systems with Transmitter Diversity," in *Proceedings of International Symposium on Personal, Indoor and Mobile Radio Communications*, vol. 2, (Hilton London Metropole Hotel, London, UK), pp. 1246–1250, IEEE, September 18-21 2000.

[112] Y. Li, "Optimum Training Sequences for OFDM Systems with Multiple Transmit Antennas," in *Proc. of Global Telecommunications Conference*, vol. 3, (San Francisco, United States), pp. 1478–1482, IEEE, November 27 - December 1 2000.

[113] A. Mody and G. Stüber, "Parameter Estimation for OFDM with Transmit Receive Diversity," in *Proceedings of Vehicular Technology Conference*, vol. 2, (Rhodes, Greece), pp. 820–824, IEEE, May 6-9 2001.

[114] Y. Gong and K. Letaief, "Low Rank Channel Estimation for Space-Time Coded Wideband OFDM Systems," in *Proceedings of Vehicular Technology Conference*, vol. 2, (Atlantic City Convention Center, Atlantic City, NJ USA), pp. 772–776, IEEE, October 7-11 2001.

[115] W. Jeon, K. Paik, and Y. Cho, "Two-Dimensional MMSE Channel Estimation for OFDM Systems with Transmitter Diversity," in *Proceedings of Vehicular Technology Conference*, vol. 3, (Atlantic City Convention Center, Atlantic City, NJ USA), pp. 1682–1685, IEEE, October 7-11 2001.

[116] F. Vook and T. Thomas, "MMSE Multi-User Channel Estimation for Broadband Wireless Communications," in *Proceedings of Global Telecommunications Conference*, vol. 1, (San Antonio, Texas, USA), pp. 470–474, IEEE, November 25-29 2001.

[117] Y. Xie and C. Georghiades, "An EM-based Channel Estimation Algorithm for OFDM with Transmitter Diversity," in *Proceedings of Global Telecommunications Conference*, vol. 2, (San Antonio, Texas, USA), pp. 871–875, IEEE, November 25-29 2001.

[118] Y. Li, "Simplified Channel Estimation for OFDM Systems with Multiple Transmit Antennas," *IEEE Transactions on Wireless Communications*, vol. 1, pp. 67–75, January 2002.

[119] H. Bölcskei, R. Heath, and A. Paulraj, "Blind Channel Identification and Equalization in OFDM-Based Multi-Antenna Systems," *IEEE Transactions on Signal Processing*, vol. 50, pp. 96–109, January 2002.

[120] H. Minn, D. Kim, and V. Bhargava, "A Reduced Complexity Channel Estimation for OFDM Systems with Transmit Diversity in Mobile Wireless Channels," *IEEE Transactions on Wireless Communications*, vol. 50, pp. 799–807, May 2002.

[121] S. Slimane, "Channel Estimation for HIPERLAN/2 with Transmitter Diversity," in *International Conference on Communications*, (New York, NY USA), IEEE, April 28 - May 2 2002.

[122] C. Komninakis, C. Fragouli, A. Sayed, and R. Wesel, "Multi-Input Multi-Output Fading Channel Tracking and Equalization Using Kalman Estimation," *IEEE Transactions on Signal Processing*, vol. 50, pp. 1065–1076, May 2002.

[123] G. Foschini, "Layered Space-Time Architecture for Wireless Communication in a Fading Environment when using Multi-Element Antennas"," *Bell Labs Technical Journal*, vol. Autumn, pp. 41–59, 1996.

[124] F. Vook and K. Baum, "Adaptive antennas for OFDM," in *Proceedings of IEEE Vehicular Technology Conference (VTC'98)*, vol. 2, (Ottawa, Canada), pp. 608–610, IEEE, 18–21 May 1998.

[125] X. Wang and H. Poor, "Robust Adaptive Array for Wireless Communications," *IEEE Transactions on Communications*, vol. 16, pp. 1352–1366, October 1998.

[126] K.-K. Wong, R.-K. Cheng, K. Letaief, and R. Murch, "Adaptive Antennas at the Mobile and Base Station in an OFDM/TDMA System," in *Proceedings of Global Telecommunications Conference*, vol. 1, (Sydney, Australia), pp. 183–190, IEEE, November 8-12 1998.

[127] Y. Li and N. Sollenberger, "Interference Suppression in OFDM Systems using Adaptive Antenna Arrays," in *Proceedings of Global Telecommunications Conference*, vol. 1, (Sydney, Australia), pp. 213–218, IEEE, November 8-12 1998.

[128] G. Golden, G. Foschini, R. Valenzuela, and P. Wolniansky, "Detection Algorithms and Initial Laboratory Results using V-BLAST Space-Time Communication Architecture," *IEE Electronics Letters*, vol. 35, pp. 14–16, January 1999.

[129] Y. Li and N. Sollenberger, "Adaptive Antenna Arrays for OFDM Systems with Cochannel Interference," *IEEE Transactions on Communications*, vol. 47, pp. 217–229, February 1999.

[130] P. Vandenameele, L. Van der Perre, M. Engels, and H. Man, "A novel class of uplink OFDM/SDMA algorithms for WLAN," in *Proceedings of Global Telecommunications Conference — Globecom'99*, vol. 1, (Rio de Janeiro, Brazil), pp. 6–10, IEEE, 5–9 December 1999.

[131] M. Speth, A. Senst, and H. Meyr, "Low complexity space-frequency MLSE for multiuser COFDM," in *Proceedings of Global Telecommunications Conference — Globecom'99*, vol. 1, (Rio de Janeiro, Brazil), pp. 2395–2399, IEEE, 5–9 December 1999.

[132] C. H. Sweatman, J. Thompson, B. Mulgrew, and P. Grant, "A Comparison of Detection Algorithms including BLAST for Wireless Communication using Multiple Antennas," in *Proceedings of International Symposium on Personal, Indoor and Mobile Radio Communications*, vol. 1, (Hilton London Metropole Hotel, London, UK), pp. 698–703, IEEE, September 18-21 2000.

[133] R. van Nee, A. van Zelst, and G. Awater, "Maximum Likelihood Decoding in a Space-Division Multiplexing System," in *Proceedings of Vehicular Technology Conference*, vol. 1, (Tokyo, Japan), pp. 6–10, IEEE, May 15-18 2000.

[134] G. Awater, A. van Zelst, and R. van Nee, "Reduced Complexity Space Division Multiplexing Receivers," in *Proceedings of Vehicular Technology Conference*, vol. 1, (Tokyo, Japan), pp. 11–15, IEEE, May 15-18 2000.

[135] A. van Zelst, R. van Nee, and G. Awater, "Space Division Multiplexing (SDM) for OFDM systems," in *Proceedings of Vehicular Technology Conference*, vol. 2, (Tokyo, Japan), pp. 1070–1074, IEEE, May 15-18 2000.

[136] P. Vandenameele, L. V. D. Perre, M. Engels, B. Gyselinckx, and H. D. Man, "A Combined OFDM/SDMA Approach," *IEEE Journal on Selected Areas in Communications*, vol. 18, pp. 2312–2321, November 2000.

[137] X. Li, H. Huang, A. Lozano, and G. Foschini, "Reduced-Complexity Detection Algorithms for Systems Using Multi-Element Arrays," in *Proc. of Global Telecommunications Conference*, vol. 2, (San Francisco, United States), pp. 1072–1076, IEEE, November 27 - December 1 2000.

[138] C. Degen, C. Walke, A. Lecomte, and B. Rembold, "Adaptive MIMO Techniques for the UTRA-TDD Mode," in *Proceedings of Vehicular Technology Conference*, vol. 1, (Rhodes, Greece), pp. 108–112, IEEE, May 6-9 2001.

[139] X. Zhu and R. Murch, "Multi-Input Multi-Output Maximum Likelihood Detection for a Wireless System," in *Proceedings of Vehicular Technology Conference*, vol. 1, (Rhodes, Greece), pp. 137–141, IEEE, May 6-9 2001.

[140] J. Li, K. Letaief, R. Cheng, and Z. Cao, "Joint Adaptive Power Control and Detection in OFDM/SDMA Wireless LANs," in *Proceedings of Vehicular Technology Conference*, vol. 1, (Rhodes, Greece), pp. 746–750, IEEE, May 6-9 2001.

[141] F. Rashid-Farrokhi, K. Liu, and L. Tassiulas, "Transmit Beamforming and Power Control for Cellular Wireless Systems," *IEEE Journal on Selected Areas in Communications*, vol. 16, pp. 1437–1450, October 1998.

[142] A. van Zelst, R. van Nee, and G. Awater, "Turbo-BLAST and its Performance," in *Proceedings of Vehicular Technology Conference*, vol. 2, (Rhodes, Greece), pp. 1282–1286, IEEE, May 6-9 2001.

[143] A. Benjebbour, H. Murata, and S. Yoshida, "Performance of Iterative Successive Detection Algorithm with Space-Time Transmission," in *Proceedings of Vehicular Technology Conference*, vol. 2, (Rhodes, Greece), pp. 1287–1291, IEEE, May 6-9 2001.

[144] M. Sellathurai and S. Haykin, "A Simplified Diagonal BLAST Architecture with Iterative Parallel-Interference Cancellation Receivers," in *Proceedings of International Conference on Communications*, vol. 10, (Helsinki, Finland), pp. 3067–3071, IEEE, June 11-14 2001.

[145] A. Bhargave, R. Figueiredo, and T. Eltoft, "A Detection Algorithm for the V-BLAST System," in *Proceedings of Global Telecommunications Conference*, vol. 1, (San Antonio, Texas, USA), pp. 494–498, IEEE, November 25-29 2001.

[146] S. Thoen, L. Deneire, L. V. D. Perre, and M. Engels, "Constrained Least Squares Detector for OFDM/SDMA-based Wireless Networks," in *Proceedings of Global Telecommunications Conference*, vol. 2, (San Antonio, Texas, USA), pp. 866–870, IEEE, November 25-29 2001.

[147] Y. Li and Z.-Q. Luo, "Parallel Detection for V-BLAST System," in *Proceedings of International Conference on Communications*, (New York, NY USA), IEEE, April 28 - May 2 2002.

[148] Y. Li and N. Sollenberger, "Interference suppression in OFDM systems using adaptive antenna arrays," in *Proceeding of Globecom'98*, (Sydney, Australia), pp. 213–218, IEEE, 8–12 November 1998.

[149] Y. Li and N. Sollenberger, "Adaptive antenna arrays for OFDM systems with cochannel interference," *IEEE Transactions on Communications*, vol. 47, pp. 217–229, February 1999.

[150] Y. Li, L. Cimini, and N. Sollenberger, "Robust channel estimation for OFDM systems with rapid dispersive fading channels," *IEEE Transactions on Communications*, vol. 46, pp. 902–915, April 1998.

[151] C. Kim, S. Choi, and Y. Cho, "Adaptive beamforming for an OFDM sytem," in *Proceeding of VTC'99 (Spring)*, (Houston, TX, USA), IEEE, 16–20 May 1999.

[152] L. Lin, L. Cimini Jr., and J.-I. Chuang, "Turbo codes for OFDM with antenna diversity," in *Proceeding of VTC'99 (Spring)*, (Houston, TX, USA), IEEE, 16–20 May 1999.

[153] M. Münster, T. Keller, and L. Hanzo, "Co–channel interference suppression assisted adaptive OFDM in interference limited environments," in *Proceeding of VTC'99 (Fall)*, vol. 1, (Amsterdam, Netherlands), pp. 284–288, IEEE, 19–22 September 1999.

[154] S. Verdu, *Multiuser Detection*. Cambridge University Press, 1998.

[155] J. Litva and T.-Y. Lo, *Digital Beamforming in Wireless Communications*. London: Artech House Publishers, 1996.

[156] P. Vandenameele, L. Van der Perre, M. Engels, B. Gyselinckx, and H. Man, "A novel class of uplink OFDM/SDMA algorithms: A statistical performance analysis," in

Proceedings of Vehicular Technology Conference, vol. 1, (Amsterdam, Netherlands), pp. 324–328, IEEE, 19–22 September 1999.

[157] F. Mueller-Roemer, "Directions in audio broadcasting," *Journal of the Audio Engineering Society*, vol. 41, pp. 158–173, March 1993.

[158] G. Plenge, "DAB — a new radio broadcasting system — state of development and ways for its introduction," *Rundfunktech. Mitt.*, vol. 35, no. 2, 1991.

[159] ETSI, *Digital Audio Broadcasting (DAB)*, 2nd ed., May 1997. ETS 300 401.

[160] ETSI, *Digital Video Broadcasting (DVB); Framing structure, channel coding and modulation for digital terrestrial television*, August 1997. EN 300 744 V1.1.2.

[161] P. Chow, J. Tu, and J. Cioffi, "A discrete multitone transceiver system for HDSL applications," *IEEE Journal on Selected Areas in Communications*, vol. 9, pp. 895–908, August 1991.

[162] P. Chow, J. Tu, and J. Cioffi, "Performance evaluation of a multichannel transceiver system for ADSL and VHDSL services," *IEEE Journal on Selected Areas in Communications*, vol. 9, pp. 909–919, August 1991.

[163] K. Sistanizadeh, P. Chow, and J. Cioffi, "Multi-tone transmission for asymmetric digital subscriber lines (ADSL)," in *Proceedings of ICC'93*, pp. 756–760, IEEE, 1993.

[164] ANSI, *ANSI/T1E1.4/94-007, Asymmetric Digital Subscriber Line (ADSL) Metallic Interface.*, August 1997.

[165] A. Burr and P. Brown, "Application of OFDM to powerline telecommunications," in *3rd International Symposium on Power-Line Communications*, (Lancaster, UK), 30 March – 1 April 1999.

[166] M. Deinzer and M. Stoger, "Integrated PLC-modem based on OFDM," in *3rd International Symposium on Power-Line Communications*, (Lancaster, UK), 30 March – 1 April 1999.

[167] R. Prasad and H. Harada, "A novel OFDM based wireless ATM system for future broadband multimedia communications," in *Proceeding of ACTS Mobile Communication Summit '97*, (Aalborg, Denmark), pp. 757–762, ACTS, 7–10 October 1997.

[168] C. Ciotti and J. Borowski, "The AC006 MEDIAN project — overview and state–of–the–art," in *Proc. ACTS Summit '96*, (Granada, Spain), pp. 362–367, 27–29 November 1996.

[169] J. Borowski, S. Zeisberg, J. Hübner, K. Koora, E. Bogenfeld, and B. Kull, "Performance of OFDM and comparable single carrier system in MEDIAN demonstrator 60GHz channel," in *Proceeding of ACTS Mobile Communication Summit '97*, (Aalborg, Denmark), pp. 653–658, ACTS, 7–10 October 1997.

[170] M. D. Benedetto, P. Mandarini, and L. Piazzo, "Effects of a mismatch in the in–phase and in–quadrature paths, and of phase noise, in QDCPSK-OFDM modems," in *Proceeding of ACTS Mobile Communication Summit '97*, (Aalborg, Denmark), pp. 769–774, ACTS, 7–10 October 1997.

[171] T. Rautio, M. Pietikainen, J. Niemi, J. Rautio, K. Rautiola, and A. Mammela, "Architecture and implementation of the 150 Mbit/s OFDM modem (invited paper)," in *IEEE*

Benelux Joint Chapter on Communications and Vehicular Technology, 6th Symposium on Vehicular Technology and Communications, (Helsinki, Finland), p. 11, 12–13 October 1998.

[172] J. Ala-Laurila and G. Awater, "The magic WAND — wireless ATM network demondtrator system," in *Proceeding of ACTS Mobile Communication Summit '97*, (Aalborg, Denmark), pp. 356–362, ACTS, 7–10 October 1997.

[173] J. Aldis, E. Busking, T. Kleijne, R. Kopmeiners, R. van Nee, R. Mann-Pelz, and T. Mark, "Magic into reality, building the WAND modem," in *Proceeding of ACTS Mobile Communication Summit '97*, (Aalborg, Denmark), pp. 775–780, ACTS, 7–10 October 1997.

[174] E. Hallmann and H. Rohling, "OFDM-Vorschläge für UMTS," in *3. OFDM Fachgespräch in Braunschweig*, 1998.

[175] "Universal mobile telecommunications system (UMTS); UMTS terrestrial radio access (UTRA); concept evaluation," tech. rep., ETSI, 1997. TR 101 146.

[176] B. M. Hochwald and S. ten Brink, "Achieving near-capacity on a multiple-antenna channel," *IEEE Transactions on Communications*, vol. 51, pp. 389–399, March 2003.

[177] L. Hanzo, W. Webb, and T. Keller, *Single- and Multi-Carrier Quadrature Amplitude Modulation: Principles and Applications for Personal Communications, WLANs and Broadcasting*. John Wiley and IEEE Press, 2000.

[178] H. Kolb Private Communications.

[179] J. Lindner Private Communications.

[180] W. Webb and L. Hanzo, *Modern Quadrature Amplitude Modulation: Principles and Applications for Wireless Communications*. IEEE Press-Pentech Pressm, 1994.

[181] J. K. Cavers, "An Analysis of Pilot Symbol Assisted Modulation for Rayleigh Fading Channels," *IEEE Transactions on Vehicular Technology*, vol. 40, pp. 686–693, November 1991.

[182] H. Harmuth, *Transmission of Information by Orthogonal Time Functions*. Berlin: Springer Verlag, 1969.

[183] H. Harmuth, "On the transmission of information by orthogonal time functions," *AIEE*, July 1960.

[184] J. Proakis, *Digital Communications*. McGraw-Hill, 1995.

[185] R. O'Neill and L. Lopes, "Performance of amplitude limited multitone signals," in *Proceedings of IEEE VTC '94*, (Stockholm, Sweden), IEEE, 8–10 June 1994.

[186] X. Li and L. Cimini, "Effects of clipping and filtering on the performance of OFDM," in *Proceedings of IEEE VTC'97*, (Phoenix, AZ, USA), pp. 1634–1638, IEEE, 4–7 May 1997.

[187] A. Garcia and M. Calvo, "Phase noise and sub–carrier spacing effects on the performance of an OFDM communications system," *IEEE Communications Letters*, vol. 2, pp. 11–13, January 1998.

[188] W. Robins, *Phase Noise in Signal Sources*, vol. 9 of *IEE Telecommunication series*. Peter Peregrinus Ltd., 1982.

[189] C. Tellambura, Y. Guo, and S. Barton, "Equaliser performance for HIPERLAN in indoor channels," *Wireless Personal Communications*, vol. 3, no. 4, pp. 397–410, 1996.

[190] T. Ojanperä, M. Gudmundson, P. Jung, J. Sköld, R. Pirhonen, G. Kramer, and A. Toskala, "FRAMES: - hybrid multiple access technology," in *Proceedings of IEEE ISSSTA'96*, (Mainz, Germany), pp. 334–338, IEEE, September 1996.

[191] M. Failli, "Digital land mobile radio communications COST 207," tech. rep., European Commission, 1989.

[192] J. Torrance and L. Hanzo, "Comparative study of pilot symbol assisted modem schemes," in *Proceedings of IEE Conference on Radio Receivers and Associated Systems (RRAS'95)*, (Bath, UK), pp. 36–41, IEE, 26–28 September 1995.

[193] R. Hasholzner, C. Drewes, and A. Hutter, "Untersuchungen zur linearen ICI-Kompensation bei OFDM," in *3.OFDM Fachgespräch*, Technische Universität Braunschweig, Germany, Sept. 1998.

[194] W. Jeon, K. Chang, and Y. Cho, "An Equalization Technique for Orthogonal Frequency-Division Multiplexing Systems in Time-Variant Multipath Channels," *IEEE Transactions on Communications*, vol. 47, pp. 27–32, January 1999.

[195] A. Hutter and R. Hasholzner, "Determination of Intercarrier Interference Covariance Matrices and their Application to Advanced Equalization for Mobile OFDM," in 5^{th} *International OFDM-Workshop 2000*, pp. 33/1–33/5, Technische Universität Hamburg-Harburg, Sept. 2000.

[196] M. Ruessel and G. Stüber, "Terrestrial digital video broadcasting for mobile reception using OFDM," *Wireless Pers. Commun.*, vol. 2, no. 3, pp. 45–66, 1995.

[197] M. Münster and L. Hanzo, "MMSE Channel Prediction for Symbol-by-symbol Adaptive OFDM Systems," in 5^{th} *International OFDM-Workshop 2000*, pp. 35/1–35/6, Technische Universität Hamburg-Harburg, September 2000.

[198] K. Fazel, S. Kaiser, P. Robertson, and M. Ruf, "A concept of digital terrestrial television broadcasting," *Wireless Personal Communications*, vol. 2, pp. 9–27, 1995.

[199] J. Kuronen, V.-P. Kaasila, and A. Mammela, "An all-digital symbol tracking algorithm in an OFDM system by using the cyclic prefix," in *Proc. ACTS Summit '96*, (Granada, Spain), pp. 340–345, 27–29 November 1996.

[200] M. Kiviranta and A. Mammela, "Coarse frame synchronization structures in OFDM," in *Proc. ACTS Summit '96*, (Granada, Spain), pp. 464–470, 27–29 November 1996.

[201] Z. Li and A. Mammela, "An all digital frequency synchronization scheme for OFDM systems," in *Proceedings of the IEEE International Symposium on Personal, Indoor and Mobile Radio Communications (PIMRC)*, (Helsinki, Finland), pp. 327–331, 1–4 September 1997.

[202] J. Bingham, "Method and apparatus for correcting for clock and carrier frequency offset, and phase jitter in multicarrier modems." U.S. Patent No. 5206886, 27 April 1993.

[203] T. de Couasnon, R. Monnier, and J. Rault, "OFDM for digital TV broadcasting," *Signal Processing*, vol. 39, pp. 1–32, 1994.

[204] P. Mandarini and A. Falaschi, "SYNC proposals." MEDIAN Design Note, January 1996.

[205] T. Keller and L. Hanzo, "Orthogonal frequency division multiplex synchronisation techniques for wireless local area networks," in *Proceedings of IEEE International Symposium on Personal, Indoor, and Mobile Radio Communications (PIMRC'96)*, vol. 3, (Taipei, Taiwan), pp. 963–967, IEEE, 15–18 October 1996.

[206] R. Steele and W. Webb, "Variable rate QAM for data transmission over Rayleigh fading channels," in *Proceeedings of Wireless '91*, (Calgary, Alberta), pp. 1–14, IEEE, 1991.

[207] H. Matsuoka, S. Sampei, N. Morinaga, and Y. Kamio, "Adaptive modulation system with variable coding rate concatenated code for high quality multi-media communications systems," in *Proceedings of IEEE VTC'96*, vol. 1, (Atlanta, GA, USA), pp. 487–491, IEEE, 28 April–1 May 1996.

[208] S.-G. Chua and A. Goldsmith, "Variable-rate variable-power mQAM for fading channels," in *Proceedings of IEEE VTC'96*, (Atlanta, GA, USA), pp. 815–819, IEEE, 28 April–1 May 1996.

[209] D. Pearce, A. Burr, and T. Tozer, "Comparison of counter-measures against slow Rayleigh fading for TDMA systems," in *IEE Colloquium on Advanced TDMA Techniques and Applications*, (London, UK), pp. 9/1–9/6, IEE, 28 October 1996. Digest 1996/234.

[210] V. Lau and M. Macleod, "Variable rate adaptive trellis coded QAM for high bandwidth efficiency applications in Rayleigh fading channels," in *Proceedings of IEEE Vehicular Technology Conference (VTC'98)*, (Ottawa, Canada), pp. 348–352, IEEE, 18–21 May 1998.

[211] J. Torrance and L. Hanzo, "Latency and networking aspects of adaptive modems over slow indoors Rayleigh fading channels," *IEEE Transactions on Vehicular Technology*, vol. 48, no. 4, pp. 1237–1251, 1998.

[212] J. Torrance, L. Hanzo, and T. Keller, "Interference aspects of adaptive modems over slow Rayleigh fading channels," *IEEE Transactions on Vehicular Technology*, vol. 48, pp. 1527–1545, September 1999.

[213] A. Czylwik, "Adaptive OFDM for wideband radio channels," in *Proceeding of IEEE Global Telecommunications Conference, Globecom 96*, (London, UK), pp. 713–718, IEEE, 18–22 November 1996.

[214] P. Chow, J. Cioffi, and J. Bingham, "A practical discrete multitone transceiver loading algorithm for data transmission over spectrally shaped channels," *IEEE Transactions on Communications*, vol. 48, pp. 772–775, 1995.

[215] L. Hanzo, C. Wong, and M. Yee, *Adaptive Wireless Transceivers*. John Wiley, IEEE Press, 2002. (For detailed contents, please refer to http://www-mobile.ecs.soton.ac.uk.).

[216] L. Hanzo, T. H. Liew, and B. L. Yeap, *Turbo Coding, Turbo Equalisation and Space-Time Coding*. Chichester, UK; Piscataway, NJ, USA: John Wiley, IEEE Press, 2002. 766 pages. (For detailed contents, please refer to http://www-mobile.ecs.soton.ac.uk.).

[217] J. Blogh and L. Hanzo, *Third-Generation Systems and Intelligent Networking*. John Wiley and IEEE Press, 2002. (For detailed contents, please refer to http://www-mobile.ecs.soton.ac.uk.).

[218] J. Torrance, *Adaptive Full Response Digital Modulation for Wireless Communications Systems*. PhD thesis, Department of Electronics and Computer Science, University of Southampton, UK, 1997.

[219] K. Miya, O. Kato, K. Homma, T. Kitade, M. Hayashi, and T. Ue, "Wideband CDMA systems in TDD-mode operation for IMT-2000," *IEICE Transactions on Communications*, vol. E81-B, pp. 1317–1326, July 1998.

[220] O. Kato, K. Miya, K. Homma, T. Kitade, M. Hayashi, and M. Watanabe, "Experimental performance results of coherent wideband DS-CDMA with TDD scheme," *IEICE Transactions on Communications.*, vol. E81-B, pp. 1337–1344, July 1998.

[221] T. Keller and L. Hanzo, "Blind-detection assisted sub-band adaptive turbo-coded OFDM schemes," in *Proceeding of VTC'99 (Spring)*, (Houston, TX, USA), pp. 489–493, IEEE, 16–20 May 1999.

[222] J. Torrance and L. Hanzo, "Optimisation of switching levels for adaptive modulation in a slow Rayleigh fading channel," *Electronics Letters*, vol. 32, pp. 1167–1169, 20 June 1996.

[223] C. Berrou, A. Glavieux, and P. Thitimajshima, "Near shannon limit error-correcting coding and decoding: Turbo codes," in *Proceedings of the International Conference on Communications*, (Geneva, Switzerland), pp. 1064–1070, May 1993.

[224] L. Bahl, J. Cocke, F. Jelinek, and J. Raviv, "Optimal decoding of linear codes for minimising symbol error rate," *IEEE Transactions on Information Theory*, vol. 20, pp. 284–287, March 1974.

[225] T. Keller, M. Muenster, and L. Hanzo, "A burst–by–burst adaptive OFDM wideband speech transceiver." submitted to IEEE JSAC, 1999.

[226] T. Keller, J. Woodard, and L. Hanzo, "Turbo-coded parallel modem techniques for personal communications," in *Proceedings of IEEE VTC'97*, (Phoenix, AZ, USA), pp. 2158–2162, IEEE, 4–7 May 1997.

[227] T. Keller and L. Hanzo, "Adaptive orthogonal frequency division multiplexing schemes," in *Proceeding of ACTS Mobile Communication Summit '98*, (Rhodes, Greece), pp. 794–799, ACTS, 8–11 June 1998.

[228] C. E. Shannon, "Communication in the presence of noise," *Proceedings of the I.R.E.*, vol. 37, pp. 10–22, January 1949.

[229] L. Piazzo, "A fast algorithm for near-optimum power and bit allocation in OFDM systems." Electronics Letters, December 1999.

[230] T. Willink and P. Wittke, "Optimization and performance evaluation of multicarrier transmission," *IEEE Transactions on Information Theory*, vol. 43, pp. 426–440, March 1997.

[231] R. Fischer and J. Huber, "A new loading algorithm for discrete multitone transmission," in *Proceeding of IEEE Global Telecommunications Conference, Globecom 96*, (London, UK), pp. 713–718, IEEE, 18–22 November 1996.

[232] S. Lai, R. Cheng, K. Letaief, and R. Murch, "Adaptive trellis coded MQAM and power optimization for OFDM transmission," in *Proceedings of VTC'99 (Spring)*, (Houston, TX, USA), IEEE, 16–20 May 1999.

[233] D. Hughes-Hartogs, "Ensemble modem structure for imperfect transmission media." U.S Patents Nos. 4,679,227 (July 1988) 4,731,816 (March 1988) and 4,833,796 (May 1989).

[234] J. Bingham, "Multicarrier modulation for data transmission: an idea whose time has come," *IEEE Communications Magazine*, pp. 5–14, May 1990.

[235] L. Godara, "Applications of antenna arrays to mobile communications, part II: Beamforming and direction-of-arrival considerations," *Proceedings of the IEEE*, vol. 85, pp. 1193–1245, August 1997.

[236] Y. Li, "Pilot-symbol-aided channel estimation for OFDM in wireless systems," in *Proceedings of VTC'99 (Spring)*, (Houston, TX, USA), IEEE, 16–20 May 1999.

[237] A. Viterbi, *CDMA: Principles of Spread Spectrum Communication*. Reading MA, USA: Addison-Wesley, June 1995. ISBN 0201633744.

[238] L. Miller and J. Lee, *CDMA Systems Engineering Handbook*. London, UK: Artech House, 1998.

[239] R. A. Scholtz, "The origins of spread spectrum communications," *IEEE Transactions on Communications*, vol. 30, no. 5, pp. 822–854, 1982.

[240] G. R. Cooper and R. W. Nettleton, "A spread-spectrum technique for high-capacity mobile communications," *IEEE Transactions on Vehicular Technology*, vol. 27, pp. 264–275, November 1978.

[241] O. C. Yue, "Spread spectrum mobile radio, 1977-1982," *IEEE Transactions on Vehicular Technology*, vol. 32, pp. 98–105, February 1983.

[242] M. Simon, J. Omura, R. Scholtz, and B. Levitt, *Spread Spectrum Communications Handbook*. New York, USA: McGraw-Hill, 1994.

[243] Y. Yoon, R. Kohno, and H. Imai, "A SSMA system with cochannel interference cancellation with multipath fading channels," *IEEE Journal on Selected Areas in Communications*, vol. 11, pp. 1067–1075, September 1993.

[244] K. Gilhousen, I. Jacobs, R. Padovani, A. Viterbi, L. Weaver Jr., and C. Wheatley III, "On the capacity of a cellular CDMA system," *IEEE Transactions on Vehicular Technology*, vol. 40, pp. 303–312, May 1991.

[245] P. Patel and J. Holtzman, "Analysis of a simple successive interference cancellation scheme in a DS/CDMA system," *IEEE Journal on Selected Areas in Communications*, vol. 12, pp. 796–807, June 1994.

[246] R. Lupas and S. Verdú, "Linear multiuser detectors for synchronous code division multiple access channels," *IEEE Transactions on Information Theory*, vol. 35, pp. 123–136, January 1989.

[247] P. Jung and J. Blanz, "Joint detection with coherent receiver antenna diversity in CDMA mobile radio systems," *IEEE Transactions on Vehicular Technology*, vol. 44, pp. 76–88, February 1995.

[248] J. Thompson, P. Grant, and B. Mulgrew, "Smart antenna arrays for CDMA systems," *IEEE Personal Communications Magazine*, vol. 3, pp. 16–25, October 1996.

[249] R. Steele and L. Hanzo, eds., *Mobile Radio Communications*. New York, USA: John Wiley and IEEE Press, 2nd ed., 1999. 1090 pages.

[250] K. Feher, *Wireless Digital Communications: Modulation and Spread Spectrum*. Englewood Cliffs, NJ: Prentice-Hall, 1995.

[251] R. Kohno, R. Meidan, and L. Milstein, "Spread spectrum access methods for wireless communication," *IEEE Communications Magazine*, vol. 33, pp. 58–67, January 1995.

[252] R. Price and E. Green Jr., "A communication technique for multipath channels," *Proceedings of the IRE*, vol. 46, pp. 555–570, March 1958.

[253] U. Grob, A. L. Welti, E. Zollinger, R. Kung, and H. Kaufmann, "Microcellular direct-sequence spread-spectrum radio system using n-path rake receiver," *IEEE Journal on Selected Areas in Communications*, vol. 8, no. 5, pp. 772–780, 1990.

[254] P. W. Baier, "A critical review of CDMA," in *Proceedings of the IEEE Vehicular Technology Conference (VTC)*, (Atlanta, GA, USA), pp. 6–10, 28 April–1 May 1996.

[255] Telcomm. Industry Association (TIA), Washington, DC, USA, *Mobile station — Base station compatibility standard for dual-mode wideband spread spectrum cellular system, EIA/TIA Interim Standard IS-95*, July 1993.

[256] A. J. Viterbi, A. M. Viterbi, and E. Zehavi, "Performance of power-controlled wideband terrestrial digital communication," *IEEE Transactions on Communications*, vol. 41, no. 4, pp. 559–569, 1993.

[257] F. Simpson and J. Holtzman, "Direct sequence CDMA power control, interleaving, and coding," *IEEE Journal on Selected Areas in Communications*, vol. 11, pp. 1085–1095, September 1993.

[258] S. Ariyavisitakul and L. Chang, "Signal and interference statistics of a CDMA system with feedback power control," *IEEE Transactions on Communications*, vol. 41, pp. 1626–1634, November 1993.

[259] S. Ariyavisitakul, "Signal and interference statistics of a CDMA system with feedback power control - Part II," *IEEE Transactions on Communications*, vol. 42, no. 2/3/4, pp. 597–605, 1994.

[260] J. G. Proakis, *Digital Communications*. Mc-Graw Hill International Editions, 3rd ed., 1995.

[261] R. W. Chang and R. A. Gibby, "A theoretical study of performance of an orthogonal multiplexing data transmission scheme," *IEEE Transactions on Communication Technology*, vol. 16, no. 4, pp. 529–540, 1968.

[262] P. V. Eetvelt, S. J. Shepherd, and S. K. Barton, "The distribution of peak factor in QPSK multi-carrier modulation," *Wireless Personal Communications*, vol. 2, pp. 87–96, 1995.

[263] V. M. DaSilva and E. S. Sousa, "Performance of orthogonal CDMA codes for quasi-synchronous communication systems," in *Proceedings of IEEE ICUPC 1993*, (Ottawa, Canada), pp. 995–999, October 1993.

[264] L. Vandendorpe, "Multitone direct sequence CDMA system in an indoor wireless environment," in *Proceedings of IEEE SCVT 1993*, (Delft, The Netherlands), pp. 4.1:1–8, October 1993.

[265] R. Prasad and S. Hara, "Overview of multi-carrier CDMA," in *Proceedings of the IEEE International Symposium on Spread Spectrum Techniques and Applications (ISSSTA)*, (Mainz, Germany), pp. 107–114, 22–25 September 1996.

[266] D. Scott, P. Grant, S. McLaughlin, G. Povey, and D. Cruickshank, "Research in reconfigurable terminal design for mobile and personal communications," tech. rep., Department of Electrical Engineering, The University of Edinburgh, March 1997.

[267] N. Yee and J. P. Linnartz, "MICRO 93-101: Multi-carrier CDMA in an indoor wireless radio channel," tech. rep., University of California at Berkeley, 1994.

[268] L.-L. Yang and L. Hanzo, "Performance of generalized multicarrier DS-CDMA over Nakagami-m fading channels," *IEEE Transactions on Communications, (http://www-mobile.ecs.soton.ac.uk/lly)*, vol. 50, pp. 956–966, June 2002.

[269] L.-L. Yang and L. Hanzo, "Slow frequency-hopping multicarrier DS-CDMAfor transmission over Nakagami multipath fading channels," *IEEE Journal on Selected Areas in Communications*, vol. 19, no. 7, pp. 1211–1221, 2001.

[270] E. A. Sourour and M. Nakagawa, "Performance of orthogonal multicarrier CDMA in a multipath fading channel," *IEEE Transactions on Communications*, vol. 44, pp. 356–367, March 1996.

[271] L.-L. Yang and L. Hanzo, "Slow frequency-hopping multicarrier DS-CDMA," in *International Symposium on Wireless Personal Multimedia Communications (WPMC'99)*, (Amsterdam, The Netherlands), pp. 224–229, September:21–23 1999.

[272] L.-L. Yang and L. Hanzo, "Blind soft-detection assisted frequency-hopping multicarrier DS-CDMA systems," in *Proceedings of IEEE GLOBECOM'99*, (Rio de Janeiro, Brazil), pp. 842–846, December:5-9 1999.

[273] S. Slimane, "MC-CDMA with quadrature spreading for wireless communication systems," *European Transactions on Telecommunications*, vol. 9, pp. 371–378, July–August 1998.

[274] I. Kalet, "The multitone channel," *IEEE Transactions on Communications*, vol. 37, pp. 119–124, February 1989.

[275] R.-Y. Li and G. Stette, "Time-limited orthogonal multicarrier modulation schemes," *IEEE Transactions on Communications*, vol. 43, pp. 1269–1272, February/March/April 1995.

[276] L. Goldfeld and D. Wulich, "Multicarrier modulation system with erasures-correcting decoding for Nakagami fading channels," *European Trans. on Telecommunications*, vol. 8, pp. 591–595, November–December 1997.

[277] E. Sousa, "Performance of a direct sequence spread spectrum multiple access system utilizing unequal carrier frequencies," *IEICE Transactions on Communications*, vol. E76-B, pp. 906–912, August 1993.

[278] B. Saltzberg, "Performance of an efficient parallel data transmission system," *IEEE Transactions on Communication Technology*, vol. 15, pp. 805–811, December 1967.

[279] C. Baum and K. Conner, "A multicarrier transmission scheme for wireless local communications," *IEEE Journal on Selected Areas in Communications*, vol. 14, pp. 512–529, April 1996.

[280] V. Dasilva and E. Sousa, "Multicarrier orthogonal CDMA signals for quasi-synchronous communication systems," *IEEE Journal on Selected Areas in Communications*, vol. 12, pp. 842–852, June 1994.

[281] L. Vandendorpe and O. V. de Wiel, "MIMO DEF equalization for multitone DS/SS systems over multipath channels," *IEEE Journal on Selected Areas in Communications*, vol. 14, pp. 502–511, April 1996.

[282] N. Al-Dhahir and J. Cioffi, "A bandwidth-optimized reduced-complexity equalized multicarrier transceiver," *IEEE Transactions on Communications*, vol. 45, pp. 948–956, August 1997.

[283] P. Jung, F. Berens, and J. Plechinger, "A generalized view on multicarrier CDMA mobile radio systems with joint detection (Part i)," *FREQUENZ*, vol. 51, pp. 174–184, July–August 1997.

[284] S. Hara and R. Prasad, "Design and performance of multicarrier CDMA system in frequency-selective Rayleigh fading channels," *IEEE Transactions on Vehicular Technology*, vol. 48, pp. 1584–1595, September 1999.

[285] V. Tarokh and H. Jafarkhani, "On the computation and reduction of the peak-to-average power ratio in multicarrier communications," *IEEE Transactions on Communications*, vol. 48, pp. 37–44, January 2000.

[286] D. Wulich and L. Goldfield, "Reduction of peak factor in orthogonal multicarrier modulation by amplitude limiting and coding," *IEEE Transactions on Communications*, vol. 47, pp. 18–21, January 1999.

[287] H.-W. Kang, Y.-S. Cho, and D.-H. Youn, "On compensating nonlinear distortions of an OFDM system using an efficient adaptive predistorter," *IEEE Transactions on Communications*, vol. 47, pp. 522–526, April 1999.

[288] Y.-H. Kim, I. Song, Seokho, and S.-R. Park, "A multicarrier CDMA system with adaptive subchannel allocation for forward links," *IEEE Transactions on Vehicular Technology*, vol. 48, pp. 1428–1436, September 1999.

[289] X. Gui and T.-S. Ng, "Performance of asynchronous orthogonal multicarrier CDMA system in frequency selective fading channel," *IEEE Transactions on Communications*, vol. 47, pp. 1084–1091, July 1999.

[290] T.-M. Lok, T.-F. Wong, and J. Lehnert, "Blind adaptive signal reception for MC-CDMA systems in Rayleigh fading channels," *IEEE Transactions on Communications*, vol. 47, pp. 464–471, March 1999.

[291] B. Rainbolt and S. Miller, "Multicarrier CDMA for cellular overlay systems," *IEEE Journal on Selected Areas in Communications*, vol. 17, pp. 1807–1814, October 1999.

[292] S.-M. Tseng and M. Bell, "Asynchronous multicarrier DS-CDMA using mutually orthogonal complementary sets of sequences," *IEEE Transactions on Communications*, vol. 48, pp. 53–59, January 2000.

[293] D. Rowitch and L. Milstein, "Convolutionally coded multicarrier DS-CDMA systems in a multipath fading channel – Part I: Performance analysis," *IEEE Transactions on Communications*, vol. 47, pp. 1570–1582, October 1999.

[294] D. Rowitch and L. Milstein, "Convolutionally coded multicarrier DS-CDMA systems in a multipath fading channel – Part II: Narrow-band interference suppression," *IEEE Transactions on Communications*, vol. 47, pp. 1729–1736, November 1999.

[295] D.-W. Lee and L. Milstein, "Comparison of multicarrier DS-CDMA broadcast systems in a multipath fading channel," *IEEE Transactions on Communications*, vol. 47, pp. 1897–1904, December 1999.

[296] N. Yee, J.-P. Linnartz, and G. Fettweis, "Multi-carrier CDMA in indoor wireless radio network," *IEICE Transactions on Communications*, vol. E77-B, pp. 900–904, July 1994.

[297] S. Kondo and L. Milstein, "On the use of multicarrier direct sequence spread spectrum systems," in *Proceedings of IEEE MILCOM'93*, (Boston, MA), pp. 52–56, Oct. 1993.

[298] V. M. DaSilva and E. S. Sousa, "Performance of orthogonal CDMA codes for quasi-synchronous communication systems," in *Proceedings of IEEE ICUPC'93*, (Ottawa, Canada), pp. 995–999, Oct. 1993.

[299] L. Vandendorpe, "Multitone direct sequence CDMA system in an indoor wireless environment," in *Proceedings of IEEE First Symposium of Communications and Vehicular Technology in the Benelux, Delft, The Netherlands*, pp. 4.1–1–4.1–8, Oct. 1993.

[300] L. L. Yang and L. Hanzo, "Blind joint soft-detection assisted slow frequency-hopping multi-carrier DS-CDMA," *IEEE Transactions on Communication*, vol. 48, no. 9, pp. 1520–1529, 2000.

[301] D.-W. Lee and L. Milstein, "Analysis of a multicarrier DS-CDMA code-acquisition system," *IEEE Transactions on Communications*, vol. 47, pp. 1233–1244, August 1999.

[302] B. Steiner, "Time domain uplink channel estimation in multicarrier-CDMA mobile radio system concepts," in *Multi-Carrier Spread-Spectrum* (K. Fazel and G. Fettweis, eds.), pp. 153–160, Kluwer Academic Publishers, 1997.

[303] K. W. Yip and T. S. Ng, "Tight error bounds for asynchronous multicarrier CDMA and their application," *IEEE Communications Letters*, vol. 2, pp. 295–297, November 1998.

[304] S. Kondo and L. Milstein, "Performance of multicarrier DS CDMA systems," *IEEE Transactions on Communications*, vol. 44, pp. 238–246, February 1996.

[305] B. M. Popovic, "Spreading sequences for multicarrier CDMA systems," *IEEE Transactions on Communications*, vol. 47, no. 6, pp. 918–926, 1999.

[306] P. Jung, P. Berens, and J. Plechinger, "Uplink spectral efficiency of multicarrier joint detection code division multiple access based cellular radio systems," *Electronics Letters*, vol. 33, no. 8, pp. 664–665, 1997.

[307] D.-W. Lee, H. Lee, and J.-S. Kim, "Performance of a modified multicarrier direct sequence CDMA system," *Electronics and Telecommunications Research Institute Journal*, vol. 19, pp. 1–11, April 1997.

[308] L. Rasmussen and T. Lim, "Detection techniques for direct sequence and multicarrier variable rate for broadband CDMA," in *Proceedings of the ICCS/ISPACS '96*, pp. 1526–1530, 1996.

[309] P. Jung, F. Berens, and J. Plechinger, "Joint detection for multicarrier CDMA mobile radio systems - Part II: Detection techniques," in *Proceedings of IEEE ISSSTA 1996*, vol. 3, (Mainz, Germany), pp. 996–1000, September 1996.

[310] Y. Sanada and M. Nakagawa, "A multiuser interference cancellation technique utilizing convolutional codes and multicarrier modulation for wireless indoor communications," *IEEE Journal on Selected Areas in Communications*, vol. 14, pp. 1500–1509, October 1996.

[311] Q. Chen, E. S. Sousa, and S. Pasupathy, "Multicarrier CDMA with adaptive frequency hopping for mobile radio systems," *IEEE Journal on Selected Areas in Communications*, vol. 14, pp. 1852–1857, December 1996.

[312] T. Ojanperä and R. Prasad, "An overview of air interface multiple access for IMT-2000/UMTS," *IEEE Communications Magazine*, vol. 36, pp. 82–95, September 1998.

[313] R. L. Peterson, R. E. Ziemer, and D. E. Borth, *Introduction to Spread Spectrum Communications*. Prentice Hall International Editions, 1995.

[314] S. W. Golomb, *Shift Register Sequences*. Holden-Day, 1967.

[315] F. Adachi, K. Ohno, A. Higashi, T. Dohi, and Y. Okumura, "Coherent multicode DS-CDMA mobile Radio Access," *IEICE Transactions on Communications*, vol. E79-B, pp. 1316–1324, September 1996.

[316] S. C. Bang, "ETRI wideband CDMA system for IMT-2000," in *Presentation material in 1st IMT-2000 Workshop*, (Seoul, Korea), pp. II–1–1 – II–1–21, KIET, August 1997.

[317] H. Rohling, K. Brüninghaus, and R. Grünheid, "Comparison of multiple access schemes for an OFDM downlink system," in *Multi-Carrier Spread-Spectrum* (K. Fazel and G. P. Fettweis, eds.), pp. 23–30, Kluwer Academic Publishers, 1997.

[318] R. Prasad, *CDMA for Wireless Personal Communications*. London: Artech House, May 1996. ISBN 0890065713.

[319] M. Schnell and S. Kaiser, "Diversity considerations forMC-CDMA systems in mobile communications," in *Proceedings of IEEE ISSSTA 1996*, pp. 131–135, 1996.

[320] W. H. Press, S. A. Teukolsky, W. T. Vetterling, and B. P. Flannery, *Numerical Recipies in C*. Cambridge University Press, 1992.

[321] S. Verdú, *Multiuser Detection*. Cambridge, UK: Cambridge University Press, 1998.

[322] E. Kuan and L. Hanzo, "Burst-by-burst adaptive multiuser detection cdma: A framework for existing and future wireless standards," *Proceedings of the IEEE*, December 2002.

[323] L. Hanzo, L.-L. Yang, E.-L. Kuan, and K. Yen, *Single- and Multi-Carrier DS-CDMA*. John Wiley and IEEE Press, 2003. 430 pages.

[324] R. Prasad, *Universal Wireless Personal Communications*. London, UK: Artech House Publishers, 1998.

[325] S. Glisic and B. Vucetic, *Spread Spectrum CDMA Systems for Wireless Communications*. London, UK: Artech House, April 1997. ISBN 0890068585.

[326] G. Woodward and B. Vucetic, "Adaptive detection for DS-CDMA," *Proceedings of the IEEE*, vol. 86, pp. 1413–1434, July 1998.

[327] S. Moshavi, "Multi-user detection for DS-CDMA communications," *IEEE Communications Magazine*, vol. 34, pp. 124–136, October 1996.

[328] A. Duel-Hallen, J. Holtzman, and Z. Zvonar, "Multiuser detection for CDMA systems," *IEEE Personal Communications*, vol. 2, pp. 46–58, April 1995.

[329] J. Laster and J. Reed, "Interference rejection in digital wireless communications," *IEEE Signal Processing Magazine*, vol. 14, pp. 37–62, May 1997.

[330] J. Thompson, P. Grant, and B. Mulgrew, "Performance of antenna array receiver algorithms for CDMA," in *Proceedings of the IEEE Global Telecommunications Conference (GLOBECOM)*, (London, UK), pp. 570–574, 18–22 November 1996.

[331] A. Naguib and A. Paulraj, "Performance of wireless CDMA with m-ary orthogonal modulation and cell site antenna arrays," *IEEE Journal on Selected Areas in Communications*, vol. 14, pp. 1770–1783, December 1996.

[332] L. Godara, "Applications of antenna arrays to mobile communications, part I: Performance improvement, feasibility, and system considerations," *Proceedings of the IEEE*, vol. 85, pp. 1029–1060, July 1997.

[333] R. Kohno, H. Imai, M. Hatori, and S. Pasupathy, "Combination of adaptive array antenna and a canceller of interference for direct-sequence spread-spectrum multiple-access system," *IEEE Journal on Selected Areas in Communications*, vol. 8, pp. 675–681, May 1998.

[334] B. J. Choi, T. H. Liew, and L. Hanzo, "Concatenated space-time block coded and turbo coded symbol-by-symbol adaptive OFDM and multi-carrier CDMA systems," in *Proceedings of IEEE VTC 2001-Spring*, p. P.528, IEEE, May 2001.

[335] W. T. Webb and R. Steele, "Variable rate QAM for mobile radio," *IEEE Transactions on Communications*, vol. 43, no. 7, pp. 2223–2230, 1995.

[336] B. Vucetic, "An adaptive coding scheme for time-varying channels," *IEEE Transactions on Communications*, vol. 39, no. 5, pp. 653–663, 1991.

[337] H. Imai and S. Hirakawa, "A new multi-level coding method using error correcting codes," *IEEE Transactions on Information Theory*, vol. 23, pp. 371–377, May 1977.

[338] G. Ungerboeck, "Channel coding with multilevel/phase signals," *IEEE Transactions on Information Theory*, vol. IT-28, pp. 55–67, January 1982.

[339] S. M. Alamouti and S. Kallel, "Adaptive trellis-coded multiple-phased-shift keying Rayleigh fading channels," *IEEE Transactions on Communications*, vol. 42, pp. 2305–2341, June 1994.

[340] S. Chua and A. Goldsmith, "Adaptive coded modulation for fading channels," *IEEE Transactions on Communications*, vol. 46, pp. 595–602, May 1998.

[341] K. J. Hole, H. Holm, and G. E. Oien, "Adaptive multidimensional coded modulation over flat fading channels," *IEEE Journal on Selected Areas in Communications*, vol. 18, pp. 1153–1158, July 2000.

[342] T. Keller, T. Liew, and L. Hanzo, "Adaptive rate RRNS coded OFDM transmission for mobile communication channels," in *Proceedings of VTC 2000 Spring*, (Tokyo, Japan), pp. 230–234, 15-18 May 2000.

[343] T. Keller, T. H. Liew, and L. Hanzo, "Adaptive redundant residue number system coded multicarrier modulation," *IEEE Journal on Selected Areas in Communications*, vol. 18, pp. 1292–2301, November 2000.

[344] T. Liew, C. Wong, and L. Hanzo, "Block turbo coded burst-by-burst adaptive modems," in *Proceedings of Microcoll'99*, (Budapest, Hungary), pp. 59–62, 21-24 March 1999.

[345] C. Wong, T. Liew, and L. Hanzo, "Turbo coded burst by burst adaptive wideband modulation with blind modem mode detection," in *ACTS Mobile Communications Summit*, (Sorrento, Italy), pp. 303–308, 8-11 June 1999.

[346] M. Yee, T. Liew, and L. Hanzo, "Radial basis function decision feedback equalisation assisted block turbo burst-by-burst adaptive modems," in *Proceedings of VTC '99 Fall*, (Amsterdam, Holland), pp. 1600–1604, 19-22 September 1999.

[347] V. Tarokh, N. Seshadri, and A. R. Calderbank, "Space-Time Codes for High Data Rate Wireless Communication: Performance Criterion and Code Construction," *IEEE Transactions on Information Theory*, vol. 44, pp. 744–765, March 1998.

[348] S. M. Alamouti, "A simple transmit diversity technique for wireless communications," *IEEE Journal on Selected Areas in Communications*, vol. 16, pp. 1451–1458, October 1998.

[349] V. Tarokh, H. Jafarkhani, and A. R. Calderbank, "Space-time block coding for wireless communications: Performance results," *IEEE Journal on Selected Areas in Communications*, vol. 17, pp. 451–460, March 1999.

[350] C. Berrou and A. Glavieux, "Near optimum error correcting coding and decoding: Turbo codes," *IEEE Transactions on Communications*, vol. 44, pp. 1261–1271, October 1996.

[351] J. Winters, "Smart antennas for wireless systems," *IEEE Personal Communications*, vol. 5, pp. 23–27, February 1998.

[352] R. Derryberry, S. Gray, D. Ionescu, G. Mandyam, and B. Raghothaman, "Transmit diversity in 3G CDMA systems," *IEEE Communications Magazine*, vol. 40, pp. 68–75, April 2002.

[353] A. Molisch, M. Win, and J. Winters, "Space-time-frequency (STF) coding for MIMO-OFDM systems," *IEEE Communications Letters*, vol. 6, pp. 370–372, September 2002.

[354] A. Molisch, M. Steinbauer, M. Toeltsch, E. Bonek, and R. Thoma, "Capacity of MIMO systems based on measured wireless channels," *IEEE Journal on Selected Areas in Communications*, vol. 20, pp. 561–569, April 2002.

[355] D. Gesbert, M. Shafi, D.-S. Shiu, P. Smith, and A. Naguib, "From theory to practice: an overview of MIMO space-time coded wireless systems," *IEEE Journal on Selected Areas in Communications*, vol. 21, pp. 281–302, April 2003.

[356] M. Shafi, D. Gesbert, D.-S. Shiu, P. Smith, and W. Tranter, "Guest editorial: MIMO systems and applications," *IEEE Journal on Selected Areas in Communications*, vol. 21, pp. 277–280, April 2003.

[357] G. Foschini Jr. and M. Gans, "On limits of wireless communication in a fading environment when using multiple antennas," *Wireless Personal Communications*, vol. 6, pp. 311–335, March 1998.

[358] S. X. Ng, B. L. Yeap, and L. Hanzo, "Full-rate, full-diversity adaptive space time block coding for transmission over Rayleigh fading channels," in *Proceedings of the IEEE VTC'05 Fall*, (Dallas, Texas), 25-28, September 2005.

[359] D. E. Goldberg, *Genetic Algorithms in Search, Optimization, and Machine Learning*. Reading, Massachusetts: Addison-Wesley, 1989.

[360] M. J. Juntti, T. Schlösser, and J. O. Lilleberg, "Genetic algorithms for multiuser detection in synchronous CDMA," in *IEEE International Symposium on Information Theory – ISIT'97*, (Ulm, Germany), p. 492, 1997.

[361] Y. Li, L. Cimini, and N. Sollenberger, "Robust channel estimation for OFDM systems with rapid dispersive fading channels," *IEEE Transactions on Communications*, vol. 46, pp. 902–915, April 1998.

[362] W. Jakes Jr., ed., *Microwave Mobile Communications*. New York, USA: John Wiley & Sons, 1974.

[363] M. C. Jeruchim, P. Balaban, and K. S. Shanmugan, *Simulation of Communication Systems*. Dordrecht; Kluwer Academic, 2000. 2nd edition.

[364] U. Fincke and M. Pohst, "Improved method for calculating vector of short length in a lattice, including a complexity analysis," *Math. Comput.*, vol. 44, pp. 463–471, April 1985.

[365] M. O. Damen, A. Chkeif, and J.-C. Belfiore, "Lattice code decoder for space-time codes," *IEEE Commun. Letters*, pp. 161–163, May 2000.

[366] M. O. Damen, H. E. Gamal, and G. Caier, "On maximum-likelihood detection and the search for closest lattice point," *IEEE Transactions on Information Theory*, vol. 49, pp. 2389–2402, October 2003.

[367] D. Pham, K. R. Pattipati, P. K. Willet, and J. Luo, "An improved complex sphere decoder for V-BLAST Systems," *IEEE Signal Processing Letters*, vol. 11, pp. 748–751, September 2004.

[368] T. Cui and C. Tellambura, "Joint channel estimation and data detection for OFDM systems via sphere decoding," in *IEEE Globcom 2004*, (Dallas, USA), pp. 3656–3660, November 2004.

[369] T. Cui and C. Tellambura, "Approximate ML detection for MIMO systems using multistage sphere decoding," *IEEE Signal Processing Letters*, vol. 12, pp. 222–225, March 2005.

[370] M. Damen, K. Abed-Meraim, and J.-C. Belfiore, "Generalised sphere decoder for asymmetrical space-time communication architecture," *Electronics Letters*, vol. 36, no. 2, pp. 166–167, 2000.

[371] T. Cui and C. Tellambura, “An efficient generalized sphere decoder for rank-deficient MIMO systems,” *IEEE Communications Letters*, vol. 9, no. 5, pp. 423–425, 2005.

[372] J. E. Gentle, *Numerical Linear Algebra for Applications in Statistics*. Berlin: Springer-Verlag, 1998.

[373] M. K. Varanasi, “Decision feedback multiuser detection: A systematic approach,” *IEEE Transactions on Information Theory*, vol. 45, pp. 219–240, January 1999.

[374] R. D. Schafer, *An Introduction to Nonassociative Algebras*. New York: Dover, 1996.

[375] H. Holma and A. Toskala, eds., *WCDMA for UMTS : Radio Access for Third Generation Mobile Communications*. John Wiley and Sons, Ltd., 2000.

[376] H. Liu and G. Xu, “Smart Antennas in Wireless Systems: Uplink Multiuser Blind Channel and Sequence Detection,” *IEEE Transactions on Communications*, vol. 45, pp. 187–199, February 1997.

[377] J. Xavier, V. Barroso, and J. Moura, “Closed-form blind channel identification and source separation in SDMA systems through correlative coding,” *International Journal on Selected Areas in Communications*, vol. 16, pp. 1506–1517, October 1998.

[378] J. Xavier, V. A. N. Barroso, and J. M. F. Moura, “Closed-form correlative coding (CFC2) blind identification of MIMO channels: isometry fitting to second order statistics,” *IEEE Transactions on Signal Processing*, vol. 49, pp. 1073–1086, May 2001.

[379] I. Bradaric, A. P. Pertropulu, and K. I. Diamantaras, “Blind MIMO FIR Channel Identification Based on Second-order Spectra Correlations,” *IEEE Transactions on Signal Processing*, vol. 51, pp. 1668–1674, June 2003.

[380] M. C. Necker and G. L. Stüber, “Totally blind channel estimation for OFDM on fast varying mobile radio channels,” *IEEE Transactions on Wireless Communications*, vol. 3, pp. 1514–1525, September 2004.

[381] W. Nabhane and H. V. Poor, “Blind Joint Equalization and Multiuser Detection in Dispersive MC-CDMA/MC-DS-CDMA/MT-CDMA Channels,” in *Proceedings MILCOM 2002*, vol. 2, pp. 814–819, 7-10 October 2002.

[382] Y. Li, N. Seshadri, and S. Ariyavisitakul, “Channel estimation for OFDM systems with transmitter diversity in mobile wireless channels,” *IEEE Journal on Selected Areas in Communications*, vol. 17, pp. 461–471, March 1999.

[383] Y. Li, J. H. Winters, and N. R. Sollenberger, “MIMO-OFDM for Wireless Communications: Signal Detection with Enhanced Channel Estimation,” *IEEE Transactions on Communications*, vol. 50, pp. 1471–1477, September 2002.

[384] S. Thoen, L. Deneire, L. V. der Perre, M. Engels, and H. D. Man, “Constrained Least Squares Detector for OFDM/SDMA-based Wireless Networks,” *IEEE Transactions on Wireless Communications*, vol. 2, pp. 129–140, January 2003.

[385] Y. Qiao, S. Yu, P. Su, and L. Zhang, “Research on an Iterative Algorithm of LS Channel Estimation in MIMO OFDM Systems,” *IEEE Transactions on Broadcasting*, vol. 51, pp. 149–153, March 2005.

[386] Y. Zeng and T. S. Ng, “A Semi-blind Channel Estimation Method for Multiuser Multi-antenna OFDM Systems,” *IEEE Transactions on Signal Processing*, vol. 52, pp. 1419–1429, May 2004.

[387] K. J. Kim and R. A. Iltis, “Joint Detection and Channel Estimation Algorithms for QS-CDMA Signals Over Time-varying Channels,” *IEEE Transactions on Communications*, vol. 50, pp. 845–855, May 2002.

[388] K. J. Kim, J. Yue, R. A. Iltis, and J. D. Gibson, “A QRD-M/Kalman Filter-based Detection and Channel Estimation Algorithm for MIMO-OFDM Systems,” *IEEE Transactions on Wireless Communications*, vol. 4, pp. 710–721, March 2005.

[389] Z. Wang, Z. Han, and K. J. R. Liu, “A MIMO-OFDM Channel Estimation Approach Using Time of Arrivals,” *IEEE Transactions on Wireless Communications*, vol. 4, pp. 1207–1213, May 2005.

[390] M. Shin, H. Lee, and C. Lee, “Enhanced Channel-estimation Technique for MIMO-OFDM Systems,” *IEEE Transactions on Vehicular Technology*, vol. 53, pp. 262–265, January 2004.

[391] F. Horlin and L. V. der Perre, “Optimal Training Sequences for Low Complexity ML Multi-channel Estimation in Multi-user MIMO OFDM-based Communications,” in *2004 IEEE International Conference on Communications*, vol. 4, pp. 2427–2431, 20-24 June 2004.

[392] T. Cui and C. Tellambura, “Joint channel estimation and data detection for OFDM systems via sphere decoding,” in *IEEE Global Telecommunications Conference, 2004 (GLOBECOM ’04)*, vol. 6, pp. 3656–3660, 29 November-3 December 2004.

[393] H. Zhu, B. Farhang-Boroujeny, and C. Schlegel, “Pilot Embedding for Joint Channel Estimation and Data Detection in MIMO Communication Systems,” *IEEE Communications Letters*, vol. 7, pp. 30–32, January 2003.

[394] J. Wang and K. Araki, “Pilot-symbol Aided Channel Estimation in Spatially Correlated Multiuser MIMO-OFDM Channels,” in *2004 IEEE 60th Vehicular Technology Conference, 2004 (VTC 2004 Fall)*, vol. 1, pp. 33–37, 26-29 September 2004.

[395] K. Yen and L. Hanzo, “Genetic Algorithm Assisted Joint Multiuser symbol Detection and Fading Channel Estimation for Synchronous CDMA Systems,” *IEEE Journal on Selected Areas in Communications*, vol. 19, pp. 985–998, June 2001.

[396] S. Chen and Y. Wu, “Maximum likelihood joint channel and data estimation using genetic algorithms,” *IEEE Transactions on Signal Processing*, vol. 46, pp. 1469–1473, May 1998.

[397] Y. S. Zhang, Y. Du, W. Zhang, X. Z. Wang, and J. Li, “A data-aided time domain channel estimation method,” in *Proceedings of the 2004 Joint Conference of the 10th Asia-Pacific Conference on Communications and the 5th International Symposium on Multi-Dimensional Mobile Communications*, vol. 1, pp. 469–473, 29 August-1 September 2004.

[398] C. E. Tan and I. J. Wassell, “Near-optimum training sequences for OFDM systems,” in *The 9th Asia-Pacific Conference on Communications (APCC 2003)*, vol. 1, pp. 119–123, 21-24 September 2003.

[399] C. Ergün and K. Hacioglu, “Multiuser detection using a genetic algorithm in CDMA communications systems,” *IEEE Transactions on Communications*, vol. 48, pp. 1374–1383, August 2000.

[400] K. Yen and L. Hanzo, "Antenna-diversity-assisted genetic-algorithm-based multiuser detection schemes for synchronous CDMA systems," *IEEE Transactions on Communications*, vol. 51, pp. 366–370, March 2003.

[401] K. Yen and L. Hanzo, "Genetic-algorithm-assisted multiuser detection in asynchronous CDMA communications," *IEEE Transactions on Vehicular Technology*, vol. 53, pp. 1413–1422, September 2004.

[402] X. Wu, T. C. Chuah, B. S. Sharif, and O. R. Hinton, "Adaptive robust detection for CDMA using a genetic algorithm," *IEE Proceedings Communications*, vol. 150, pp. 437–444, 10 December 2003.

[403] J. Akhtman and L. Hanzo, "Reduced-Complexity Maximum-Likelihood Detection in Multiple-Antenna-Aided Multicarrier Systems," in *Proceedings of the 5th International Workshop on Multi-Carrier Spread Spectrum Communications*, (Oberpfaffenhofen, Germany), 14-16 September 2005.

[404] J. Akhtman and L. Hanzo, "Novel Optimized-Hierarchy RSA-aided Space-Time Processing Method," Mobile VCE Core 3 Programme - Wireless Enablers 2.2: ICR-WE2.2.1, University of Southampton, Southampton, UK, May 2005.

[405] M. Jiang and L. Hanzo, "Improved Hybrid MMSE Detection for Turbo Trellis Coded Modulation Assisted Multi-User OFDM Systems," *IEE Electronics Letters*, vol. 40, pp. 1002–1003, August 2004.

[406] N. Seshadri, "Joint data and channel estimation using blind Trellis search techniques," *IEEE Transactions on Communications*, vol. 42, pp. 1000–1011, February–April 1994.

[407] R. Raheli, A. Polydoros, and C.-K. Tzou, "Per-survivor processing: A general approach to MLSE in uncertain environments," *IEEE Transactions on Communications*, vol. 43, pp. 354–364, February/March/April 1995.

[408] J. Holland, *Adaptation in Natural and Artificial Systems*. Ann Arbor, Michigan: University of Michigan Press, 1975.

[409] M. Jiang and L. Hanzo, "Novel MUD Techniques Designed for OFDM/MC-CDMA," Mobile VCE Core 3 Programme - Wireless Enablers 2.2: Deliverable D-WE2.2.2, University of Southampton, Southampton, UK, June 2004.

[410] R. L. Haupt and S. E. Haupt, *Practical Genetic Algorithms*. New Jersey, USA: John Wiley & Sons, Ltd, 2nd ed., 2004. ISBN 0-471-45565-2.

[411] Z. Michalewicz, *Genetic Algorithms + Data Structures = Evolution Programs*. New York, USA: Springer-Verlag, 2nd ed., 1994.

[412] S. M. Kay, *Fundamentals of Statistical Signal Processing, Estimation Theory*. Prentice Hall, New Jersey, 1993.

[413] R. Gallager, "Low-density parity-check codes," *IEEE Transactions on Information Theory*, pp. 21–28, 1962.

[414] M. C. Davey, *Error-Correction Using Low Density Parity Check Codes*. PhD thesis, University of Cambridge, UK, 1999.

[415] C. Berrou, A. Glavieux, and P. Thitimajshima, "Near shannon limit error-correcting coding and decoding: Turbo codes," in *Proc. of International Conference on Communications*, (Geneva, Switzerland), pp. 1064–1070, IEEE, May 1993.

[416] C. Berrou and A. Glavieux, "Near optimum error-correcting coding and decoding: Turbo codes," *IEEE Transactions on Communications*, vol. 44, pp. 1261–1271, October 1996.

[417] M. Jiang, S. X. Ng, and L. Hanzo, "Hybrid iterative multi-user detection for channel coded space division multiple access ofdm systems," *IEEE Transactions on Vehicular Technology*, vol. 55, pp. 115 – 127, January 2006.

[418] R. C. de Lamare and R. Sampaio-Neto, "Adaptive MBER Decision Feedback Multiuser Receivers in Frequency Selective Fading Channels," *IEEE Communications Letters*, vol. 7, no. 2, pp. 73–75, February 2003.

[419] C.-C. Yeh and J. R. Barry, "Adaptive Minimum Bit-Error Rate Equalization for Binary Signalling," *IEEE Transactions on Communications*, vol. 48, no. 7, pp. 1226–1235, July 2000.

[420] S. Chen, A. K. Samingan, B. Mulgrew, and L. Hanzo, "Adaptive Minimum-BER Linear Multiuser Detection for DS-CDMA Signals in Multipath Channels," *IEEE Transactions on Signal Processing*, vol. 49, no. 6, pp. 1240–1247, June 2001.

[421] D. Gesbert, "Robust Linear MIMO Receivers: A Minimum Error-Rate Approach," *IEEE Transactions on Signal Processing*, vol. 51, no. 11, pp. 2863–2871, November 2003.

[422] B. Mulgrew and S. Chen, "Adaptive Minimum-BER Decision Feedback Equalizers for Binary Signalling," *EURASIP Signal Processing Journal*, vol. 81, no. 7, pp. 1479–1489, 2001.

[423] M. R. Aaron and D. W. Tufts, "Intersymbol Interference and Error Probability," *IEEE Transactions on Information Theory*, vol. IT-12, pp. 26–34, January 1966.

[424] E. Shamash and K. Yao, "On the Structure and Performance of a Linear Decision Feedback Equalizer Based on the Minimum Error Probability Criterion," in *Proceedings of the International Conference on Communications (ICC)*, (Minneapolis, Minnesota, USA), pp. 25F1–25F5, 17-19 June 1974.

[425] P. Galko and S. Pasupathy, "Optimal Linear Receiver Filters for Binary Digital Signals," in *Proceedings of the International Conference on Communications (ICC)*, pp. 1H.6.1–1H.6.5, 1982.

[426] S. Chen, E. Chng, B. Mulgrew, and G. Gibson, "Minimum-BER Linear-Combiner DFE," in *Proceedings of International Conference on Communications (ICC)*, (Dallas, Texas, USA), pp. 1173–1177, 23-27 June 1996.

[427] C. C. Yeh and J. R. Barry, "Approximate Minimum Bit-Error Rate Equalization for Binary Signaling," in *Proceedings of International Conference on Communications (ICC)*, vol. 1, (Montreal, Canada), pp. 1095–1099, 8-12 June 1997.

[428] N. B. Mandayam and B. Aazhang, "Gradient Estimation for Sensitivity Analysis and Adaptive Multiuser Interference Rejection in Code-Division Multiple-Access Systems," *IEEE Transactions on Communications*, vol. 45, no. 6, pp. 848–858, July 1997.

[429] C. C. Yeh and J. R. Barry, "Approximate Minimum Bit-Error Rate Equalization for Pulse-Amplitude and Quadrature Amplitude Modulation," in *Proceedings of International Conference on Communications (ICC)*, vol. 1, (Atlanta, Georgia, USA), pp. 16–20, 7-11 June 1998.

[430] C. C. Yeh, R. R. Lopes, and J. R. Barry, "Approximate Minimum Bit-Error Rate Multiuser Detection," in *Proceedings of IEEE Global Telecommunications Conference (GLOBECOM)*, vol. 1, (Sydney, Australia), pp. 3590–3595, 8-12 November 1998.

[431] S. Chen, B. Mulgrew, E. S. Chng, and G. Gibson, "Space Translation Properties and the minimum-BER Linear-Combiner DFE," *IEE Proceedings on Communications*, vol. 145, no. 5, pp. 316–322, October 1998.

[432] S. Chen and B. Mulgrew, "The Minimum-SER Linear-Combiner Decision Feedback Equalizer," *IEE Proceedings on Communications*, vol. 146, no. 6, pp. 347–353, December 1999.

[433] I. N. Psaromiligkos, S. N. Batalama, and D. A. Pados, "On Adaptive Minimum Probability of Error Linear Filter Receivers for DS-CDMA Channels," *IEEE Transactions on Communications*, vol. 47, no. 7, pp. 1092–1102, July 1999.

[434] B. Mulgrew and S. Chen, "Stochastic Gradient Minimum-BER Decision Feedback Equalisers," in *Proceedings of IEEE Symposium on Adaptive Systems for Signal Processing, Communication and Control*, (Lake Louise, Alberta, Canada), pp. 93–98, 1-4 October 2000.

[435] X. Wang, W.-S. Lu, and A. Antoniou, "Constrained Minimum-BER Multiuser Detection," *IEEE Transactions on Signal Processing*, vol. 48, no. 10, pp. 2903–2909, October 2000.

[436] S. Chen, A. K. Samingan, B. Mulgrew, and L. Hanzo, "Adaptive Minimum-BER Linear Multiuser Detection," in *Proceedings of IEEE International Conference of Acoustics, Speech and Signal Processing (ICASSP)*, (Salt-Lake City, Utah, USA), pp. 2253–2256, 7-11 May 2001.

[437] A. K. Samingan, S. Chen, and L. Hanzo, "Adaptive Minimum-BER Linear Multiuser Detection for CDMA Signals in Multipath Channels with 4-QAM Constellation," *IEE Electronics Letters*, vol. 37, no. 11, pp. 721–723, 24 May 2001.

[438] S. Chen, B. Mulgrew, and L. Hanzo, "Least Bit Error Rate Adaptive Nonlinear Equalizers for Binary Signalling," *IEE Proceedings Communications*, vol. 150, no. 1, pp. 29–36, February 2003.

[439] S. Chen, L. Hanzo, and N. N. Ahmad, "Adaptive Minimum Bit Error Rate Beamforming Assisted Receiver for Wireless Communications," in *Proceedings of IEEE International Conference of Acoustics, Speech and Signal Processing (ICASSP)*, vol. IV, (Hong Kong, China), pp. 640–643, 6-10 April 2003.

[440] M. Y. Alias, A. K. Samingan, S. Chen, and L. Hanzo, "Multiple Antenna Aided OFDM Employing Minimum Bit Error Rate Multiuser Detection," *IEE Electronics Letters*, vol. 39, no. 24, pp. 1769–1770, 27 November 2003.

[441] J.H. Winters, "Smart Antennas for Wireless Systems," *IEEE Personal Communications*, vol. 5, no. 1, pp. 23–27, February 1998.

[442] J. Blogh and L. Hanzo, *3G Systems and Intelligent Networking*. John Wiley and IEEE Press, 2002.

[443] D. E. Goldberg, *Genetic Algorithms in Search, Optimization, and Machine Learning*. Reading, Massachusetts: Addison-Wesley, 1989.

[444] L. Hanzo, L-L. Yang, E-L. Kuan and K. Yen, *Single- and Multi-Carrier DS-CDMA: Multi-User Detection, Space-Time Spreading, Synchronisation, Networking and Standards*. Chichester, UK:: John Wiley and Sons, 2002.

[445] J. Holland, *Adaptation in Natural and Artificial Systems*. Ann Arbor, Michigan: University of Michigan Press, 1975.

[446] J. J. Grefenstette, *Genetic Algorithms for Machine Learning*. Kluwer academic Publishers, 1993.

[447] H. Adeli and S. L. Hung, *Machine Learning: Neural Networks, Genetic Algorithms and Fuzzy Systems*. John Wiley & Sons Inc., 1994.

[448] S. K. Pal and P. P. Wong, *Genetic Algorithms for Pattern Recognition*. CRC Press, 1996.

[449] M. D. Vose, *The Simple Genetic Algorithm: Foundations and Theory (Complex Adaptive Systems)*. Cambridge, Massachusetts: MIT Press, 1999.

[450] H. Dawid, *Adaptive Learning by Genetic Algorithms: Analytical Results and Applications to Economic Models (Lecture Notes in Economics and Mathematical Systems)*. Springer-Verlag Berlin and Heidelberg GmbH & Co. KG, 1996.

[451] M. Gen and R. Cheng, *Genetic Algorithms and Engineering Optimisation (Wiley Series in Engineering Design & Automation)*. John Wiley & Sons Inc., 2000.

[452] M. J. Juntti, T. Schlosser, and J. O. Lilleberg, "Genetic Algorithms for Multiuser Detection in Synchronous CDMA," in *Proceedings of IEEE Symposium on Information Theory*, (Ulm, Germany), p. 492, 29 June-4 July 1997.

[453] X. F. Wang, W.-S. Lu and A. Antoniou, "Genetic-algorithm-based Multiuser Detector for Multiple-access Communications," in *Proceedings of IEEE International Symposium on Circuits and Systems*, vol. 4, (Monterey, CA, USA), pp. 534–537, 31 May-3 June 1998.

[454] C. Ergun and K. Hacioglu, "Multiuser Detection Using a Genetic Algorithm in CDMA Communications Systems," *IEEE Transactions on Communications*, vol. 48, no. 8, pp. 1374–1383, August 2000.

[455] S. Abedi and R. Tafazolli, "A New CDMA Multiuser Detection Technique Using an Evolutionary Algorithm," *IEE Proceedings: Communications*, vol. 148, no. 6, pp. 393–399, December 2001.

[456] M. G. Shayesteh, M. B. Menhaj, and B. G. Nobary, "A Modified Genetic Algorithm for Multiuser Detection in DS/CDMA," *IEICE Transactions on Communications*, vol. E86-B, no. 8, pp. 2377–2388, August 2003.

[457] K. Yen and L. Hanzo, "Genetic Algorithm Assisted Joint Multiuser Detection and Fading Channel Estimation for Synchronous CDMA Systems," *IEEE Journal on Selected Areas in Communications*, vol. 19, no. 6, pp. 985–998, June 2001.

[458] K. Yen and L. Hanzo, "Antenna-diversity-assisted Genetic-algorithm-based Multiuser Detection Schemes for Synchronous CDMA Systems," *IEEE Transactions on Communications*, vol. 51, no. 3, pp. 366–370, March 2003.

[459] S. X. Ng, K. Yen, and L. Hanzo, "TTCM Assisted Genetic-algorithm Aided Reduced-Complexity Multiuser Detection," *Electronics Letters*, vol. 38, no. 14, pp. 722–724, 4 July 2002.

[460] A. Wolfgang, N. N. Ahmad, S. Chen and L. Hanzo, “Genetic Algorithm Assisted Error Probability Optimisation for Beamforming,” *IEE Electronics Letters*, vol. 40, no. 5, pp. 320–322, 4 March 2004.

[461] Y. Du and K. T. Chan, “Feasibility of Applying Genetic Algorithms in Space-time Block Coding Multiuser Detection Systems,” in *Proceedings of the IASTED International Conference on Wireless and Optical Communications*, vol. 3, (Banff, Canada), pp. 469–473, 2-4 July 2003.

[462] M. Mitchell, *An Introduction to Genetic Algorithm*. Cambridge, Massachusetts: MIT Press, 1996.

[463] C.-T. Chiang and C.-Y. Chang, “An Improved Genetic Algorithm Based on Eugenic Population for Multiuser Detection in DS-CDMA Systems,” in *Proceedings of IEEE Region 10 Annual International Conference (TENCON)*, vol. 2, (Beijing, China), pp. 984–987, 28-31 October 2002.

[464] A. Wolfgang, N. N. Ahmad, S. Chen, and L. Hanzo, “Genetic Algorithm Assisted Minimum Bit Error Rate Beamforming,” in *Proceedings of IEEE Vehicular Technology Conference (VTC-Spring)*, (Milan, Italy), pp. 142 – 146, 17-19 May 2004.

[465] M. Y. Alias, S. Chen and L. Hanzo, “Genetic Algorithm Assisted Minimum Bit Error Rate Multiuser Detection in Multiple Antenna Aided OFDM ,” in *Proceedings of IEEE Vehicular Technology Conference (VTC-Fall)*, (Los Angeles, California, USA), p. To be published, September 2004.

[466] T. H. Liew, B. J. Choi, and L. Hanzo, “Space-time block coded and space-time trellis coded OFDM,” in *Proceedings of IEEE VTC 2001-Spring*, p. P.533, IEEE, May 2001.

[467] J. Akhtman and L. Hanzo, “Channel estimation methods for OFDM and MC-CDMA systems,” tech. rep., University of Southampton, July 2004. Mobile VCE Core 3 Programme - Wireless Enablers 2.2.